MODELING AND SIMULATION OF GRID INTERFACED PV SYSTEM

A DISSERTATION SUBMITTED IN PARTIAL FULFILLMENT OF THE REQUIREMENTS FOR THE AWARD OF THE DEGREE OF

MASTER OF TECHNOLOGY
IN
POWER SYSTEM

(ELECTRICAL ENGINEERING)

SUBMITTED BY:

URVASHI MEENA
(2K15/ PSY/ 16)

UNDER THE SUPERVISION OF

Prof. Rachana Garg

DEPARTMENT OF ELECTRICAL ENGINEERING

DELHI TECHNOLOGICAL UNIVERSITY
(Formerly Delhi College of Engineering)
Bawana Road, Delhi-110042
INDIA
2017

DEPARTMENT OF ELECTRICAL ENGINEERING

DELHI TECHNOLOGICAL UNIVERSITY

(Formerly Delhi College of Engineering)

Bawana Road, Delhi-110042

CERTIFICATE

I, **Urvashi Meena** Roll No. 2K15/PSY/16, a student of M. Tech. (Power System), hereby declare that the dissertation titled "**Modeling and Simulation of Grid Interfaced PV System**" is a bonafide record of the work carried out by me under the supervision of **Prof. Rachana Garg** of Electrical Engineering Department, Delhi Technological University in partial fulfilment of the requirement for the award of the degree of Master of Technology and has not been submitted elsewhere for the award of any other Degree or diploma.

Place: Delhi **(Urvashi Meena)**

Date:

(Prof. Rachana Garg)

SUPERVISOR

ACKNOWLEDGEMENT

I would like to express my sincere gratitude to Prof. Rachana Garg for her guidance and assistance in the dissertation. The technical discussions with her were always been very insightful, and I will always be indebted to her for all the knowledge she shared with me. Her prompt responses and availability despite her constantly busy schedule were truly appreciated. She always helped me in all the technical and non-technical issues. Without her consistent support, encouragement and valuable inputs, this dissertation would not have become possible.

I would like to express my deep gratitude to Prof. Madhusudan Singh, Head of Department of Electrical Engineering for providing his support during my project. I would also like to thank Dr. Priya Mahajan and the other entire faculty and staff of electrical engineering department, DTU.

I would also like to thank to Ms Nikita Gupta and Ms Pallavi Verma (research scholars of DTU), my batch-mates and friends who encouraged and helped me in completing the dissertation.

Finally, I express my deep sincere thanks to my Parents who motivated and encouraged me for higher studies, without which it wouldn't have been possible.

Delhi, 2017 Urvashi Meena

ABSTRACT

The concern of environment due to green house gases and global warming have forced grid designers to design a smarter power system that has potential to integrate renewable energy sources with the power grid. Solar and wind power generators, now, have become standard electrical energy sources. In contrast to fossil fuels, which are quickly being drained, renewable energy sources are regularly recharged and environmental friendly. The human activities contribute to the global warming of the planet. Today depleting fossil fuels is not the only concern, but also its rising prices which are affecting the economic stability worldwide. The photovoltaic (PV) generation system is one of the best renewable energy sources available to meet out the energy crisis. It is safe, clean, pollution-free, and it requires less maintenance and inexhaustible. Solar photovoltaic system may be implemented as standalone system or grid connected system.

In recent years, the power generation through solar PV systems have shown rapid growth all over the world .There has been a remarkable increase in the grid interfaced PV systems being connected to the distribution end. These systems require high quality, low harmonic distortion and current injection into the grid. Inorder to fulfill these objectives, careful consideration of the inverter control is required.

In this work, modeling and simulation of grid interfaced 8 kW solar photovoltaic system is presented under different load and atmospheric conditions. The MPPT algorithms for tracking maximum power are presented. The inverter control for integrating the PV system to the grid is presented. The three phase inverter works as a multi-tasking device, which not just supplys power to the grid as power converter but also behaves as harmonic eliminator. The inverter controlling operation is performed on the system using three different control algorithms, under different load and environmental conditions in MATLAB/SIMULINK. These inverter control schemes are implemented to have reduced harmonics in the source current occuring due to various loads in the system. The system further involves the implementation of LCL filter between the PV array and distribution grid, providing reduced THD.Hence, the system have better power quality with reduced THD.

TABLE OF CONTENTS

LIST OF FIGURES

LIST OF TABLES

LIST OF SYMBOLS

RE	Renewable energy
SECI	Solar Energy Corporation of India
JNNSW	Jawaharlal Nehru National Solar mission
MNRE	Ministry of New and Renewable Energy
SPV	Solar Photovoltaic
MPPT	Maximum power point tracking
P&O	Perturb and observe
INC	Incremental and Conductance
PV	Photovoltaic
AC	Alternating Current
VSI	Voltage source Inverter
CCVSI	Current controlled voltage source inverter
IGBT	Insulated Gate Bipolar Transistor
PWM	Pulse Width Modulation
DC	Direct Current
SRFT	Synchronous Reference Frame Theory
ISCT	Instantaneous symmetrical component theory
PFC	Power factor correction
PLL	Phase Locked Loop
HCC	Hysteresis Current Controller
PCC	Point of Common Coupling
DG	Distributed generation
W	Watts
KWh	Kilowatt hour
GW	Giga watt
THD	Total Harmonic Distortions
Var	Reactive Volt Ampere

CHAPTER 1

INTRODUCTION

1.1 General

Electrical energy is the primary need for the economic development of a nation. We need energy in different walks of life, whether it is cooling our homes, cooking, charging our laptops or having bath. The degree of energy consumption of a nation depicts the standard of living of it people. With the growing population and modernization electrical energy demand is also growing. To meet this increasing energy demand, electric generation must be raised. The world's total energy production has been increased from 21.6 trillion kWh in 2012 to 24.4 trillion kWh in 2015 and is estimated to be 25.8 trillion kWh in 2020 and would reach about 36.5 trillion kWh by 2040[1]. Today fossil fuels (Non-Renewable resource) are one of the major sources of electrical energy. Cheaper and abundant energy availability is essentially required for all living beings in different walks of life. With the increased rate of consumption of energy, fossil fuel energy sources are soon depleting followed by huge energy crisis. Increased use of non-renewable resources can contaminate environment to a great extent resulting in greenhouse gas emission, causing global warming. To overcome such pollution hazards and greenhouse gas emissions like carbon dioxide and mercury, today's generation is now switching from conventional energy sources to the renewable energy sources. Renewable energy sources are environmental friendly sources of energy. Thus to provide a better future for the upcoming generations, renewable source of energy need to be developed.

1.2 Classification of Energy Sources

The energy sources can be broadly classified into following two categories:

i. Non-renewable energy sources
ii. Renewable energy source

1.2.1 Non-Renewable Energy Sources

These resources are obtained from fossil fuel. They took billions of years to turn into a source of energy, and will soon run out as they are used at a much faster rate, than their replacement. As these sources cannot be formed again in a short period of time they are known to be exhaustible in nature. Fig. 1.1 shows types of non-renewable energy sources.

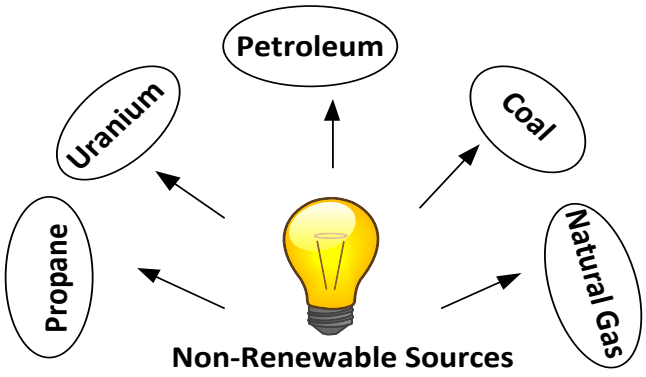

Fig. 1.1 Non-Renewable energy resources

1.2.2 Renewable Energy Sources

Renewable energy sources do not dissipate with time rather gets recycled will the small passage of time. Thus these sources of energy can be used repeatedly without any fear of extinction. Fig 1.2 shows types of renewable energy sources.

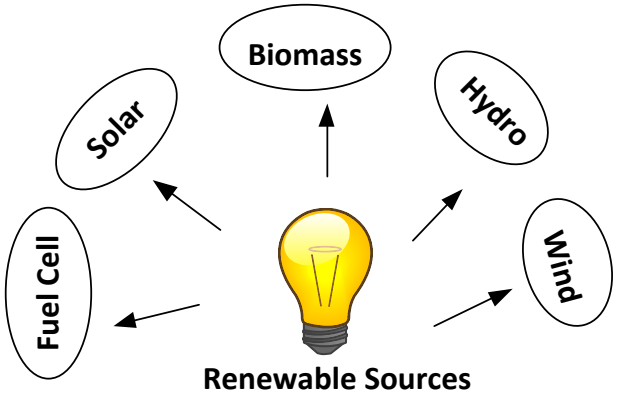

Fig. 1.2 Renewable energy sources

Current total power generating capacity of India is 330.26 GW of which RE (Renewable energy) capacity is 57.26 GW (17.33% of generating capacity (as on March 2017) and has

a huge potential of renewable energy sources. The estimation of renewable energy in India is shown in Fig. 1.3[2]

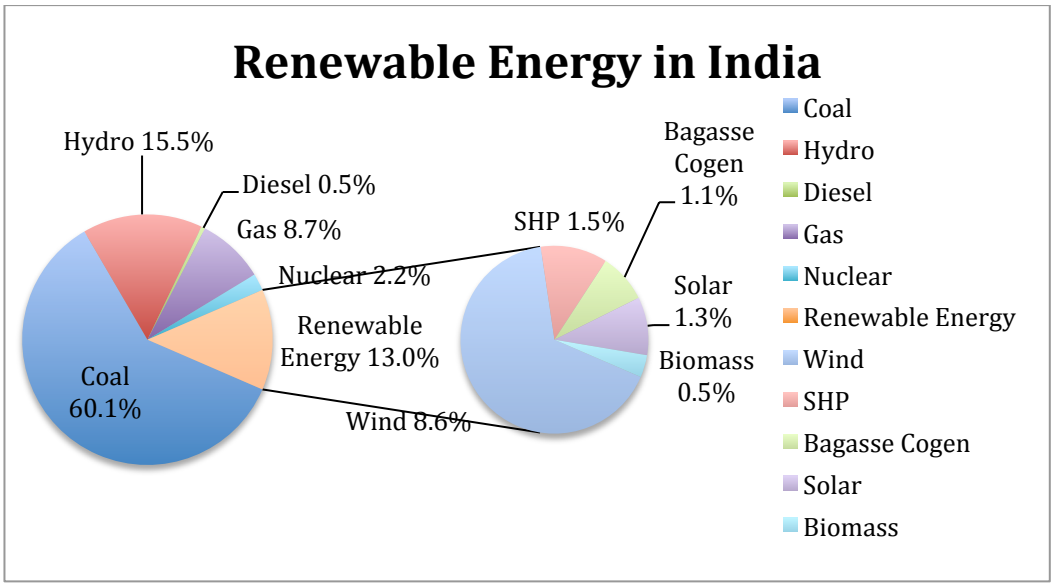

Fig. 1.3 Renewable energy in India

The photovoltaic (PV) generation process is one of the foremost renewable energy mode accessible to meet out the energy crisis. It is risk-free, clean, pollution-free, requires very less maintenance and is present in abundance. The geographical position of India is fairly suitable for application of solar energy plants. Solar power in India is a growing field. With this panorama, India has framed future solar energy utilization roadmap through Jawaharlal Nehru National Solar Mission (JNNSM) with a objective of generating 20000 MW of grid interfaced solar power by 2022[3-4]. With its ecofriendly nature, virtually limitless supply and global availability- solar energy is very important energy resource. The solar energy source is a practical solution to mark the continuous power demand in the power industry by employing photovoltaic (PV) system. Thus considering the geographical and social-economic feature of this country, PV approach is the best solution to meet the demand. The map of the solar irradiation across India is shown in Fig. 1.4.

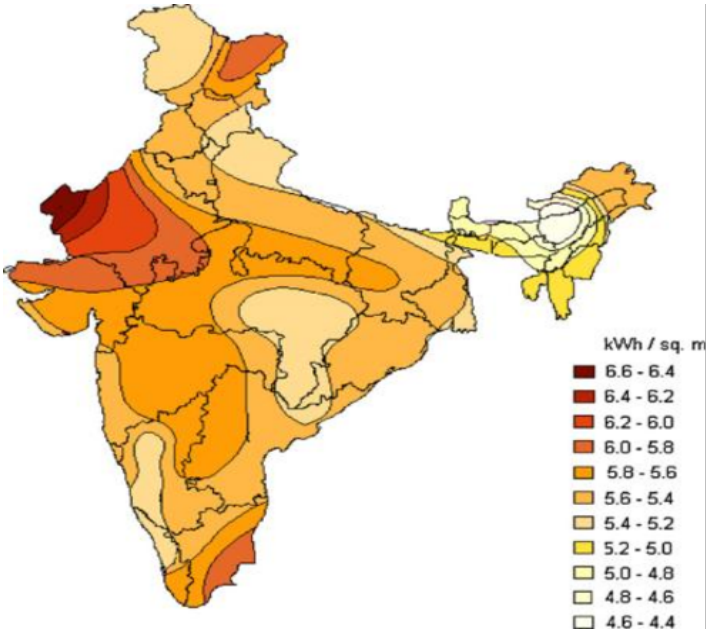

Fig. 1.4 Solar irradiation across India

Solar Photovoltaic systems are used to produce electricity. The solar energy gets converted to electrical energy through photovoltaic process and therefore these systems are known as solar photovoltaic (PV) system as shown in Fig.1.5.Power generating PV systems are employed on a large-scale either in large farms connected to the utility grid or on the rooftops of houses which provide cleaner source of electricity generation.

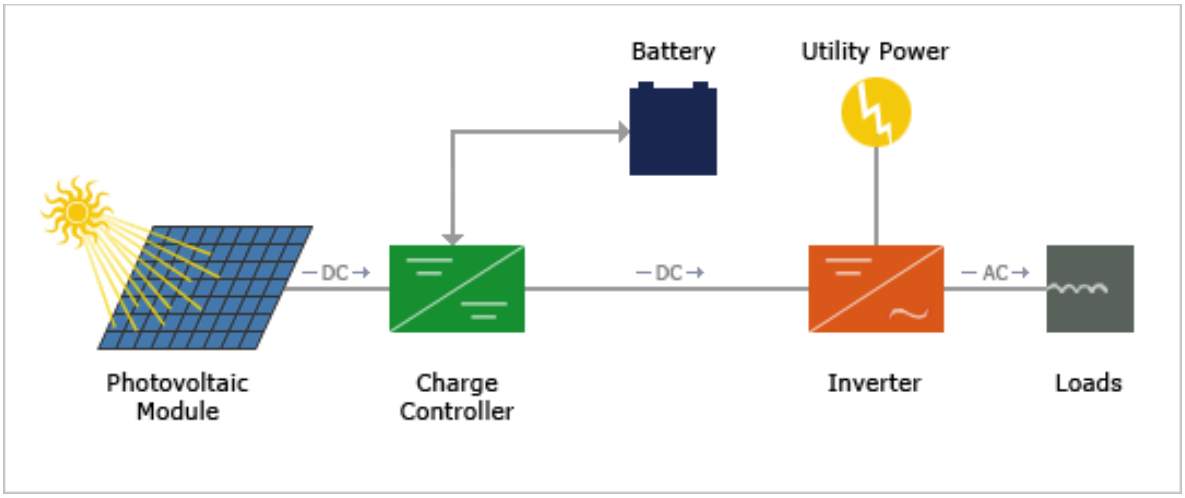

Fig. 1.5 Solar Photovoltaic system

The photovoltaic system can be employed as: (a) off-grid system where PV array deliver power to local consumers (loads which are not coupled with grid) such systems are known as standalone system (b) Grid connected system where PV array is coupled with grid and

can deliver power to the loads connected to grid, such systems are known as grid connected PV system. PV systems can be installed on the facades and rooftops of houses, offices and buildings. They are installed in large fields to produce power at bigger scale. PV system has been applied in various fields in India. Some important photovoltaic power generating units in India with their commissioned generating capacity as on 22 February 2017 are Kamuthi solar power project Tamil Nadu with 648 MW capacity, Charanka solar park Gujrat with 221 MW capacity, Welspun solar project in Madhya Pradesh with capacity 151 MW,Badla Solar park Rajasthan having 115 MW capacity, Sakri solar plant Maharashtra with 125MW capacity etc. As India is blessed with abundant solar energy thus solar PV generation seems more attractive, than other renewable source of energy.

PV application in India includes off-grid systems and small capacity installation for public streetlights, traffic lights and household power back up and lanterns in rural districts. Now a day, they are also used to supply power to water pumps for harvesting and to small industrial units. On the other hand in India there are large government firms like railways, telecom and other organizations, which consume power generated from PV solar system. The installed capacity of India is 308 GW (as of November 2016).Table I shows the current status of Solar PV systems installed in different areas involving 308 MW of Solar Rooftop Projects sanctioned by MNRE and 49.677 MW Commissioned.

Table I Present status of installed Rooftop PV system in India [2]

Area	**Installed by SECI (MW)**	**Installed by States(MW)**	**Total Installed (MW)**
Private enterprise	11.36	12.71	24.07
Government	2.36	4.893	7.253
Institutions	3.215	4.131	8.346
Hospital	1.6	0.47	2.07
Religious institution	0.12	7.52	7.64
Residential	0	0.298	0.298
Total	**18.655**	**31.022**	**49.677**

1.3 Motivation

Different technologies are being developed all over the world and especially in India to take advantage of the solar energy. To visualise India as SOLAR INDIA as mentioned in JNNSM,the prime focus should be towards developing an environment for solar energy development in the country.

In the recent times there has been remarkable development in the PV based projects both in grid-connected and Standalone form. So, it calls for investigation of the working of solar PV system and the understanding of the performance of solar generating units which would result in better investment decisions and beneficial government plans.

1.4 Objective

The primary objective of this thesis work is to design, simulate and study the performance of a grid connected solar PV system under various loads and atmospheric conditions. Fig. 1.6 shows the schematic diagram of grid interfaced solar PV system.

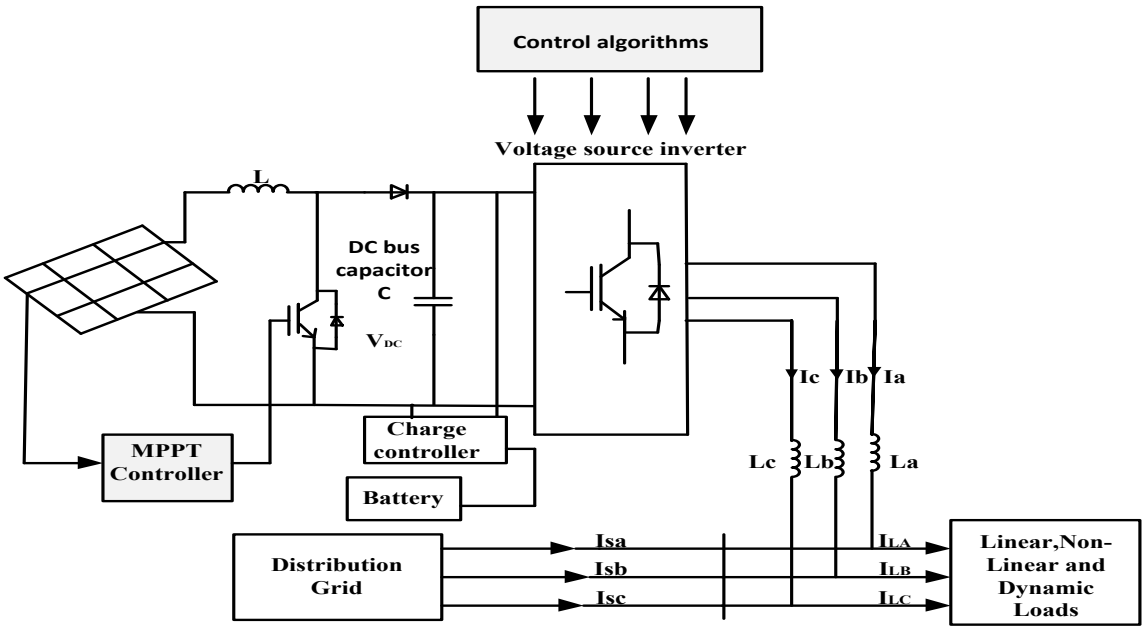

Fig. 1.6 Grid interfaced PV system

Large-scale solar photovoltaic system integration to grid poses a set of challenges such as voltage fluctuation, reactive power compensation, voltage dips/swells, voltage flicker,

voltage unbalance, harmonics etc. The DC-AC converter connected to the grid limits these power quality issues to a great extent. Thus, the output power quality to the grid is preserved. The PI controller regulates the DC-bus voltage (the DC link between the two power converters) to have a balanced power flow in the system.

Installation of PV system comes up with various challenges, among which withdrawing maximum power from sun with varying environmental conditions is the most important challenge. PV cell has nonlinear characteristics. Further, solar irradiation and varying temperature conditions also affect its power output. MPPT algorithm is used to track the maximum power from the PV array according to the variation in the temperature and irradiation [5].

The contents of the thesis are briefly outlined here.

i. Grid interfaced PV system has been modeled with a PV array generating an active power of 8 kW and simulated in MATLAB Simulink version 15.
ii. Two MPPT techniques to extract maximum power from the PV array, namely P&O and INC has been studied and the one with better results (P&O) is implemented to the grid interfaced system.
iii. Further three control algorithms for PV inverter control have been analysed.
iv. The inverter control with best THD results is further improved by replacing L filter by LCL filter between the PV array and distribution grid.

1.5 Thesis Organization

This dissertation has been arranged in six chapters. With the first chapter introducing the significance of solar energy, motivation and objective of this work.

Chapter 2, covers the literature review of the achievements in past years and current research undertaking in the field of the grid-interfaced PV systems and its controlling.

Chapter 3, presents the basics of Photovoltaic system, DC-DC converter, MPPT techniques, and PV inverter.

Chapter 4, presents the controlling of PV inverter through different control algorithms.

Chapter 5, gives simulation results of grid interfaced PV system with different load conditions for power factor correction mode (PFC) in MATLAB environment using SIMULINK.

Chapter 6, presents the summary of the dissertation and conclusion ,as well as the future scope of this work.

CHAPTER 2

LITERATURE REVIEW

2.1 General

This chapter aspires to give a concise literature review of grid interfaced PV system. A lot of research work has been surveyed in context with maximum power point techniques(MPPT) and control techniques for dc- ac converter applied in grid connected PV system. The prime emphasis of this literature review is on following points:

i. Modeling of PV cell.
ii. MPPT algorithms to extract maximum power.
iii. Inverter control techniques.

2.2. Modeling of PV Cell

Ideal PV cell constitutes an ideal current source in parallel with a diode. The cell output characteristics vary with the variation in the atmospheric condition and shows non-linear behavior. Pritam et al. [6] gives the modeling of a non-conventional solar energy generation system. A grid-interfaced PV system with the controlling of harmonics is presented in this paper. Considering this system, a testing set up for assuring the viability of the strategy proposed.

Jincy Philip et al. [7] give a control algorithm for a standalone solar photovoltaic diesel-battery based hybrid system. The battery energy storage system (BESS) is integrated into the diesel engine generator set for the cocrdinated load management and power flow within the system.

S. Sumathi et al. [8] book provides a detailed study of solar and wind energy design and simulation. For this cause, an illustrative framework has been presented using models designed in MATLAB/SIMULINK. This book also puts light on the current trends of soft computing techniques in solar and wind energy system through elaborate description of practical cases and their Simulink models.

Dasgupta et al [9] and Augustin McEvoy et al. [10] gives a complete overview of grid-interfaced SPV systems, which includes characteristic curves, grid-interfaced configurations, various inverter topologies (both for single and three phase system), control

techniques, maximum power point tracking (MPPT) algorithm, and ways to detect anti-islanding.

Himanshu Sekhar Sahu et al. [11] explains under partial shading condition, the modules of the PV aaray receive different levels of solar radiation, so the power generation of the PV system decreases.

M. G. Villalva et al. [12] presents a method of design and simulation of solar PV array to obtain the of the nonlinear I–V equation through regulation of the curve at three places i.e. open circuit, maximum power point, and short circuit.

2.3. MPPT algorithms to extract maximum power

SPV array exhibits the non-linear behaviour when observed under varrying enviromental conditions.Consequently its output characteristic changes and therefore it is very necessary to track the maximum power ponit of the solar array.A significant amount of work has been done for advancing the maximum power point techniques.

J. A. Gow et al. [13] proposed an entire SPV power electronic conversion system in Simulink model in order to interface a proposed converter and the PV array. The converter takes in the changing parameters (i.e. irradiance and temperature) as input variables and gives outputs the I-V characteristic with the system operating at MPP.

Wei Jiang et al. [14] presents the principle of operation of controlling of Boost converter in current mode. The mathematical equations are formulated by the application of KCL and KVL theory for two different working conditions. The models working in CCM and DCM are respectively developed using MATLAB/Simulink. The Boost converter nonlinear behavior is then observed through simulation model.

Nikita Gupta et al [15] propose PV module controlling through a asymmetrical fuzzy logic control in micro grid. In this work it has been explained that there is considerable change in the dc bus voltage during the load change transients and the performance using asymmetrical fuzzy logic control the voltage is maintained better than the conventional controller.

Mukhtiar Singh et al. [16] proposes a new approach to assess the behavior of SPV Array and grid interfaced inverter control technique. The design of this model includes the

conversion of the basic network equation of the solar cell into simpler order along with the impact of varying solar irradiation and temperature. This paper presents an effective MPPT control technique and grid interfaced Photovoltaic array using DC/DC/AC Converter
S. Rustemli et al.[11], Kinal Kachhiya et al. [18] and H. Atlas et al. [19] develops the comparison of the performance of boost and injected boost converter for Maximum Power Point Tracking (MPPT) and different MPPT techniques.
M.Latha Devi et al. [20] presents the modeling and matlab simulation of incremental conductance algorithm to trac maximum power point which is implemented through lift cuk converter.

M. Abdulkadir et al. [21] proposes the design and modeling of dc- dc boost converter with modified incremental and conductance algorithm on matlab simulink platform. The system is tested with solar panel ICO-SPC 100W module under different operating conditions.

Muhammad Afroz Akhtar et al. [22] presents the maximum power extraction from the PV panel by using Phase Modulated Converter and incremental conductance algorithm. The simulation results are taken under different enviromental conditions.

Himanshu Kumar et al. [23] proposes variable incremental conductance method for maximum power point tracking of a solar PV panel. This method is differs from existing MPPT methods as there is no proportional integral loop.

Trishan Esram et al. [24] presents the various algorithms for maximum power point tracking of solar photovoltaic (SPV) arrays.

Tarek Selmi et al. [25] and M.A Elgendy et al. [26] shows the mathematical modeling of a solar PV cell with a single diode and double diode arrangements. A patented algorithm is used to implement the model of the double diode arrangement in the cell on MATLAB/Simulink platforf. Perturb and observe (P&O) control technique is used to track the MPP.

Macro Liserre et al. [27] presents detailed design procedure and simulation model of LCL-filter based active rectifier.The resulting system is stable and the grid current harmonics gets reduced remarkably in low as well as high frequency ranges.

Leonardo Augusto Serpa et al. [28] proposes the addition of LCL-filter to the conventional DPC to have reduced harmonics in the system. The system is analysed for both dynamic and steady state.

A. Reznik et al. [29] gives the designing of LCL-filter for grid interfaced inverters with adetailed study of how to reduce harminics.

2.4. Inverter Control Techniques

In a grid interfaced SPV system, it is very important that the inverter's output magnitude and frequency is well defined.To have reduced THD in the inverter output, different inverter control schemes can be used.

Prakash Chittora et al. [30] proposed a notch filter based extraction of harmonic current and compensation technique in a three-wire distribution system using avoltage source converter. The technique uses shunt compensation to mitigate harmonic current.

Bhim Singh et al. [31] proposed the modeling of a $3-\phi$ DSTATCOM (Distribution Static Compensator) and its controlling technique on the basis of interrelation and cross interrelation operation approach to improve power quality under different loads in a distribution system.

B. N. Singh et al. [32] presented current-controlled voltage source inverters (CC-VSI) as active filter using three-pole/four-pole topologies. The filter system implements power balance theory using TMS320C31 DSP.

El-Samahy et al. [33] studies the impact of the Distributed Generation (DG) on power quality and delivered its advantages and disadvantages.

Bhattacharya et al. [34] proposes modeling of controller using synchronous reference for a series hybrid active filter. This work explains the basic controller structure of synchronous reference frame and marks it's functioning in case the controller loop gain is not unity.

Bhim singh et al. [35] proposes the application of SPV power generating system to achieve unity power factor or to have voltage regulation at PCC.

Rejil et al. [36] presents design and Simulink model of active filter with the application of synchronous frame theory.

Nikita Gupta et al. [37] developed a 10 kW photovoltaic array and studied it considering different load. The inverter control technique used is synchronous reference frame theory (SRFT) to produce gate signals for controlling the inverter.

Ravi Nath Tripathi et al. [38] gives the design to connect Photovoltaic (PV) system's operation in indirect current control condition with the application of Synchronous Reference Frame theory(SRFT).
Da silva et al. [39] and [40] presents a control strategy called phase-locked loop (PLL) to synthesize unit vector by applying the synchronous reference frame (SRF).

U. Koteswara Rao et al. [41] and Sunil Kumar et al. [42] described the instantaneous symmetrical component theory(ISCT). The theory is applied to study different control techniques for load compensation with varying input voltages. With balanced input voltages, each of these technique results into identical compensation characteristics.
Arindam Ghosh et al. [43] proposes a different method for reference currents extraction of an active filter and/or a static compensator. It is considered that the compensator is interfaced to a load which can be in any configuration, either star or delta. There may be unbalanced load, which might also fetch harmonic currents. The aim of the compensation technique is to achieve balanced load and keep the power factor on supply end within desired range. The instantaneous symmetrical component theory is implemented to deliver three phase reference currents, which are further given to the system to obtain the results required. Authors also suggest an appropriate compensator model to trace the reference currents in a hysteresis band control technique.
Mahesh K. Mishra et al. [44], Naresh K. Kummari, Asheeshet al. [45] and Dinesh Kumar, Rajesh et al. [46] have examined load compensation methods with unbalanced and diformed voltages. Two different compensation techniques are discussed. The first section discuss, synchronous detection and modified equal current techniques implemented under the unbalanced sinusoidal source voltages. The second section discusses, instantaneous symmetrical component theory implementation for load compensation where drawing positive sequence is suggested and is examined under unbalanced source voltages and the source voltages, which are not sinusoidal.

Arun Kumar Verma et al. [47] presents a Photovoltaic (PV) power generating system employing 4-leg voltage source converter (VSC), connected to a 4-wire distribution system. The inverter control technique implemented is Modified Instantaneous Symmetrical Component Theory (MIST). This technique is employed to evaluate reference currents for controlling the converter. The control technique used also provides load balancing and power factor correction.

Manoj Kumar et al [48] proposes a method called dual voltage source inverter (DVSI) to have improved power quality and stability of a microgrid. The control technique used is instantaneous symmetrical component theory (ISCT) so that DVSI can function in grid sharing and grid injecting cases.

G. Bhuvaneswari et al. [49] explained Icosø technique, which is implemented to a three-phase shunt active filter to obtain harmonic and reactive power compensation, required by the non-linear loads. The model is demonstrated on Simulink platform and the signals are introduced to hardware through basic analog circuits and comparison of results is given.

Bhim Singh et al. [50] propose the design of a DSTATCOM (Distributed Static Compensator) employing of a 3-leg VSC (voltage source converter) and a zigzag transformer to obtain load compensation and the neutral current compensation in 3-phase 4-wire distribution system. A modified IcosΦ technique is implemented regulating the DSTATCOM in power factor correction (PFC) and zero voltage regulation (ZVR) modes at PCC (point of common coupling).

Kamatchi Kannan et al. [51] propose the design of a Photovoltaic (PV) array or DC-DC boost converter operated through battery supplying a $3-\phi$ three-wire DSTATCOM to provide reactive power compensation, reduced harmonic in source current and load compensation in the distribution system. The two control techniques namely Synchronous Reference Frame theory (SRFT) and Icosø technique are implemented to provide switching gate pulses to the converter which would result after the comparison of the source current with the reference current through Hysteresis based Pulse Width Modulation (PWM).

G. Bhuvaneswari et al. [52] propose Icosø algorithm which is implemented on a $3-\phi$ shunt active filter imparting harmonic and reactive power compensation as required by the non-linear system. The model is demonstrated on Simulink platform and the signals are introduced to hardware through basic analog circuits and comparison of results is given.

2.5 Conclusion

Significant amount of work has been done in the field of grid interfaced SPV system. This chapter covers a brief literature review of the work done so far on the relevant topics i.e. SPV design, MPPT algorithms, inverter control techniques and LCL filter design.

CHAPTER 3
MATHEMATICAL DESIGN OF GRID INTERFACED SPV SYSTEM

3.1 General

Solar PV plants have now become standard sources of electrical energy. Solar cells inside the solar panel fetch the light from the sun and convert it to electricity. A PV system mainly constitutes solar cells or PV cells, DC-DC Boost converter, DC-AC inverter etc. This chapter includes the basics of PV cell and its modelling, and a brief description of the DC-DC boost converter, MPPT algorithms, PV inverter and its modeling.

3.2 Solar Photovoltaic (SPV) System

Solar PV system can be classified into two broad categories viz. standalone system and grid

Interfaced PV system [6- 9]:

3.2.1 Standalone SPV system

Stand-alone PV systems are commonly known as direct-coupled PV systems. These systems are designed to supply output power of a PV module or array directly to DC or AC electrical loads. Stand-alone PV systems are not connected to the utility grid and are therefore also known as off-Grid PV system. Some of the standalone PV systems are directly coupled i.e there is no electrically energy storage. These systems use maximum power point tracking (MPPT) between the array output and load. Fig. 3.1 shows the the standalone PV system directly-coupled with load.

The direct coupled solar PV systems are used in various applications such as agriculture where solar PV array can be directly connected to run the pump.Series/parallel configurations of the module can be used to achieve particular pump capacity.

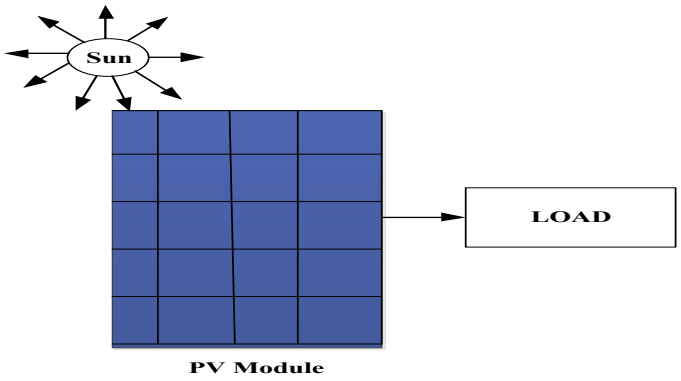

Fig. 3.1 Block diagram of Direct-coupled standalone SPV system

Some standalone systems use batteries for energy storage[7]. Fig. 3.2 shows the schematic diagram of a stand-alone solar system delivering power to both DC and AC loads with battery storage system.

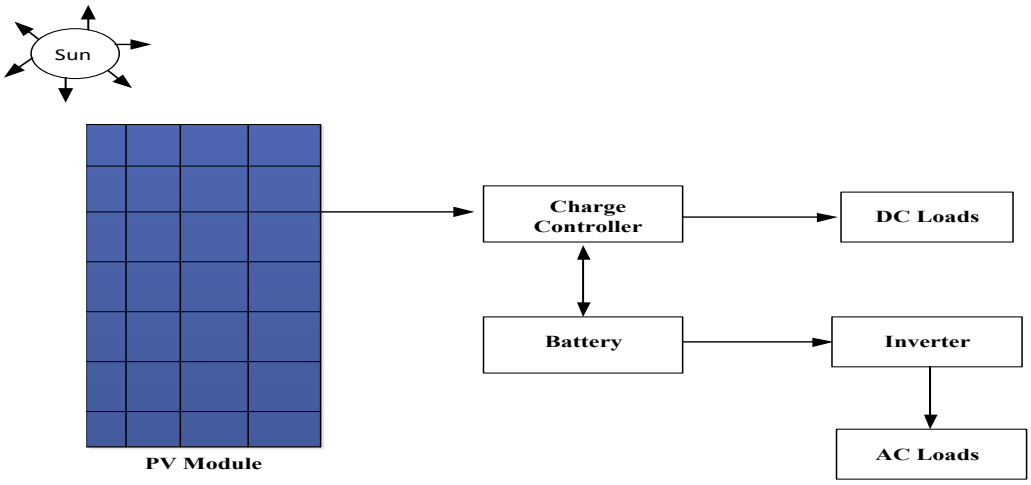

Fig. 3.2 Block diagram of Standalone SPV system with battery storage

The systems comprising of batteries require charge controllers. These controllers prevent discharging and overcharging of the batteries. The charge controller maintains the current output and checks the voltage from surpassing the maximum value for charging the batteries. The charge controller's output is connected to the battery bank through a dual DC cutoff disconnect. During the sunlight hours, the system supplies DC power to the load and charges the battery simultaneously. The role of the controller is to ensure that the PV arrays should provide ample output power to sustain the demands of loads connected while sizing the batteries. Sizing of the battery bank is influenced by various factors, such as the

duration of an uninterrupted power supply to the load or the duration when there is less or no radiation from the sun.

3.2.2 Grid-interfaced SPV system

The PV systems which are coupled with the utility grid is called grid connected PV systems. In grid connected PV system, energy flow is bi-directional. If the load demand is less than the output of PV power generation, the excess power from PV is fed to the grid and when the load demand exceeds than the PV power generation, the remaining load power is supplied by the grid as shown in Fig. 3.3. The primary component in grid-connected PV systems is the inverter. The inverter converts the DC power produced by the PV array into AC power consistent with the voltage, frequency and power quality requirements of the utility grid.

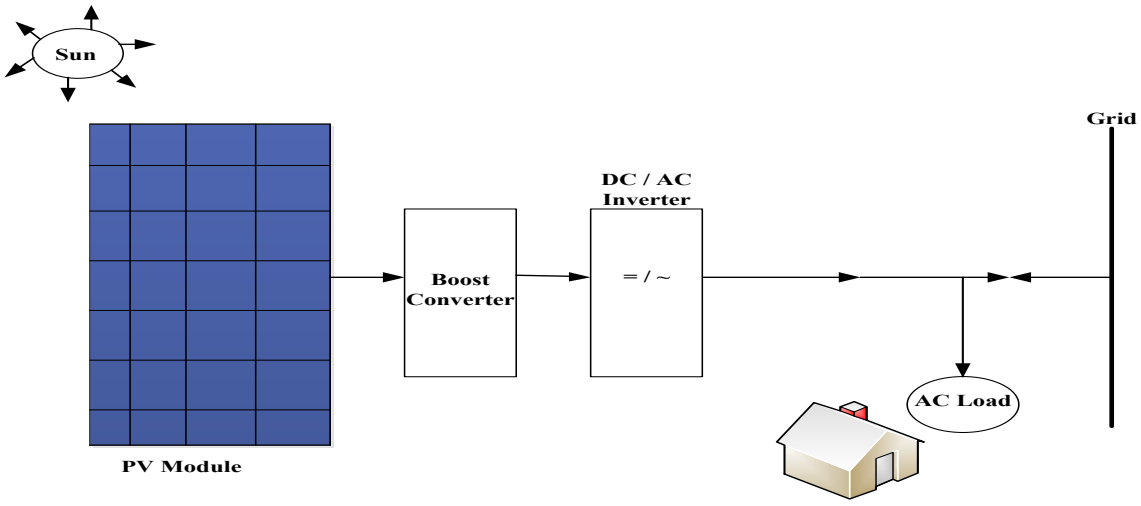

Fig. 3.3 Block diagram of Grid interfaced SPV system

3.3 Elements of Grid connected PV system

The various components of grid connected PV system are:

i. Solar Photovoltaic array.
ii. DC-DC boost converter.
iii. MPPT Controller.
iv. PV Inverter and its modeling.

3.3.1 Solar PV Array

The fundamental component of a PV system is a solar cell. A solar cell can roughly generate about 1 or 2 W of power. To achieve higher power output, a number of cells can be grouped together to form PV modules and further higher power can be obtained by grouping a number of PV modules to form PV arrays as shown in the Fig. 3.4

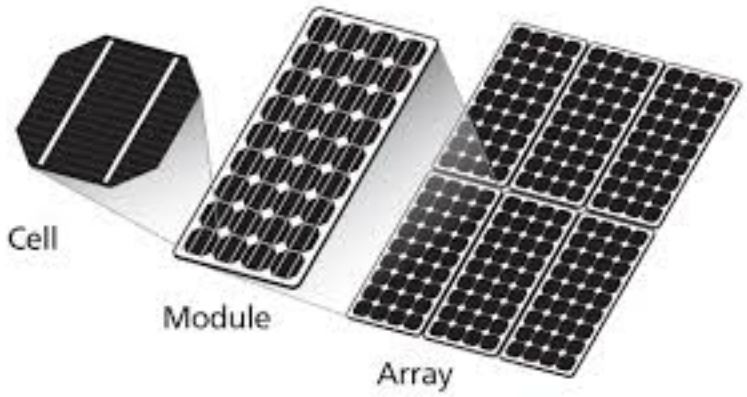

Fig. 3.4 Solar Photovoltaic cell, Module and Array.

Several solar arrays combine to form a solar PV system.The solar PV system also consists of some other components such as charging battery controller, MPPT controller and dc-ac converter and switchgear components.The complete system performance depends on the efficiency or the performance of its individual components[8].

PV cell can be made up of various semiconductor materials but for commercial use mono-crystalline silicon and polycrystalline silicon are preferred. An individual PV cell can agenerate about 0.6V. The solar cells works on the principle based on the photovoltaic effect, i.e. the development of a potential difference at the junction of two different materials in reaction to electromagnetic radiation. Fig.3.5 shows the principle of generation of photocurrent in a PV cell. In a photovoltaic cell when sunrays fall on its surface, some amount of the solar energy gets absorbed in the semiconductor material. If the energy absorbed by the semiconductor is greater than its band gap energy, the electrons jumps from the valence band to the conduction band, forming electron hole pairs. The electrons in the conduction band can move freely. The electric field present in the PV cell pushes free electrons to take a particular path. The unidirectional flow of these electrons forms current and can be extracted through a metal plate on top and bottom of PV cell for external use.

When sun radiations strikes the cell surface, the photons are absorbed by the semiconductor atoms and deliver free electrons from the negative layer[10]. These free electron finds its way toward the positive layer through an external circuit connecting the two resulting in the formation of electric current.

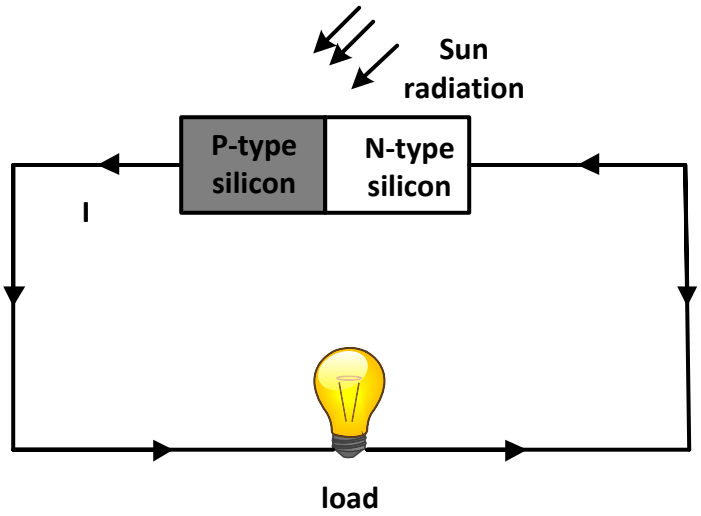

Fig.3.5. Photocurrent generation principle

The basic circuit of an ideal solar cell and a practical solar cell is as shown in Fig.3.6. The practical modelling of a solar cell includes an ideal solar cell along with a series resistance (R_s) and a parallel resistance (R_p).

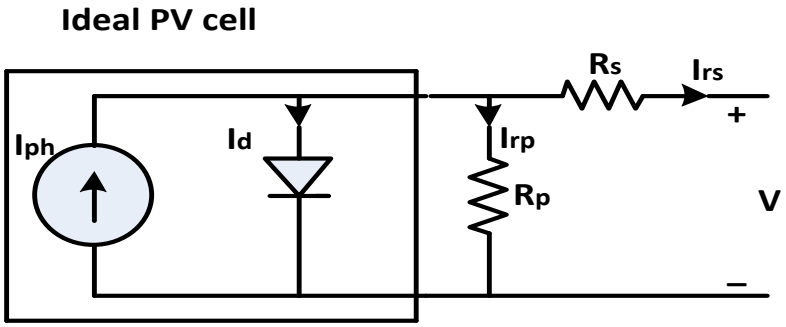

Fig. 3.6 Equivalent circuit diagram of a practical SPV cell.

The theory of semiconductors gives basic eqn., that mathematically describes the I-V characteristics of an ideal PV cell given by eqn. (3.1) to eqn. (3.3):

$$I = I_{ph} - I_d \tag{3.1}$$

Where, $I_d = I_{rs}\left[exp\left(\frac{qv}{aKT}\right) - 1\right]$ (3.2)

Therefore, $I = I_{ph} - I_{rs}\left[exp\left(\frac{qv}{aKT}\right) - 1\right]$ (3.3)

where, I_{ph} is the current drawn by the absorption of photon energy and is directly proportional to the incident solar radiation. Therefore, I_{ph} represents the photocurrent, I_d is the diode current, I_{rs} is the reverse saturation or leakage current of the diode, q is the electron charge $(1.60217646 \times 10^{-19}\text{C})$,'$\propto$' is the diode ideality constant, K is the Boltzmann constant($1.3806503 \times 10^{-23}$ J/K) and T(in Kelvin) is the temperature. Fig.3.7 shows the I-V curve obtained from eqn. (3.1).

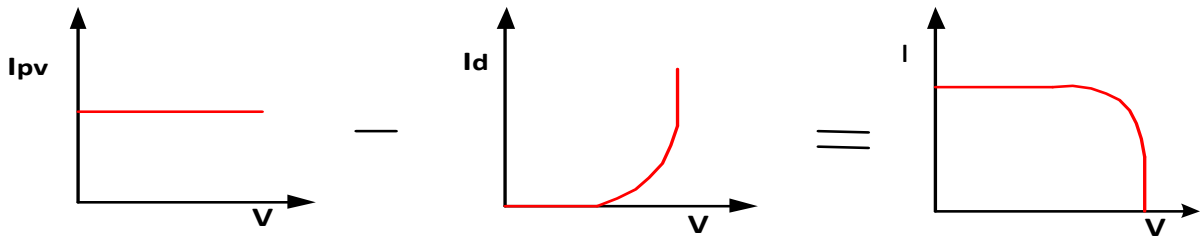

Fig. 3.7 Equivalent I–V curve of a SPV cell

The eqn. (3.3) gives the equation of an ideal PV cell I-V characteristics and not that of a practical one. Practically the PV arrays consist of several interconnected PV cells and the characteristics observed at the terminals of the PV array need to include additional resistive parameters to the basic eqn. (3.3). Hence, the modified eqn. for practical PV array is shown in eqn. (3.4):

$$I = I_{ph} - I_{rs}\left[exp\left\{\frac{(V+R_SI)}{V_Ta}\right\} - 1\right] - \frac{V+R_SI}{Rp} \quad (3.4)$$

Now, if the array is formed by a number of parallel cell connections (N_p), the saturation current is expressed as $I_{ph} = I_{ph}N_P$, $I_{rs} = I_{rs}N_P$. Thus, the overall eqn. can be given as eqn. (3.5) :

$$I = I_{ph}N_p - N_pI_{rs}\left[exp\left\{\frac{q(V+IRs)}{N_sakT}\right\} - 1\right] - \frac{V+IR_S}{R_P} \quad (3.5)$$

The photocurrent is highly influenced by the solar irradiance and cell temperature as shown in eqn. (3.6)

$$I_{ph} = I_{sc} * \frac{I_{rr}}{1000}[1 + (T - T_0) * \alpha] \quad (3.6)$$

Where $V_T = \frac{N_SkT}{q}$ is the thermal voltage of the array with cells Ns connected in series, $R_S$is the series resistance of the array and Rp is the parallel resistance, T_0 is reference

temperature which is 25^0 C, T is the operating temperature (K) which may lie in the range 20 to 65^0C, α is the short-circuit current temperature coefficient at short circuit condition and I_{sc} is the PV cell's Short-circuit current at 25°C.

3.3.1.1 Characteristics of PV Array

The photocurrent is highly influenced by the amount of solar radiation striking its surface and the ambient temperature[11]. The I-V characteristic curve for current versus voltage and P-V characteristic curve for power versus voltage of the solar PV system are shown in Fig. 3.8, (a) and (b) respectively with 1000 W/m^2 radiation and 25^0 C temperature. Both the characteristic curves show nonlinear behaviour. Maximum power point (MPP) is the point at which the output power of PV array is maximum corresponding to a particular value of voltage (V_{mpp}).The respective voltage (V_{mpp}) and current (I_{mpp}) at Maximum Power Point (MPP) are also highlighted in the Fig. 3.8.

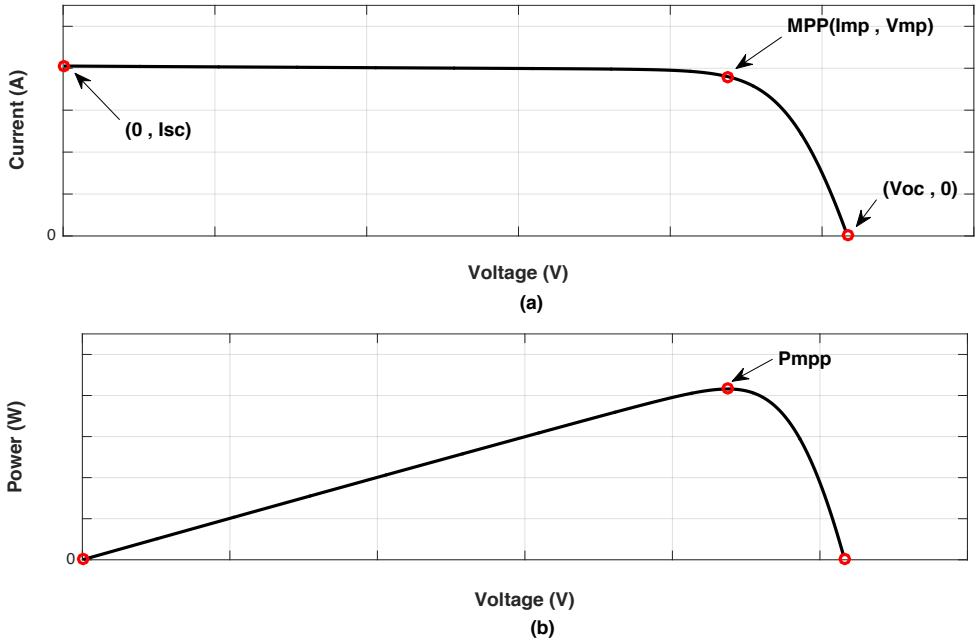

Fig. 3.8. a) I-V curve b) P-V curve of a practical SPV module

Each point on the curve gives the corresponding power and voltage expressed in watts and volts respectively. The knee of the P-V curve represents the maximum output power point. This power gives the rating of the PV panel[12]. This output power of PV module is based

on two factors i.e. PVs output voltage V_{mp} and PVs output current I_{mp} and given as $P_{mp} = V_{mp} * I_{mp}$.

This thesis work includes a solar PV array of 8kW at 1000W/m2 of solar radiation, and at 25^0C of temperature. The complete details of the rating and specifications of devices and components of the system are mentioned in appendix-I.

3.3.1.2 Effect of change in temperature and irradiation on P-V and I-V characteristics

The solar panels show nonlinear characteristic curve and are highly influenced by the intensity of solar irradiation striking its surface and ambient temperature[13-14].

A) Effect of Change in Irradiance

The output power of PV array depends on the PV output voltage and current. The I-V and P-V characteristic curves at 25^0C constant temperature and changing irradiance, are shown in the Fig. 3.9. The change in the power output of PV array is observed by varrying the irradiance from 200W/m^2 to 1000W/m^2.With the increase in the solar irradiance the output power of the PV array also increases.

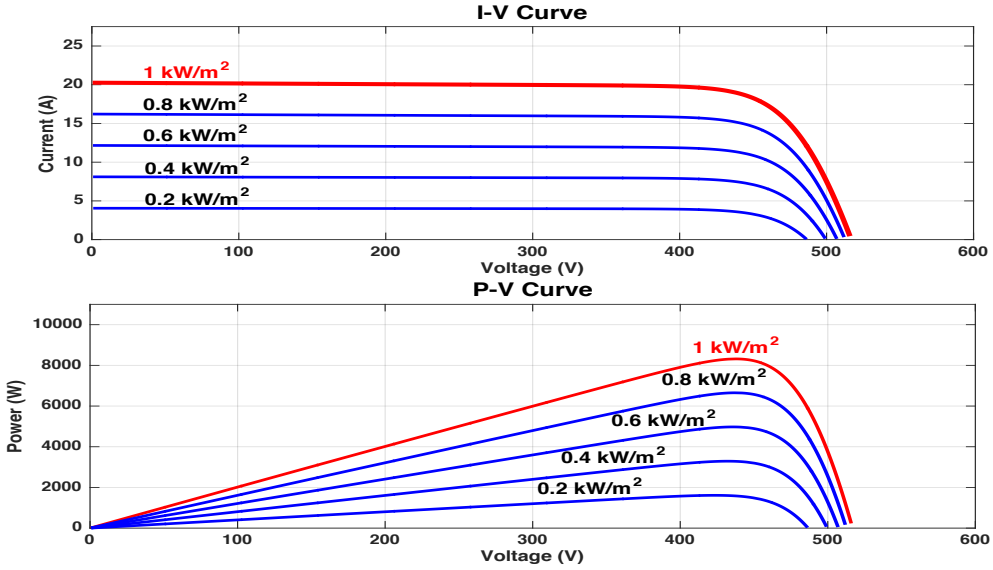

Fig 3.9. I-V and P-V Characteristic curves of the SPV array at constant temperature and changing radiation

B) Effect of Change in temperature

The I-V characteristics and P-V characteristics of PV array at a constant irradiance of 1000W/m^2 and varying temperature are shown in the Fig. 3.10. The Figure clearly states that increasing temperature from 25^{0}C to 65^{0}C causes reduction in voltage and a slight increase in current. Thus the resultant output power gets reduced.

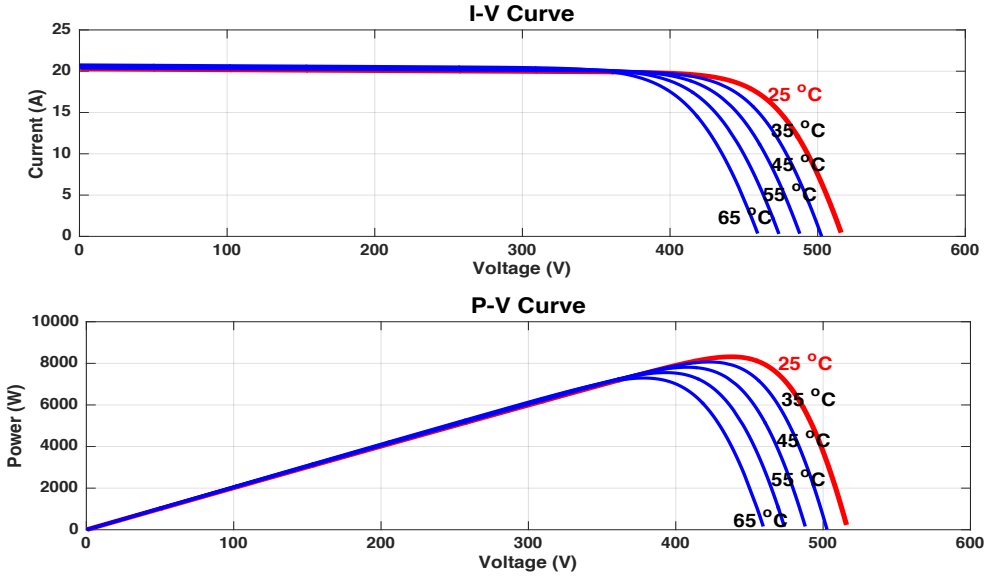

Fig. 3.10 I-V and P-V Characteristic curves of the SPV array with changing temperature and constant radiation

Finlay, observing the system by keeping one parameter constant and varrying the other it can be concluded that solar irradiance has direct relation and temperature has inverse relation with output power of PV module. This simply depicts with increase in the intensity of sun radiation, the output power rises, increase in the temperature, the power comes down.

3.3.2 DC-DC Converter

As stated earlier voltage generated by the photovoltaic module varys with the variation in the intensity of sun irradiance and temperature, but the system output need a constant voltage to process and handle the electric energy parameters in the system (i.e. the voltages, currents, frequency). This calls for a power electronic interface.Thus the power electronics converters used include DC-DC converter and DC-AC converter (Inverter). These converters are required due to the mismatch between the power supply available and the power supply required by the loads.

The DC-DC Converter is used to convert uncontrolled DC input from the PV array to controlled DC output at a desired voltage level. The converter use MPP Tracking algorithm (elaborated later) to adjust its operating point to the optimal operating voltage of the PV array.

The DC-DC converter types used in the grid connected PV system are as follows:

i. Boost converter,
ii. Buck converter ,
iii. Buck –boost converter etc.

In this work DC-DC boost converter have been used.

3.3.2.1 DC-DC Boost Converters

The PV array output voltage is boosted to a higher voltage, using a DC-DC boost converter and is also known as step-up converter. The designing of boost converter include two semiconductor switches and a storage component [15]. Fig.3.11 shows the equivalent circuit diagram of a boost converter. When the switch is closed the inductor gets charged by the available source either through PV module or battery and stores energy. In this duration diode blocks the flow of current, maintaining a constant load current which is being supplied by the discharging capacitor. When the switch is open the diode conducts and the energy stored in the inductor discharges and charges the capacitor. Hence, the load current stays constant throughout the cycle.

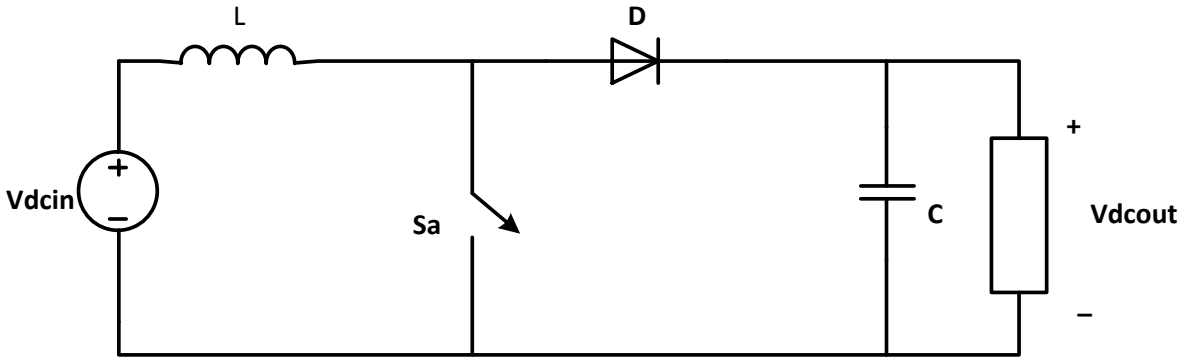

Fig 3.11 Circuit diagram of Boost converter

The Boost converter design used in the PV system include maximum power point tracking (MPPT) controller inorder to ensure the power generated by solar module is maximum and

the system is operating at or near to the MPP. A converter lacking such controllers can only regulate the output voltage of PV module, but it does not ensure that the PV system is operating at MPP, resulting into inefficient operation. Thus, it proves to be a very significant component of the system which keeps a track of the MPP in different conditions to ensure that the available maximum power is extracted from the PV array.

3.3.2.2 Design of DC-DC Boost Converter

DC-DC boost converter mainly designed to perform two main operations. One is to boost the dc voltage level to suitable level such that it can be converted into the desired ac voltage and the other is to ensure the PV panel operates at maximum power point. A boost converter provides the control of the PV panel output voltage so that the PV Panel operate at maximum output operating point and maintain the Voltage input to the Inverter. This thesis work implements DC-DC boost converter to raise the PV array voltage to 800 V maintaining the point of operation at or near MPP simultaneously.

The filtering elements of the converter include Inductor (L) and Capacitor(C) and their designing [15] is given by eqn. (3.7) and (3.8):

$$L = \frac{V_{in}D}{\Delta i_i f} \tag{3.7}$$

where, L is the value of an inductor for boost converter.

$$C = \frac{I_{OC}D}{\Delta v f} \tag{3.8}$$

Eqn. (3.9) gives the duty cycle (D) of the converter.

$$D = 1 - \frac{V_{in}}{V_{oc}} \tag{3.9}$$

where V_{in} and V_{oc} are the input and output voltages of boost converter, Δi_i is the input current ripple and can be up to 6% of input current, Δv is output voltage ripple and it can be up to 3% of the output voltage V_o and the switching frequency f is taken as 10kHz.

3.3.3 Maximum Power Point tracking (MPPT) Techniques / Controller

The output of PV module is hugely influenced by atmospheric conditions. Under different atmospheric condition, the output voltage of photovoltaic module will be different. Thus the maximum output power of solar array changes with the variations in environment. The

maximum output power of photovoltaic array is achieved only at a particular voltage value, i.e the maximum power point voltage. Thus, forcing the PV system to work at or near the maximum power point is called the maximum power point tracking (MPPT). The Maximum Power Point Tracking (MPPT) algorithms are usually implemented through power electronic circuits such as boost converter to obtain maximum power from the solar system. In recent years a number of MPPT techniques have been developed. These techniques use voltage and current output of the PV system, which are regulated by changing the duty cycle of DC-DC Boost converter in order to obtain MPP**.**

There are different algorithms [16] used to track the maximum power point (MPP). Some of the most popular algorithms are :

1) Perturb and Observe
2) Incremental Conductance method
3) Fractional short circuit current
4) Fractional open circuit voltage
5) Fuzzy logic
6) Neural networks etc.

The selection of the algorithm to be implemented in a system depends on various factors such as the time taken to track the MPP, application cost and the simplicity of execution. The Incremental and conductance is a bit complex technique while Perturb and Observe technique is very simple from application point of view. This thesis work implements both incremental and conductance algorithm and Perturb and Observe (P&O) algorithm in boost converter for tracking maximum power point(MPP) and their MPP tracking is compared.

3.3.3.1 Perturb and Observe Algorithm

P&O maximum power tracking technique require two sensors one to sense the voltage and the other to sense current of PV module. The sensed values are fed to the MPPT controller to track the maximum power point and accordingly generates control signal for DC-DC boost converter. The output signal generated on comparision of this control signal with a high frequency (10 kHz) saw-tooth waveform, regulates the duty cycle of a DC-DC boost converter to track the MPP of the specific system.

The P&O algorithm works on the principle of introducing perturbation to the operating point of the system to achieve maximum power output[17-19]. The algorithm keeps a track of instentaneous values of PV current and voltage and its power calculation and pushes the working point to reach the MPP. The PV module output power is perturbed by small steps until the maximum power point is reached. If a system is considered to have P_1 (power output) calculated by measuring the initial values of voltage and current $V_1$and I_1 respectively and the perturbation added be C. Then P_2 is calculated by measuring the new instentaneous values V_2 and I_2. If the P_2 reads positive i.e increment in power, the system will keep on perturbing in the same direction. The moment P_2 reads negative i.e decreament in power, the controller will bring the operating point back to MPP by adding a negative increment. When the maximum power point is achieved, the system operating point will oscillate constantly around that point. Thus controller continuously tracks this operating point and regulates the voltage of the solar module to perform at MPP.

The algorithm for P &O MPPT is shown in Fig. 3.12. The algorithm indicates that the sensed values of voltage and current are taken as input to the controller and change in the duty cycle is the output. A small perturbation (0.01) is induced in the system. This perturbation reflects a change in power of the PV array. If the change followed by the perturbation is positive i.e power increases, then the perturbation is continued (Duty cycle + c) in the same direction.Just after the MPP, the power starts decreasing and so the perturbation reverses (Duty cycle − c) at that instant.

The main drawback of the P&O algorithm is, it doesn't produce a stable response with rapid changes in irradiance.

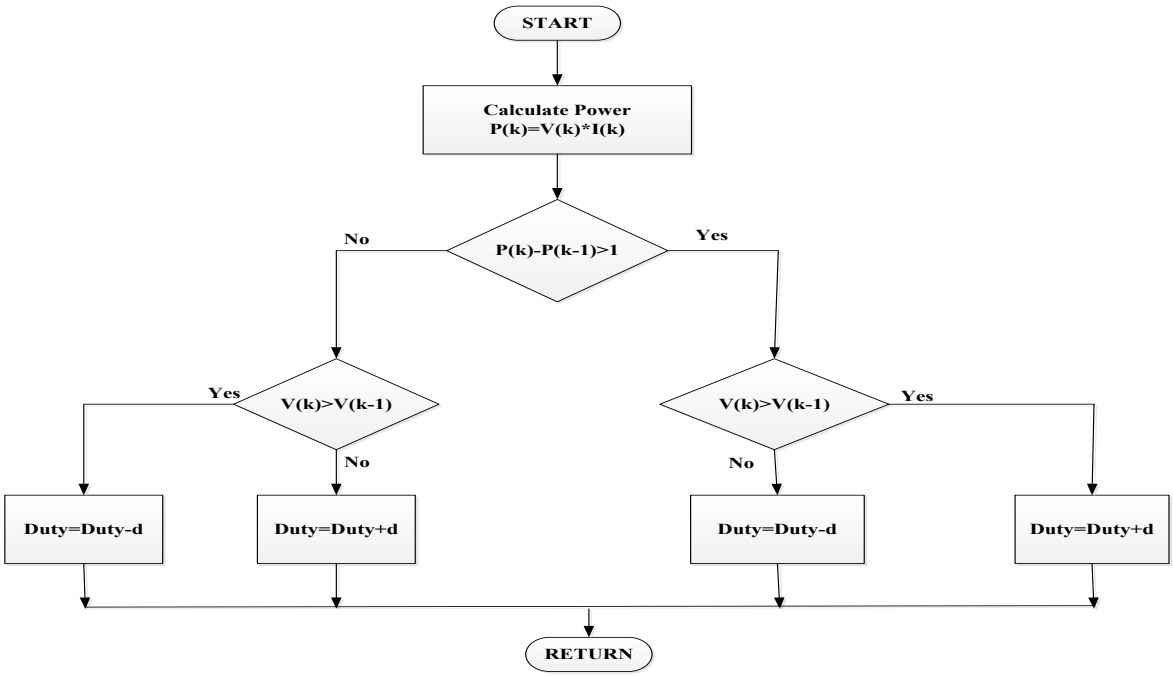

Fig 3.12 P &O Algorithm for MPPT

3.3.3.2 Incremental Conductance algorithm

Maximum Power Point Tracking algorithms are used to operate PV arrays such that they can produce all the power they are capable of producing. The incremental conductance algorithm is based on the fact that the slope of the power versus voltage curve is zero at maximum power point. This algorithm involves two sensors to sense the output voltage and current of the PV module. In this method the terminal voltage of the array is varied according to the MPP voltage with the variation in incremental and instantaneous conductance of the PV module [20-21]. The slope of the P-V curve of the array is zero at the MPP, positive on the left of the MPP and negative on the right of the MPP as shown in Fig. 3.13.

This algorithm follows some basic relational equations given as follows,

$$\frac{dI}{dV} = -\frac{I}{V} \quad \text{At MPP}$$

$$\frac{dI}{dV} > -\frac{I}{V} \quad \text{Left of MPP}$$

$$\frac{dI}{dV} < -\frac{I}{V} \quad \text{Right of MPP} \qquad (3.10)$$

where I and V represents output current and voltage of the PV array respectively.The left side of each equation mentioned above presents incremental conductance of the PV array while the right side presents the instentaneous conductance.Maximum power point is achieved when the variation in the output conductance is equal the negative of the instentaneous conductance[22-23].

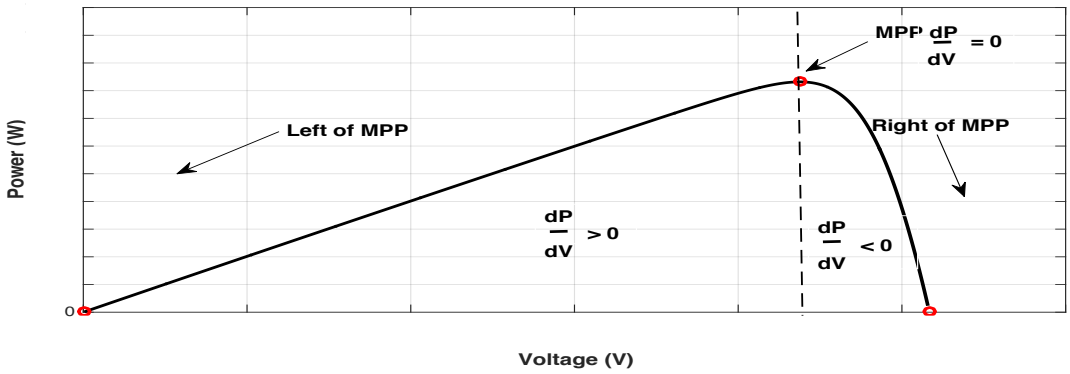

Fig 3.13 Basic idea of Incremental and Conductance method

The incremental conductance algorithm for MPPT is shown in Fig. 3.14. The algorithm indicates that the sensed values of voltage and current are taken as input to the controller and change in the duty cycle is the output.

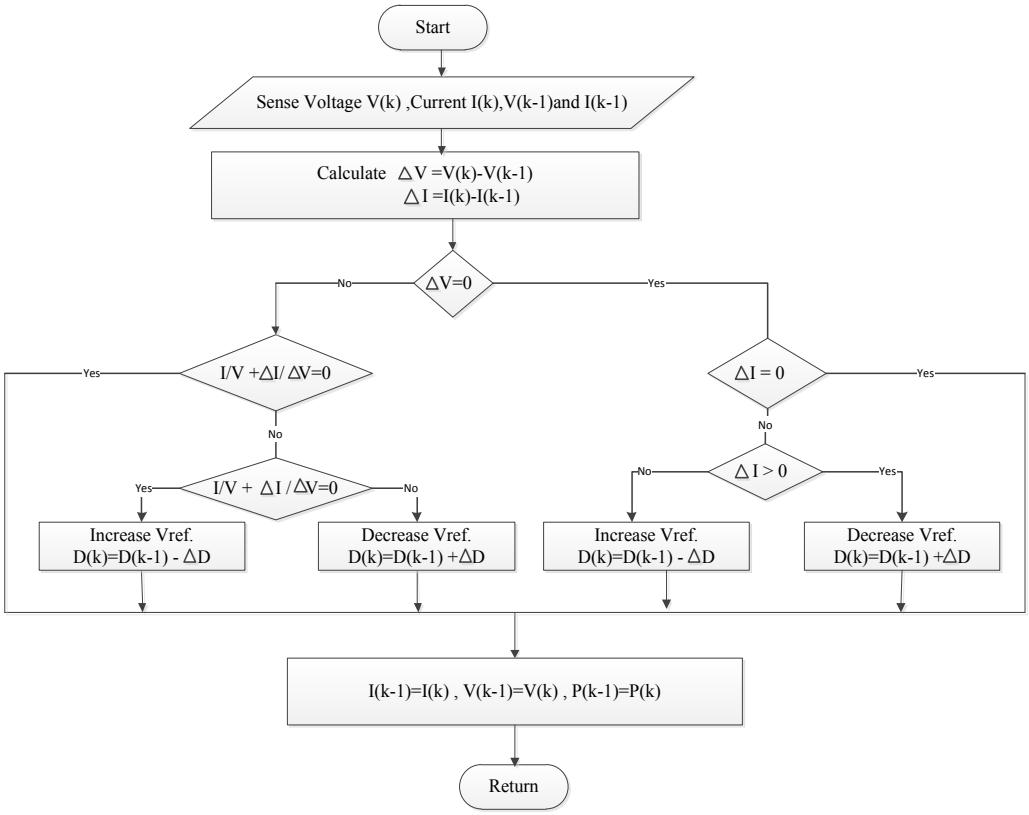

Fig 3.14 Incremental and Conductance Algorithm for MPPT

3.3.4 Photovoltaic Inverter

The DC to AC inverter is one of the important elements in grid-connected PV power generating systems. Three-phase inverter used in the system converts PV array's DC voltage output to three-phase AC voltage In order to integrate PV system to the 3-Phase grid a DC-DC Boost converter and a PV inverter are required. The PV inverter used is basically a voltage source converter (VSI) to convert the dc voltage output of the boost converter to 3-phase ac voltage of desired magnitude and frequency. VSI finds high application in distribution generation (DG) systems due its compactness, good efficiency and control of power flow. VSI [24]are mainly classified into two categories: Voltage controlled Voltage Source Inverter (VCVSI) and Current controlled Voltage source Inverter (CCVSI).

In VCVSI the filter parameter i.e Decoupling Inductor plays very important role in the power flow of system therefore its size must be cosidered very carefully. For example in weak grid where the voltage drops considerably, there the inverter has to supply both the

active and the reactive power by increasing the size of the inductor. Moreover, correction of power factor is not possible in VCVSI [25] .However the unity power factor can be maintained using CCVSI. So, the CCVSI has been opted for the present work. The PV inverter is shown in Fig 3.13.

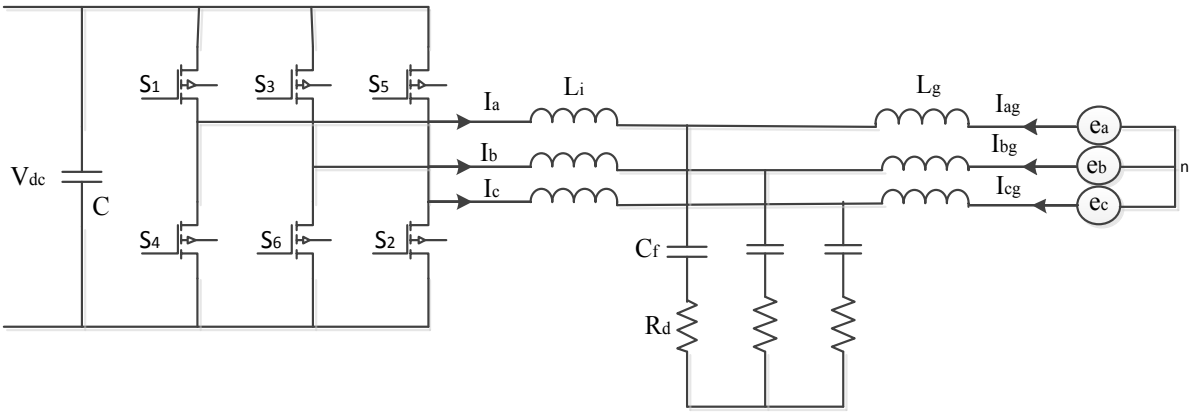

Fig 3.13 LCL connecting Voltage Source Inverter and Grid

The switches used in inverter are IGBTs with anti parallel diodes to provide load balancing and compensates for the reactive power and harmonics of the loads. IGBT give very low switching loss and on-state voltage drop, improving the efficiency of the system. Its controlling is simple even in systems with high voltage and high current. These switches are turned on and off through a gate driver circuit.

The VSI consists of capacitors to filter the DC link voltage. The PV inverter or VSI behaves like an active shunt compensator and imparts both reactive power and harmonics compensation with load balancing.

3.3.4.1 Design of VSI

PV inverter used in the system a 3-phase VSI, having six IGBTs with anti-parallel diodes forming a bridge structure [26]. The voltage and current ratings of IGBTs used are 2500kV and 1500A respectively. The computation of DC link voltage to be preserved across the VSI and interfacing inductor calculations are as follows:

i. DC link Voltage

The magnitude of DC bus voltage depends on the instantaneous power received by the PV inverter and it must be greater than voltage magnitude at point of common coupling. For a three phase VSC with a DC link capacitor, the DC bus voltage is given by eqn. (3.9).

$$v_{DC} = (2\sqrt{2}v_l)/\sqrt{3}m \quad (3.9)$$

Where, m is the modulation index and taken as 0.9, and $v_l$is AC terminal voltage of VSI and is equal to 415 V (RMS line to line). The selected magnitude of dc bus voltage is 800V in this thesis work.

ii. Coupling Inductor (L_f)

The VSI interfacing inductance L_f depends upon the current ripple Δi_r, DC bus voltage $v_{DC}$and switching frequency $f_s = 10kHz$, therefore its calculation is given by eqn. (3.10),

$$L_f = \frac{\sqrt{3}\, m\, v_{DC}}{12hfs\Delta i} \quad (3.10)$$

Where, Δi_r=5% of phase current, h =1.2 is overload factor and m = 0.9 is modulation index. The calculated value of L_f is 6.34mH and is taken to be 7mH in this work.

The inductor (L_f) is a filtering element which will bound the amount of circulating current in the circuit.

3.3.4.2 Design of LCL Filter

To increase the power density of PV inverter, LCL-type filters are preferred over L- or LC-type filters at the inverter output. With the increase in the converter power rating, the size and cost of the power converters reduces by employing *LCL*-filters compared to the other filters [27-28]. However the main limitation of the LCL-type filters is their implicit resonance frequency, which produces problems in stability and therefore specific control techniques are required.

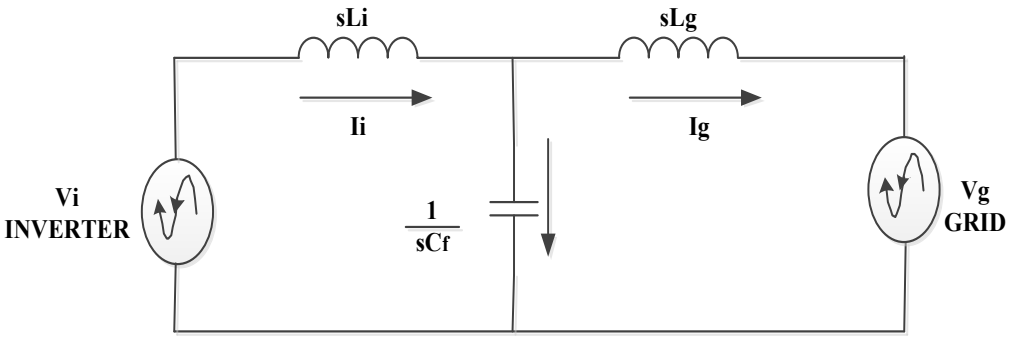

Fig 3.14 LCL Filter inserted between inverter end and grid.

The filter design involves following parameters:

V_{ph}- inverter phase output voltage, P_n-rated power, V_{dc}-dc bus voltage, k is the attenuation factor and f_s-switching frequency.

The base values of impedance and capacitance are given by equations (3.11) and (3.12) respectively [29]. Thus, the filter values are obtained with reference to the base values:

$$Z_b = \frac{{E_n}^2}{P_n} \tag{3.11}$$

$$C_b = \frac{1}{\omega_g Z_b} \tag{3.12}$$

The filtering elements include two inductors one on the inverter side (L_{inv}) and other towards the grid (L_g) and a Capacitor (C_f) and their designing is given by equations (3.13), (3.15) and (3.16) respectively.

$$L_{inv} = \frac{V_{dc}}{16.\Delta L_{max} f_s} \tag{3.13}$$

The maximum current ripple at the inverter output is given by (3.14)

$$\Delta I_{Lmax} = 0.1 \times \frac{P_n \sqrt{2}}{3.V_{ph}} \tag{3.14}$$

$$L_g = \frac{\sqrt{\frac{1}{k^2}+1}}{C_f {\omega_{sw}}^2} \tag{3.15}$$

For designing filter capacitance, the maximum power factor variation seen by the grid is considered to be 5%; consequently the capacitance of the system is as follows

$$C_f = 0.05 C_b \tag{3.16}$$

where C_b is the base capacitance value.

Conclusion

The modeling of photovoltaic array and its basic I-V and P-V characteristics have been introduced. The study of these characteristics show that output of a PV system changes with change in the environmental conditions. The mathematical model of DC-DC boost converter and PV inverter are also presented followed by description of two MPPT algorithms namely Perturb and Observe and Incremental and Conductance.

CHAPTER 4

PV INVERTER CONTROL TECHNIQUES

4.1 General

The increased use of power electronic based components and non-linear loads in the power system results in the generation of harmonic currents followed by poor power-quality in the system[30]. The system presented, is a grid interfaced PV system employing a three-phase VSI to connect PV system to three-phase distribution grid. The inverter used also compensates for power quality issues. Based on different processing techniques and the sensed parameters there are several inverter control algorithms. This chapter presents three different control algorithms for the grid connected inverter to compensate power quality issues.

4.2 PV inverter Control Techniques

The main objective of these control schemes is to withdraw fundamental component of the current from the sensed parameters according to the system requirement. Some conventional control algorithms studied here are as follows:

(i) Synchronous Reference Frame (SRF) Theory

(ii) Instantaneous Symmetrical Component Theory(ISCT)

(iii) Icosineφ control algorithm

The mathematical description of each control algorithm is given in the following section.

4.2.1 Synchronous Reference Frame theory (SRFT)

The synchronous reference frame theory (SRFT) is also reffered as d-q theory. This technique is build on time-domain evaluation of reference signal. It can operate either for steady-state or transient state ,as well as for general voltage and current waveforms. It allows controlling the active power filters. Another significant characteristic of this theory is the ease of calculation, which includes simple algebraic calculation. The SRF controller

structure basically consists of direct (d-q-0) and inverse $(d\text{-}q\text{-}0)^{-1}$ park transformations[31]. The block diagram of control technique based on SRF theory is shown in Fig.4.1.

The SRFT is an indirect control approach used for the evaluation of reference AC currents, which are further used to generate gate pulses for controlling PV inverter. In this method, Load current, PCC voltage and dc bus voltage values are sensed and are taken as the feedback signal. The SRF theory involves the extraction of synchronously rotating d-q components. The sensed load currents are converted from the 3-φ currents (i_{Labc}) to (d-q-0) frame using Park's transformation[32-34]. The voltages on grid side are given in eqn. (4.1) to eqn. (4.3)

$$v_{sa} = V_m \sin(\omega t) \tag{4.1}$$

$$v_{sb} = V_m \sin(\omega t - {}^{2\pi}/_{3}) \tag{4.2}$$

$$v_{sc} = V_m \sin(\omega t + {}^{2\pi}/_{3}) \tag{4.3}$$

The fundamental component of load current are given in eqn. (4.4) to eqn. (4.6):

$$i_{La} = I_m \sin(\omega t - \theta_n) \tag{4.4}$$

$$i_{Lb} = I_m \sin(\omega t - {}^{2\pi}/_{3} - \theta_n) \tag{4.5}$$

$$i_{Lc} = I_m \sin(\omega t - {}^{2\pi}/_{3} - \theta_n) \tag{4.6}$$

SRF procures the fundamental component of load currents by transforming load current signals from abc frame to d-q reference frame using park's transformation given by eqn. (4.7)

$$\begin{bmatrix} i_{Ld} \\ i_{Lq} \\ i_{L0} \end{bmatrix} = \frac{2}{3} \begin{bmatrix} \cos\omega t & \cos(\omega t - {}^{2\pi}/_{3}) & \cos(\omega t + {}^{2\pi}/_{3}) \\ \sin\omega t & \sin(\omega t - {}^{2\pi}/_{3}) & \sin(\omega t + {}^{2\pi}/_{3}) \\ 1/2 & 1/2 & 1/2 \end{bmatrix} * \begin{bmatrix} i_{La} \\ i_{Lb} \\ i_{Lc} \end{bmatrix} \tag{4.7}$$

The d-axis and q- axis currents consist of both fundamental and harmonic components given by eqn. (4.8) and eqn. (4.9):

$$i_d = i_{dDC} + i_{dAC} \tag{4.8}$$

$$i_q = i_{qDC} + i_{qAC} \tag{4.9}$$

The harmonics term includes the entire harmonics component having ac characteristics. While the dc component gives the fundamental term. These currents are passed through low pass filter (LPF) to acquire only the dc components and separate out the harmonics from reference signal. Thereafter, the reference signals contain only the dc quantities.

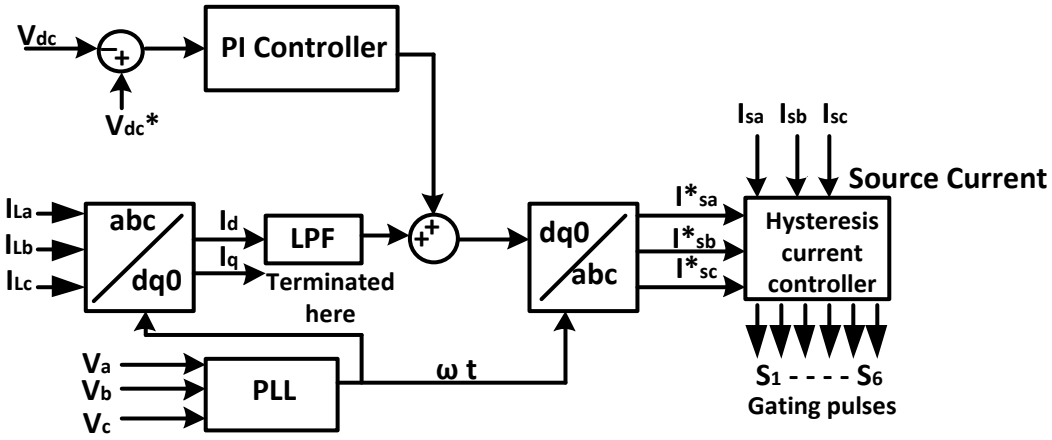

Fig. 4.1 SRF theory to extract reference current

When the grid interfaced system is operating in power factor(PFC) correction mode to obtain unity power factor, the control algorithm considers the grid should provide direct axis component of load current and active power component of current which are essential components for the regulation of the DC bus voltage to a desired constant value and to feed inverter losses (i_{loss}). The PI controller is used to regulate the dc bus voltage to desired reference value and gives the active power transfer to compensate inverter losses.

Thus active power requirement of load and the power required to maintain DC voltage at inverter DC terminals to a constant value has to be accomplished by the grid and hence these powers are added. To maintain DC bus voltage constant, the sensed DC voltage is compared with the reference signal and the error generated is fed into a PI controller, thus producing an output current (i_{loss}) proportional to the loss in DC voltage. Therefore i_W is the current required to compensate the losses and is given by eqn.(4.10)

$$i_{loss}(n) = i_{loss}(n-1) + K_p\big(V_{dce}(n) - V_{dce}(n-1)\big) + K_i * V_{dce}(n) \quad (4.10)$$

where, K_p and K_i represents the proportional and integral gain of PI controller and $V_{dce}(n)$ is error between the measured DC terminal voltage and the reference DC voltage signal of 800V given by eqn. (4.11),

$$V_{dce}(n) = V_{dc}^{*}(n) - V_{dc}(n) \tag{4.11}$$

The active ac reference grid current i_{active}^{*} can be given by eqn. (4.12),

$$i_{active}^{*} = i_{dc} + i_{loss} \tag{4.12}$$

The active power component of reference AC currents must be in phase with the PCC voltage. Therefore a 3-φ PLL is applied to synchronize these reference signals with the PCC voltage. The park's transformation angle ωt gives the synchronous angular position obtained by the PLL action. Then reverse Park's transformation is applied on the resultant the *d-q-0* reference frame currents ($i_d^{*} = i_{active}^{*},\ i_q^{*} = 0, i_0^{*}$) and reference source current ($\mathrm{i_{sa,}^{*}i_{sb,}^{*}i_{sc,}^{*}}$) in *a-b-c* frame are obtained given by eqn. (4.13)

$$\begin{bmatrix} i_{sa}^{*} \\ i_{sb}^{*} \\ i_{sc}^{*} \end{bmatrix} = \begin{bmatrix} \cos\omega t & \sin\omega t & 1 \\ \cos\left(\omega t - {}^{2\pi}/_{3}\right) & \sin\left(\omega t - {}^{2\pi}/_{3}\right) & 1 \\ \cos\left(\omega t + {}^{2\pi}/_{3}\right) & \sin\left(\omega t + {}^{2\pi}/_{3}\right) & 1 \end{bmatrix} * \begin{bmatrix} i_d^{*} \\ i_q^{*} \\ i_0^{*} \end{bmatrix} \tag{4.13}$$

These reference source currents generated on applying reverse Park's transformation calculated from eqn. (4.13) are further fed to hysteresis current controller (HCC) along with sensed source currents, to obtain switching signal for PV inverter. The hysteresis band current controller is used to maintain the source currents ($\mathrm{i_{sa}, i_{sb}, i_{sc}}$) close to three phase reference currents ($\mathrm{i_{sa,}^{*}i_{sb,}^{*}i_{sc,}^{*}}$).

4.2.1.1 Phase Locked Loop

A phase locked loop (PLL) is a system which synchronizes its output signal with a given input signal or reference signal both in frequency and in phase. It is a non-linear closed loop control system which can change the frequency of a controlled oscillator automatically according to the frequency and phase of the input signal to have an output having similar frequency and phase as that of the input or reference signal.

The synchronous Reference Frame PLL (SRF PLL) is used for synronizing the phase angle of 3-phase signals .Their performance is quite similar to a linear PLL .The only difference between the two is SRF PLL includes a Phase Detector (PD) block in its circuit. It involves Park's Transformation of a 3-phase signal in phase detection. The block diagram of the Three-phase Phase locked loop is shown in Fig 4.2. This PLL is used in controlling the PV inverter. PLL produces phase angle $\omega t, which$ ranges from 0 to 2π, and synchronized to zero crossing of the phase 'a' fundamental component [35-37].

.

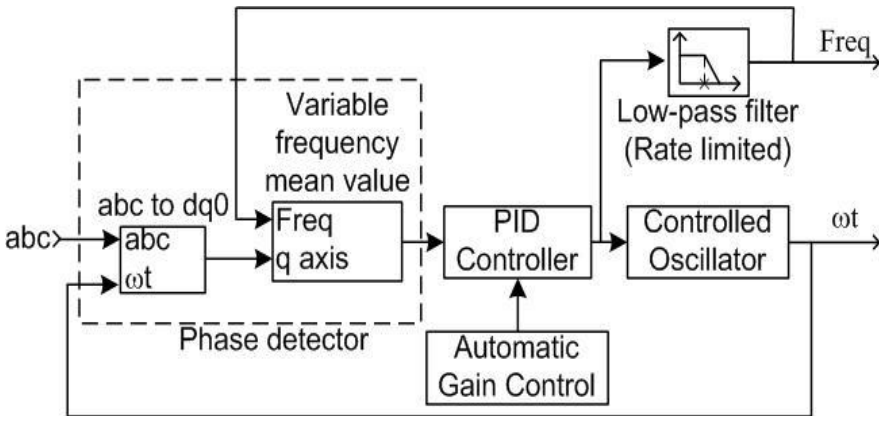

Fig 4.2 Block Diagram of 3-φ PLL

An internal oscillator provides the angular speed required for converting the three-phase input signal of PLL to the d-q-0 rotating frame. Then q-axis signal obtained after the transformation, which is proportional to the phase difference between the input *a-b-c* signal and the internal oscillator-rotating frame, is filtered through a mean variable frequency block. The filtered output is fed to a PID controller having an optional automatic gain control (AGC) to maintain the phase difference to 0 by controlling the controlled oscillator. The PID output, corresponding to the angular velocity, is filtered and converted to frequency in Hz and the controlled oscillator output is the angle (ωt) varying between 0 & 2π rad.

4.2.1.2 Hysteresis Current Controller (HCC)

The switching signals for the inverter are produced using synchronized pulse width modulation (PWM) method or hysteresis current control method[38]. Hysteresis current controller is used because of its Due to its fast response with peak current limiting capability and ease of execution hysteresis current controller is preferred. Besides hysteresis current control scheme offers the drawback of having wide switching frequency variation, which may be excessively high, and can result in rise of converter switching losses caused due to increased number of switching per cycle. This method is simplest from implementation point of view, requiring just the value of error traced, which is basically the difference between of the grid side current (i_{sa}, i_{sb}, i_{sc}) and the current references ($i_{sa}^*, i_{sb}^*, i_{sc}^*$).

This method involves the switching of actual source currents in an asynchronous procedure of ramping the actual current up and down such that it follows the reference current. When the source current is exceeds the upper limit of the hysteresis, it turns on a negative voltage switching function and causes the source current to decrease. And if the current reaches the lower limit of the hysteresis, then it turns on a positive voltage switching function to increase the source current. The hysteresis band limit considered in this analysis is 0.2. The actual current waveform tracking using a hysteresis current controller is shown in Fig. 4.3

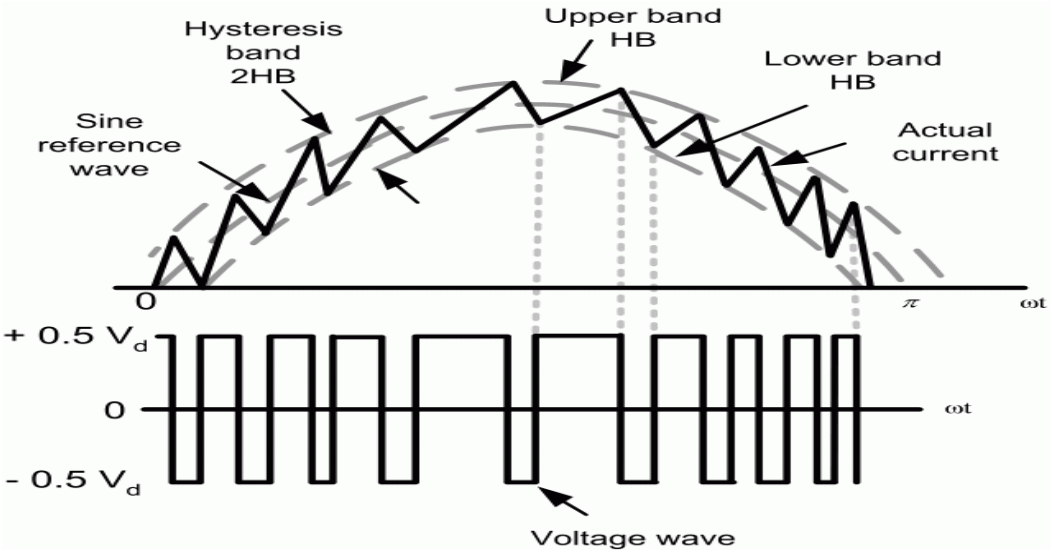

Fig. 4.3 Hysteresis current control technique.

The internal structure of hysteresis current controller is shown in Fig 4.4. At the output of HCC six gating pulses are generated which are fed to the six IGBT switches of VSC. In VSC each phase is having two switches, therefore the output of HCC also contains two pulses for each phase.

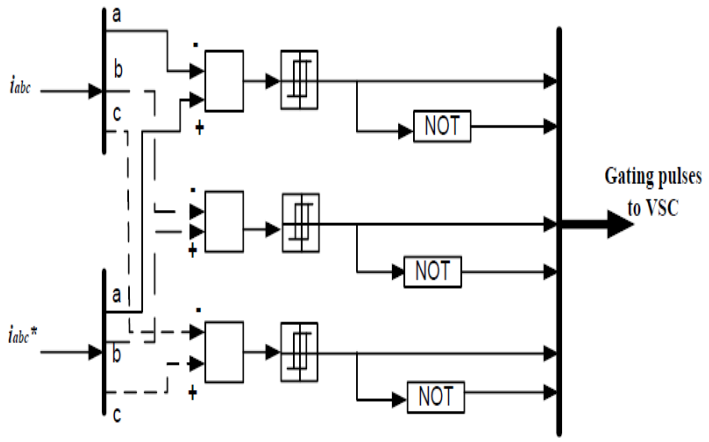

Fig 4.4 Schematic Diagram of Hysteresis Current Controller

4.2.2 Instantaneous Symmetrical Component Theory (ISCT)

The instantaneous symmetrical components theory is mainly used reduce harmonic components and improve power factor [39-43] etc. The inverter control algorithm based on instantaneous symmetrical component theory can compensate almost any kind of unbalance and harmonics in the load. For a set of three-phase currents or voltages, the instantaneous symmetrical components are given by eqn. (4.14) and eqn. (4.15),

$$\begin{bmatrix} i_{a_0} \\ i_{a_1} \\ i_{a_2} \end{bmatrix} = \frac{1}{\sqrt{3}} \begin{bmatrix} 1 & 1 & 1 \\ 1 & \alpha & \alpha^2 \\ 1 & \alpha^2 & \alpha \end{bmatrix} \begin{bmatrix} i_a \\ i_b \\ i_c \end{bmatrix} \tag{4.14}$$

Similarly three-phase instantaneous voltages are given by

$$\begin{bmatrix} v_{a_0} \\ v_{a_1} \\ v_{a_2} \end{bmatrix} = \frac{1}{\sqrt{3}} \begin{bmatrix} 1 & 1 & 1 \\ 1 & \alpha & \alpha^2 \\ 1 & \alpha^2 & \alpha \end{bmatrix} \begin{bmatrix} v_{sa} \\ v_{sb} \\ v_{sc} \end{bmatrix} \tag{4.15}$$

where, α is a complex operator and is mathematically stated as $\alpha = e^{\frac{j2\pi}{3}}$,$\alpha^2 = e^{\frac{j4\pi}{3}}$. The instantaneous components of currents, $i_{a_1}$and $i_{a_2}$are complex time varying quantities and are complex conjugate of each other. This same is follows for the quantities $v_{a_1}$and v_{a_2}.The terms $i_{a_0}$and $v_{a0}$are real quantities.These instantaneous symmetrical components are used to develop mathematical model for load compensation etc.

Thus the PV inverter use instantaneous symmetrical component theory control algorithm provides the reference current evaluation, balancing of load, harmonics suppression and power factor correction. The schematic diagram for the ISCT inverter control algorithm is

shown in the Fig.4.5.The reference source current are extracted using PCC voltage (v_{sa}, v_{sb}, v_{sc}), source currents (i_a, i_b, i_c), load currents (i_{la}, i_{lb}, i_{lc}) and DC link voltage (v_{dc}) of the grid interfaced PV system. Initially the control algorithm of inverter involves the computation of instantaneous positive sequence values of load side currents and utility grid side voltages on application of instantaneous symmetrical component theory.

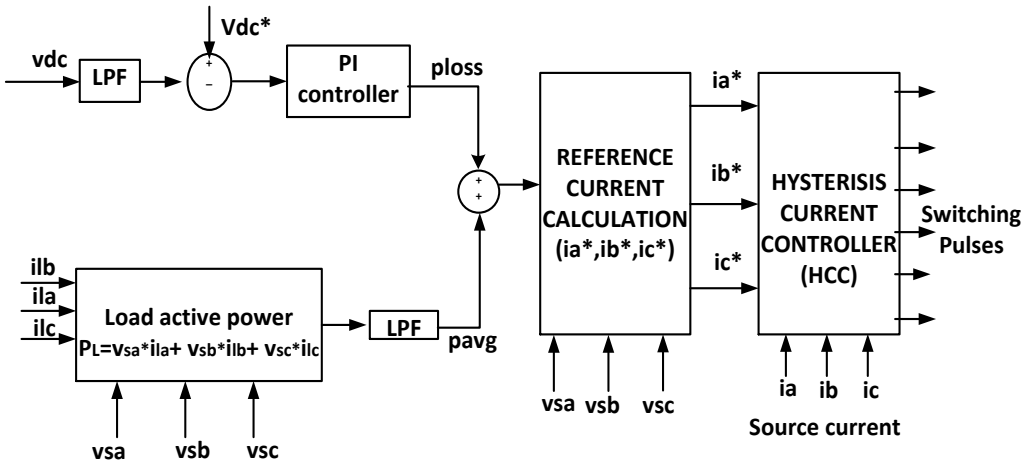

Fig. 4.5. Block Diagram of ISCT for Reference Source Current Extraction.

The main motive of the control algorithm is to produce balanced supply current. So, the current on the source side is given by eqn. (4.16):

$$i_a + i_b + i_c = 0 \tag{4.16}$$

Positive sequence values of voltage and current are required to achieve the balanced source current. On application of symmetrical component theory, positive sequence component can be derived using the eqn. (4.17) and also from the point of view of source power factor, we have

$$\angle v_{a1} = \angle i_{a1} + \phi \tag{4.17}$$

$$\angle\{v_{sa} + \alpha v_{sb} + \alpha^2 v_{sc}\} = \angle\{i_a + \alpha i_b + \alpha^2 i_c\} + \phi \tag{4.18}$$

Where v_{a1} and i_{a1} are positive sequence values and $\emptyset$ is the phase shift between supply voltage and current. Under the condition of balanced supply voltage, the eqn. mentioned above can be rewritten using the eqn. (4.19):

$$\tan^{-1}\left(\frac{k_1}{k_2}\right) = \tan^{-1}\left(\frac{k_3}{k_4}\right) + \phi \tag{4.19}$$

where,

$$k_1 = \sqrt{3/2}\,(v_{sb} - v_{sc}) \;,\; k_2 = \frac{3}{2}(v_{sb})$$

$$k_3 = \sqrt{3/2}\,(i_b - i_c) \,,\; k_4 = \left(i_a - i_{\frac{b}{2}} - i_{\frac{c}{2}}\right) \tag{4.20}$$

$$\gamma = \tan\phi/\sqrt{3} \tag{4.21}$$

On solving the eqn. (4.17)- (4.20) gives resultant in eqn. (4.22):

$$(v_{sb} - v_{sc} - \gamma v_{sa})i_a + (v_{sc} - v_{sa} - \gamma v_{sb})i_b + (v_{sa} - v_{sb} - \gamma v_{sc})i_c = 0 \tag{4.22}$$

If $\gamma = 0$, source current (i_a, i_b, i_c) are in phase with voltages(v_{sa}, v_{sb}, v_{sc}) which indicates the inverter will supply the reactive power demand of the load. If $\gamma \neq 0$ i.e. in the cases other than zero, the source may supplies or absorbs the reactive power.

The active power demand of the load is supplied by the source in power factor correction mode. Thus average power demand is given by eqn. (4.23)

$$P_{avg.} = v_{sa}i_a + v_{sb}i_b + v_{sc}i_c \tag{4.23}$$

where $P_{avg.}$ is average active power which is acquired after removing the harmonics on passing through LPF filter. The active power of the load can be computed using eqn. (4.24):

$$P_l = v_{sa}i_{la} + v_{sb}i_{lb} + v_{sc}i_{lc} \tag{4.24}$$

The PI (proportional integral) controller is used to maintain the DC link voltage, given by eqn. (4.25):

$$P_{loss} = K_{pd}V_{dcei} + K_{id}\int V_{dce}\,dt \tag{4.25}$$

where $V_{dce} = v_{dc}^{*} - v_{dc}$= error. v_{dc}^{*} is the sensed voltage of DC bus and v_{dc} is the reference voltage of DC bus. K_{pd} and K_{id} are the proportional and integral gain of the PI controller of the inverter control algorithm over the DC link voltage.

The PI controller limits the losses occurring due to switching. Hence it provides $P_{loss}, which$ compensates the switching losses in the converter. Therefore, the net power given by eqn. (4.26):

$$P_{avg.} + P_{loss} = v_{sa}i_a + v_{sb}i_b + v_{sc}i_C \tag{4.26}$$

On solving eqn. (4.16), (4.21) and (4.25), the reference currents are achieved using eqn. (4.27):

$$i_a^{*} = [v_{sa} + (v_{sb} - v_{SC})\gamma](P_{avg.} + P_{loss})/A$$

$$i_b^{*} = [v_{sb} + (v_{sc} - v_{sa})/\gamma](P_{avg.} + P_{loss})/A$$

$$i_c^{*} = [v_{sc} + (v_{sa} - v_{sb})/\gamma](P_{avg.} + P_{loss})/A \tag{4.27}$$

where $A = \sum(v_{sa}^2 + v_{sb}^2 + v_{sc}^2)$ and $\gamma = 0$ for the grid interfaced PV system in PFC mode.

Hence the obtained reference currents are compared with actual source currents(i_a, i_b, i_c) using hysteresis current controller (HCC) which further provides six pulse output required for the switching of PV Inverter.

4.2.3 Icosϕ Control Algorithm:

The 'Icosϕ' algorithm is applied to obtain the fundamental component of the active part of the load current. In each phase a LPF and sample & hold circuit is used to tune to fundamental frequency.Thus the desired amplitude of the mains current in each phase is obtained. These three-phase voltages are act as templates to obatain unit amplitude sine waves which in same phase as the mains voltages. Then the product of the two quantities is obtained i.e. of the amplitude Icosϕ and the unit sine wave for each phase to get the desired currents[45-47].

The 3-ϕ inverter involves a self-sustaining DC bus capacitor which can itself produce the required reactive power and harmonic compensation. The voltage fluctuations in this

capacitor are used to estimate the extra power loss due to switching in the inverter. The current amplitude corresponding to this loss is calculated and added to the active component (Icosϕ) of the fundamental load current in each phase.

This inverter control algorithm generates reference currents for the 3-ϕ PV inverter depending on the real part of the load current. Thus the current obtained from the supply mains have no reactive component and is purely sinusoidal i.e. unity power factor is achieved with no reactive component. Thus this control algorithm gives good harmonic compensation, simulateously maintaining unity power factor at the source side.

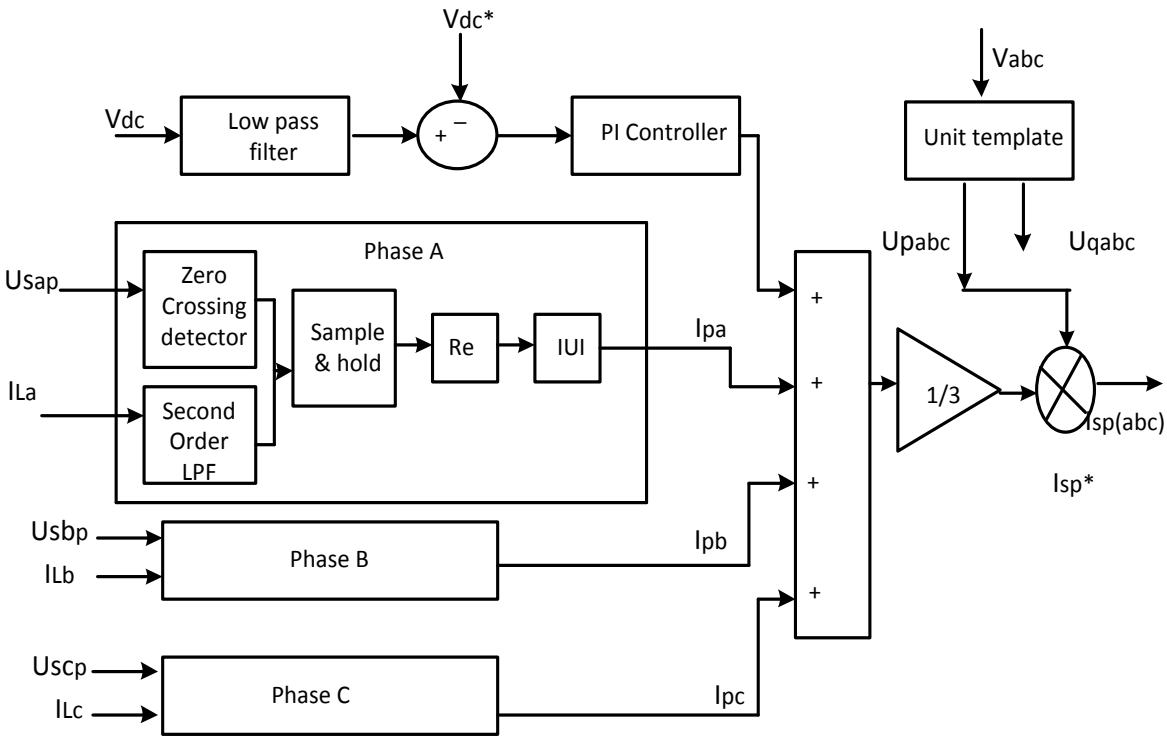

Fig 4.6 Block diagram of Icosø for extracting reference source currents.

The 'Icosø' based inverter control algorithm is shown in Fig.4.6. The implementation of the algorithm involves measurement of the sensed values of the PCC voltage (v_a, v_b, v_c), the source currents(i_a, i_b, i_c),the load currents(i_{La}, i_{Lb}, i_{Lc}), and the DC link voltage $(V_{dc})$of the inverter. The reference source currents are finally obtained by the product of Icosϕ and Isinϕ component of load currents with unit templates[48-50] .

Let, the load current can be given by eqn.(4.28)

$$i_{La} = \sum_{k=1}^{k=\infty} I_{Lak} \sin(k\omega t - \phi_{ak})$$

$$i_{Lb} = \sum_{k=1}^{k=\infty} I_{Lbk} \sin(k\omega t - \phi_{bk} - 120^0)$$

$$i_{Lc} = \sum_{k=1}^{k=\infty} I_{Lck} \sin(k\omega t - \phi_{ck} - 240^0) \quad (4.28)$$

where $\phi_{(abc)1}$ and $\phi_{(abc)k}$ are phase angles of fundamental and k[th] harmonic current in a,b and c phases, $I_{L(abc)1}$ and $I_{L(abc)k}$ are amplitude of fundamental and k[th] harmonic current in a,b, and c phases.

The magnitude of fundamental load currents' active component is given by eqn. (4.29):

$$|Re(I_{La1})| = |I_{La}| cos\phi_a$$

$$|Re(I_{Lb1})| = |I_{Lb}| cos\phi_b$$

$$|Re(I_{Lc1})| = |I_{Lc}| cos\phi_c \quad (4.29)$$

The amplitude of fundamental load current's active component (Icos∅) is obtained at the zero crossing of the unit template which is in phase with PCC voltage. A set of low pass filters is used for shifting the load currents by +90°. The filters with cut-off frequency of 50Hz are used to extract the fundamental component of load current. A zero crossing detector and a sample and hold network are implemented to extract reference currents in the (Icos∅) algorithm.

When source currents are in balanced condition, the magnitude of reference source currents' active component is given by eqn. (4.30):

$$I_{sp}^{*} = (|I_{la}| cos\emptyset_a + |I_{lb}| cos\emptyset_b + |I_{lc}| cos\emptyset_c + I_d)/3 \quad (4.30)$$

where, $|I_{la}| cos\emptyset_a$, $|I_{lb}| cos\emptyset_b$ and $|I_{lc}| cos\emptyset_c$ are the magnitude of the load active currents and I_d is the output of the DC link voltage PI controller for the self supporting bus of the inverter which can be expressed as:

$$P_{loss} = K_{pdc} V_{dcei} + K_{idc} \int V_{\mathrm{dcei}}\, dt \quad (4.31)$$

where $V_{\mathrm{dcei}} = v_{\mathrm{dc}} * - v_{\mathrm{dc}}$ is the error in DC link voltage, $v_{\mathrm{dc}} *$ = reference DC link voltage of inverter and v_{dc} = actual DC link voltage of inverter respectively. K_{pdc} and K_{idc} are the proportional and integral gains of the PI controller over the DC link voltage of inverter given by eqn. (4.31).

Likewise the amplitude of fundamental load currents' reactive component(Isin∅) can be also obtained at the zero crossing of the unit template in quadrature of PCC voltage from the filtered fundamental load currents. Thus the magnitude of reactive component of the reference source currents can be given as.

$$I_{sp}^{*} = \frac{(|I_{la}|cos\emptyset_a + |I_{lb}|cos\emptyset_b + |I_{lc}|cos\emptyset_c + I_d)}{3} \quad (4.32)$$

Similarly, the magnitude of reactive component of reference source current is given by eqn. (4.33)

$$I_{sq}^{*} = \frac{(|I_{la}|sin\emptyset_a + |I_{lb}|sin\emptyset_b + |I_{lc}|sin\emptyset_c + I_d)}{3} \quad (4.33)$$

In power factor correction mode I_{sq}^{*} is kept zero.

Now, Unit amplitude templates are in-phase and quadrature component of source voltage, which are of unit magnitude. They are used to provide phase difference to different components of current. For calculation of unit amplitude template, first terminal voltage,v_m, is calculated by the formula given in eqn.(4.34), where v_a, $v_b$and$v_c$are phase voltages of the supply line.

$$v_m = Sqrt(\{(2/3)(v_{sa}^2 + v_{sb}^2 + v_{sc}^2)\}) \quad (4.34)$$

Thereafter each phase voltages is divided by terminal voltage, to provide unit amplitude with the phase angle of actual phase voltage supply. The in-phase components are portrayed by u_{pa}, u_{pb}andu_{pc}, for phase a, b and c respectively and the quadrature components are portrayed by u_{qa}, u_{qb}andu_{qc}, for phase a, b and c respectively[51-52]. The computation of unit templates are given in eqn.(4.35) to (4.38).

$$U_{pa} = \frac{v_a}{v_m},\ U_{pb} = \frac{v_b}{v_m},\ U_{pc} = \frac{v_c}{v_m} \quad (4.35)$$

$$U_{qa} = -\frac{U_{pb}}{\sqrt{3}} + \frac{U_{pc}}{\sqrt{3}} \quad (4.36)$$

$$U_{qb} = \sqrt{3}\frac{U_{pa}}{2} + \frac{(U_{pb} - U_{pc})}{2\sqrt{3}} \quad (4.37)$$

$$U_{qc} = -\sqrt{3}\frac{U_{pa}}{2} + \frac{(U_{pb} - U_{pc})}{2\sqrt{3}} \quad (4.38)$$

Thus, three phase source currents' active component are extracted using in-phase unit templates as follows:

$$i_{sap}^{*} = I_{sp}^{*} U_{pa}$$

$$i_{sbp}^{*} = I_{sp}^{*} U_{pb}$$

$$i_{scp}^{*} = I_{sp}^{*} U_{pc} \quad (4.39)$$

The required three phase reference source currents can be achieved from eqn. (4.40) .

$$i_{sa}^{*} = I_{sap}^{*}$$

$$i_{sb}^{*} = I_{sbp}^{*}$$

$$i_{sc}^{*} = I_{scp}^{*} \quad (4.40)$$

The reference currents are then compared with actual source currents (i_{sa}, i_{sb}, i_{sc}) using hysteresis current controller (HCC) that results in the required six pulses for providing control signals to PV Inverter.

4.3 Conclusion

In this chapter, an elaborate description of different control algorithms for PV inverter control is presented. On studying the control algorithms, one can conclude that SRF is axis transformation based technique. ISCT is also transform-based theory. And Icosø is an inverter control algorithm, which involves the tuning of the fundamental frequency and sample, and hold circuits through the load current in every phase by the implementation of a low pass filter.

CHAPTER 5

SIMULATION RESULTS AND DISCUSSION

5.1 General

In this chapter the two algorithm for maximum power point tracking is analyzed and further the performance of a grid interfaced PV system using three-phase inverter employing three different inverter is studied using MATLAB-Simulink version-15. The control algorithms are compared on the basis of different loads and environmental conditions [53].

5.2 Proposed System

An 8kW solar PV array is designed at 1000W/m^2 of solar irradiation, and at 25^{o}C is connected to a three phase 415V, 50 Hz AC utility grids through a three-phase inverter. Fig. 5.1 shows the block diagram of proposed grid interfaced solar PV system.

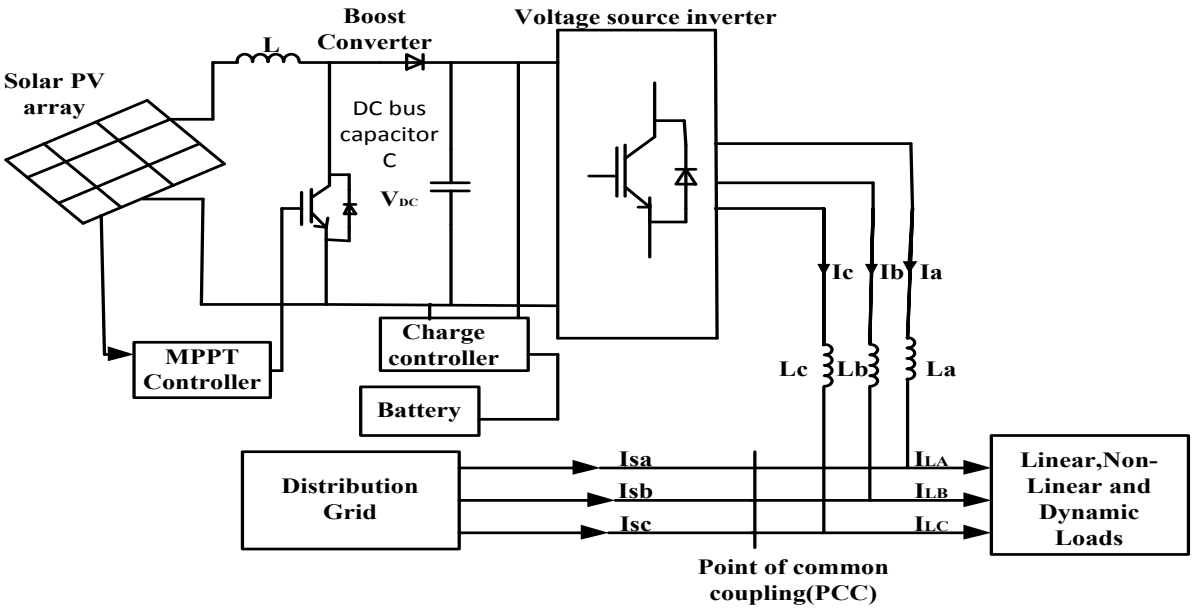

Fig 5.1 Grid interfaced Solar PV system

The system is studied under different loads namely star connected balanced linear loads, non-linear loads, unbalanced non-linear loads and dynamic loads. Interfacing inductor (L_f) is used at the point of common coupling (PCC) of PV inverter and distribution grid.

The grid interfaced solar PV system is modeled using MATLAB-Simulink toolbox. The MATLAB model of the same is shown in Fig. 5.2.

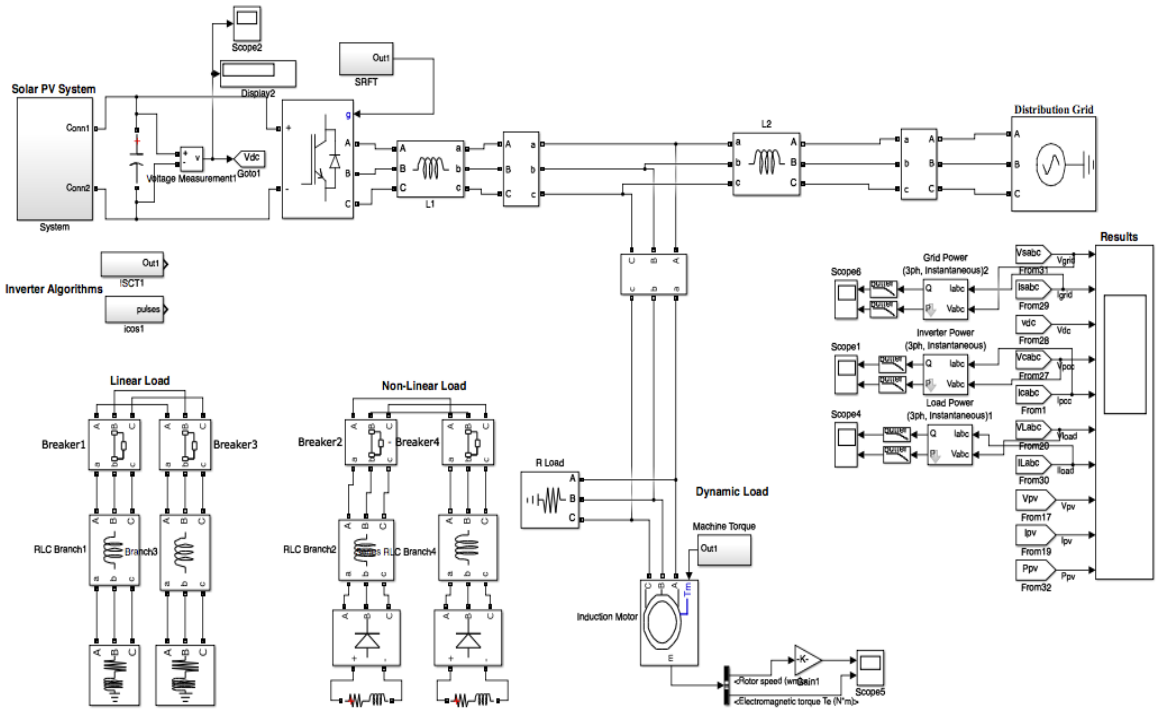

Fig. 5.2 Simulink model of the grid interfaced SPV system

All the parameters ratings are mentioned in the appendix-I. The simulation results of grid side voltage and current, dc bus voltage, PCC voltage and current, load voltage and current, PV voltage and current, PV power under different loads are displayed for different inverter control techniques.

5.3 Simulation results of the system presented:

The solar photovoltaic array is first subjected to different MPPT algorithms namely P&O and INC, and one with better MPP tracking (P&O) is implemented to the proposed system. The simulation results of the proposed system for various loads under varying atmospheric conditions are presented. Three different control algorithms viz. SRFT, ISCT and ICOSØ are used for controlling the inverter.

5.3.1 MPPT Algorithms

The simulation results of the solar photovoltaic system with perturb and observe algorithm is compared with Incremental and conductance algorithm. The Voltage versus time curve and power versus time curve on application of incremental and conductance method is

shown in Fig. 5.3 and 5.4 respectively. It is observed from the curves that output voltage and power had perturbations before obtaining a constant value. Also the output voltage and power so obtained was not of desired value. In contrast the output voltage versus time curve and power versus time curve on implementing P&O algorithm showed better results as shown in Fig. 5.5 and 5.6 respectively. The output voltage and power obtained by this technique are of desired value, hence P&O is implemented in the grid interfaced PV system.

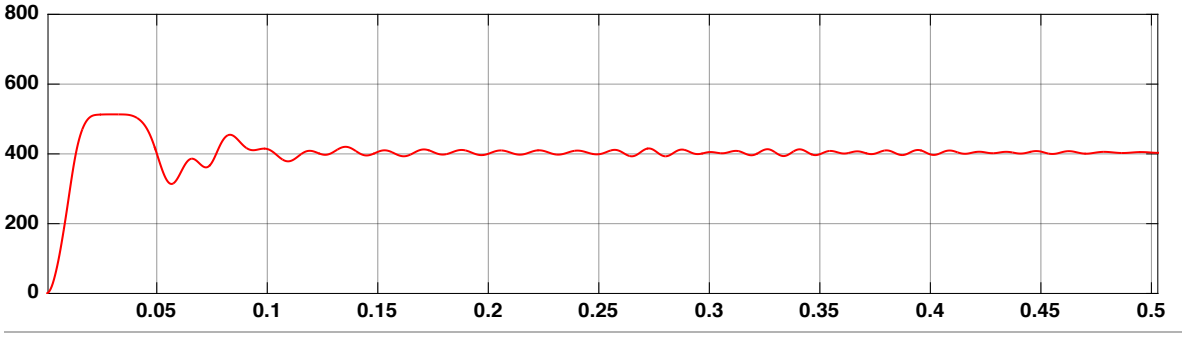

Fig. 5.3 Voltage versus time curve using INC MPPT algorithm with 1kW/m^2 irradiance and 25^0 C temperature.

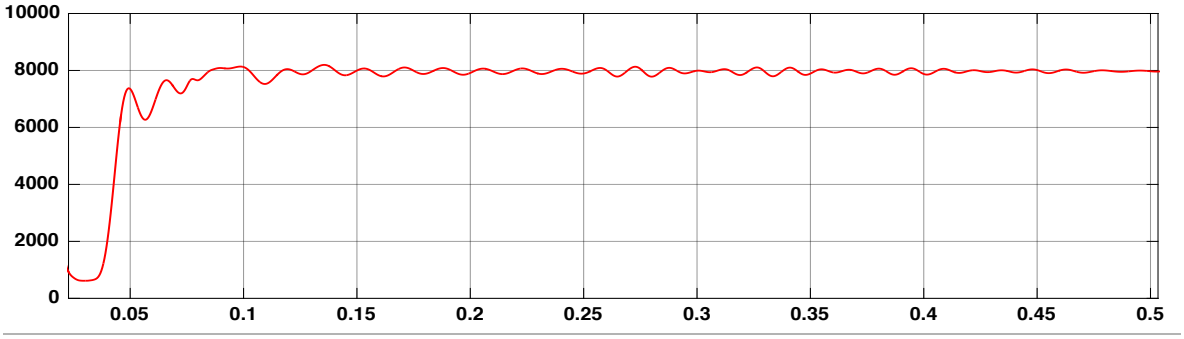

Fig. 5.4 Power versus time curve using INC MPPT algorithm with 1kW/m^2 irradiance and 25^0 C temperature.

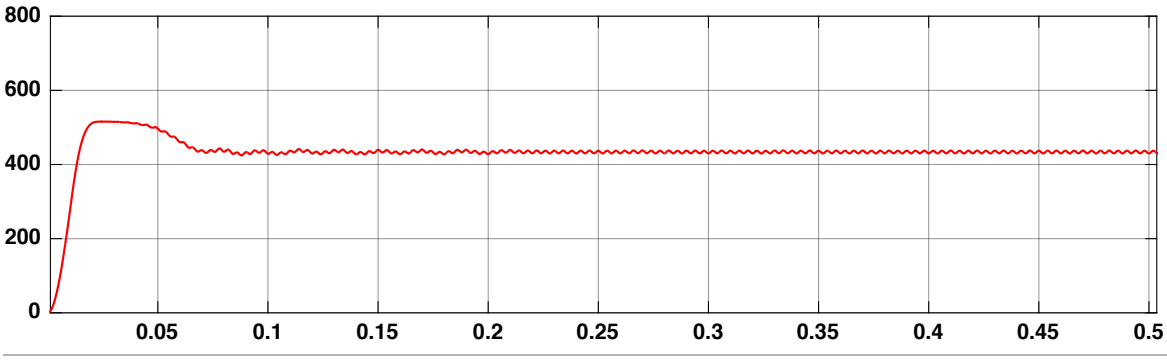

Fig. 5.5 Voltage versus time curve using P&O MPPT algorithm with 1kW/m^2 irradiance and 25^0 C temperature.

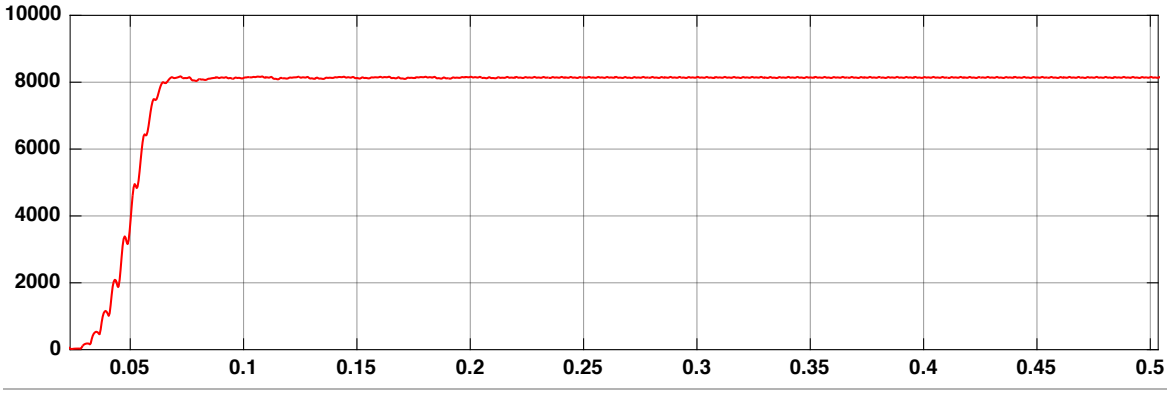

Fig. 5.6 Power versus time curve using P&O MPPT algorithm with 1kW/m^2 irradiance and 25^0 C temperature.

5.3.2 Solar PV inverter control techniques.

Three different inverter control algorithm are implemented on grid interfaced PV system on the MATLAB/Simulink platform.

5.3.2.1 Synchronous Reference Frame (SRF) Theory based control technique

An elaborate description of the theory and its control technique has already been covered in section (4.2.1). The Simulink model for SRF theory is shown in Fig. 5.7.

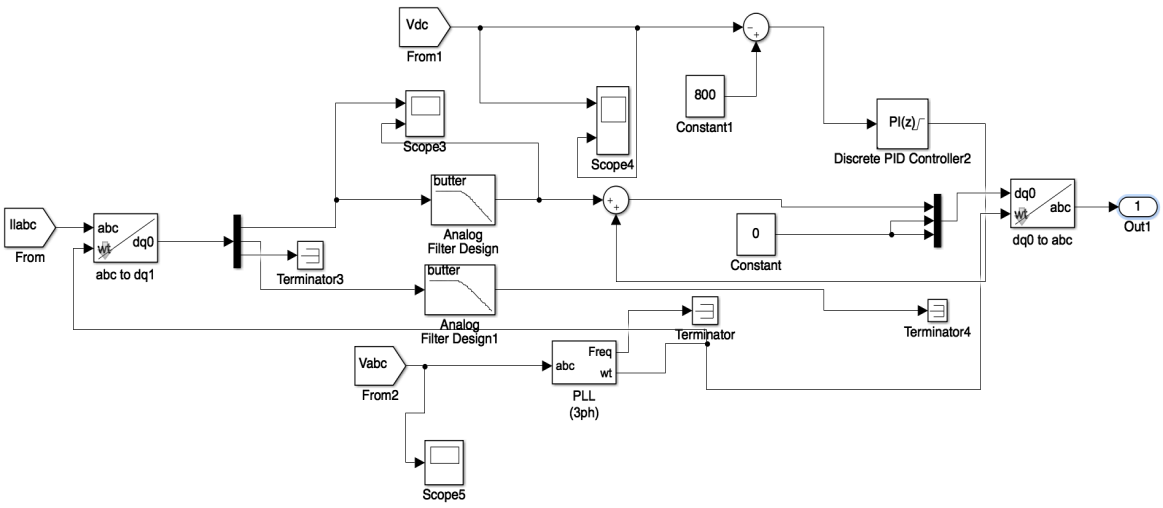

Fig.5.7. Simulink model of SRFT for reference current extraction

A. Performance of grid interfaced Solar PV system with balanced linear load :

The simulation results of grid interfaced Solar PV system with balanced linear load are shown in Fig. 5.8 and Fig. 5.9. The load is instantaneously decreased from 0.3sec to 0.6sec. Thus the respective variation in various parameters can be observed due to the load change. The simulation results show that V_{dc} remains constant and grid current decreases to meet the load demand, maintaining balanced, sinusoidal waveform with unity power factor. Keeping temperature constant the irradiation of the solar PV system is decreased from 1000 W/m^2 to 500 W/m^2 from 0.7 sec. to 0.85 sec, as shown in Fig. 5.8. Keeping irradiation constant the temperature is increased from 25^{0}C to 50^{0}C as shown in Fig. 5.9 respectively. With the variation in these input parameters i.e reduction in solar irradiation or increased temperature, the solar PV power generation gets reduced and vice versa. So, the grid supplies the remaining load demand. Under all the parameter variations mentioned above, DC bus and PCC voltages are maintained and grid current remains balanced. The THD level of grid current is 2.23% and PCC current is 1.25% as shown in Fig.5.10, which is maintained within the IEEE limits. The active power delivered to the load is the total of the grid power and SPV power. For the above changes, the system both active and reactive power balance of the system is shown in Fig. 5.11 and Fig. 5.12. The grid supply is maintained at unity power factor as shown in Fig. 5.13.

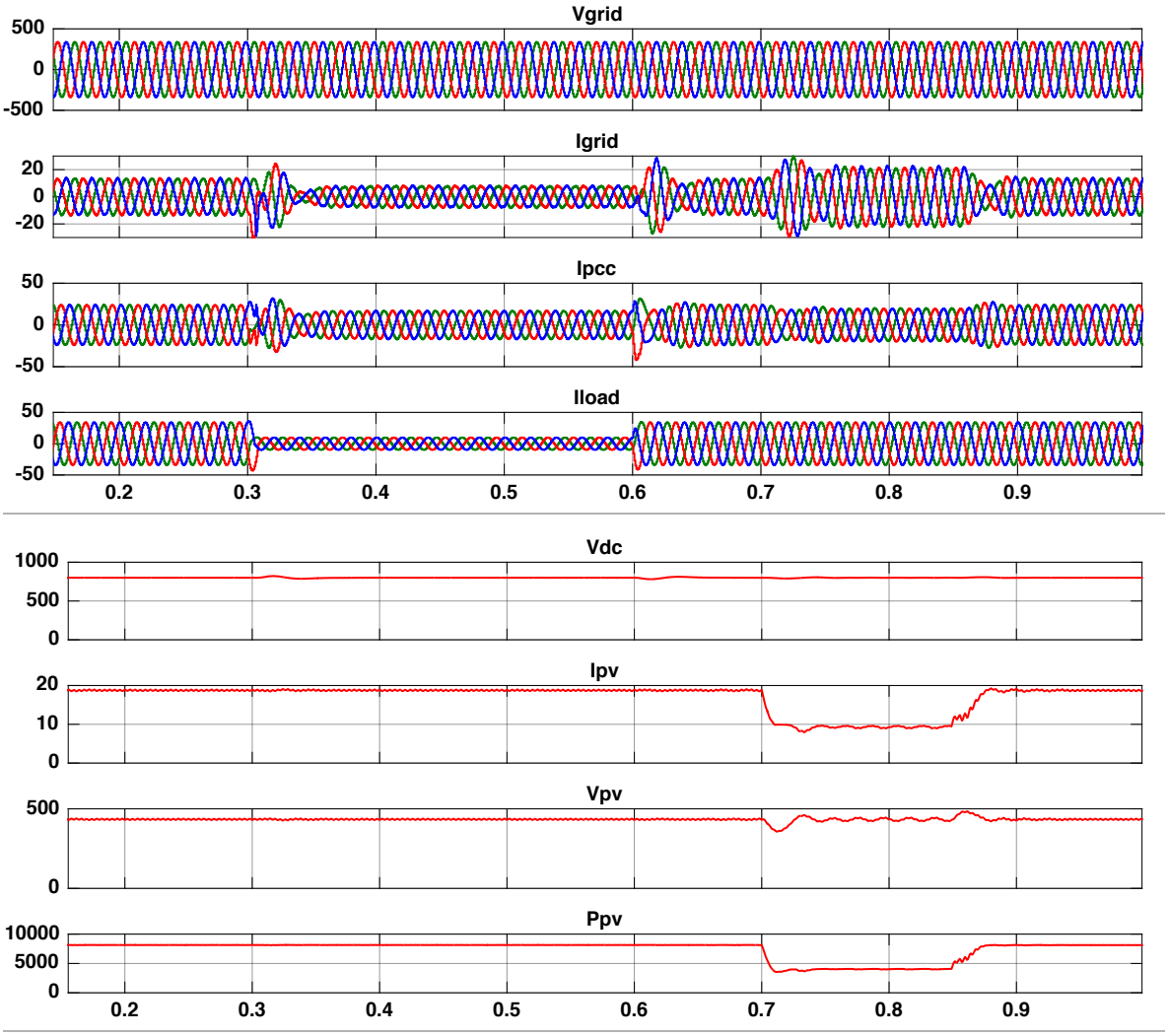

Fig. 5.8. Performance of grid interfaced PV system for balanced linear load under varying load with changing radiation (SRFT).

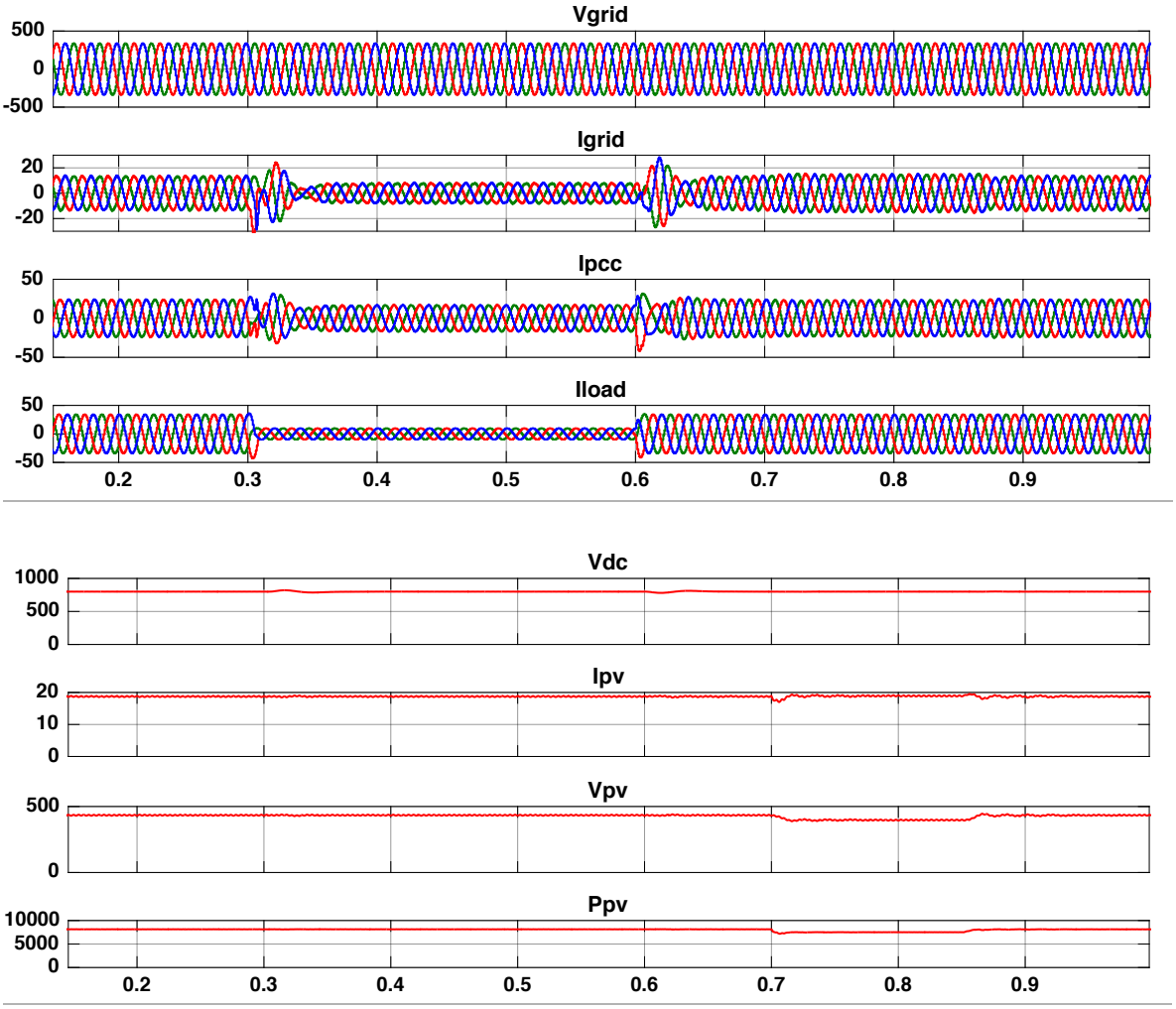

Fig. 5.9. Performance of grid interfaced PV system for balanced linear load under varying load with changing temperature(SRFT).

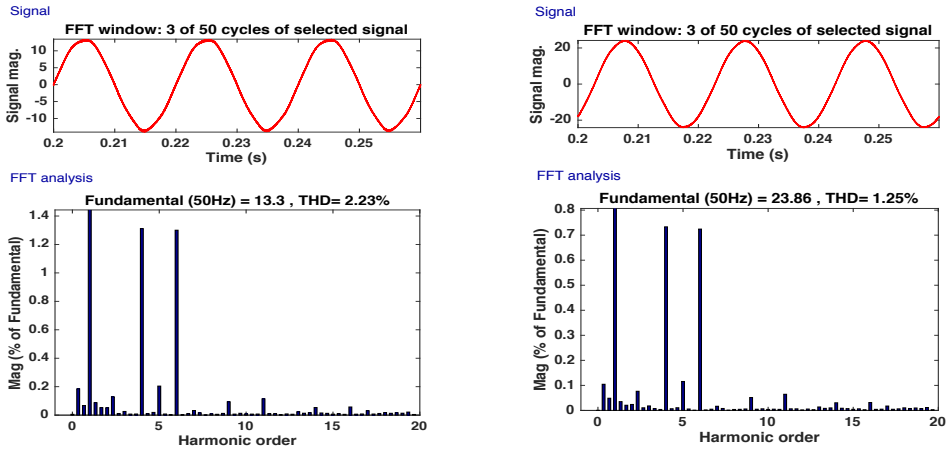

Fig.5.10 Waveform and THD for Grid Current (I_{grid}) and PCC current (I_{PCC}) for linear load(SRFT).

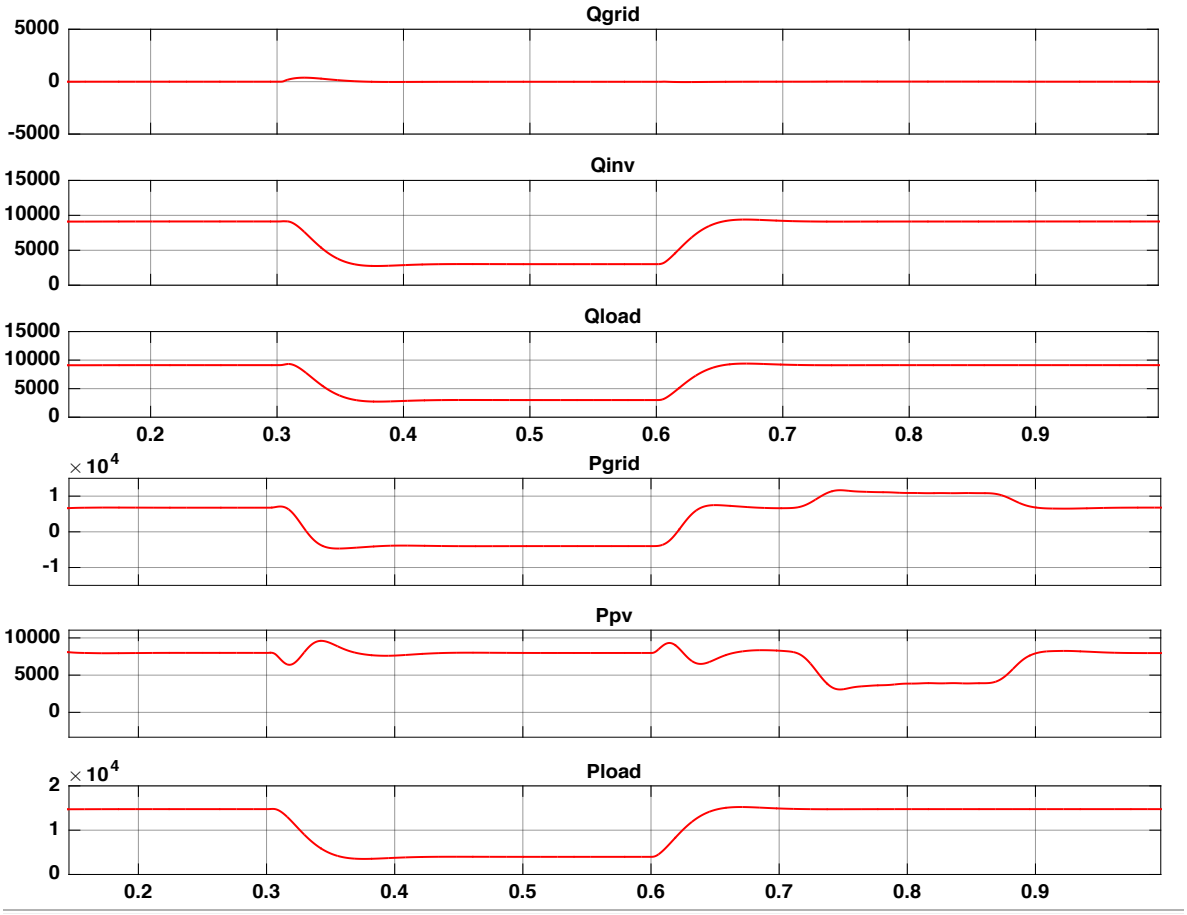

Fig.5.11 Power flow at different points in the system for linear load with varying load and changing radiation(SRFT).

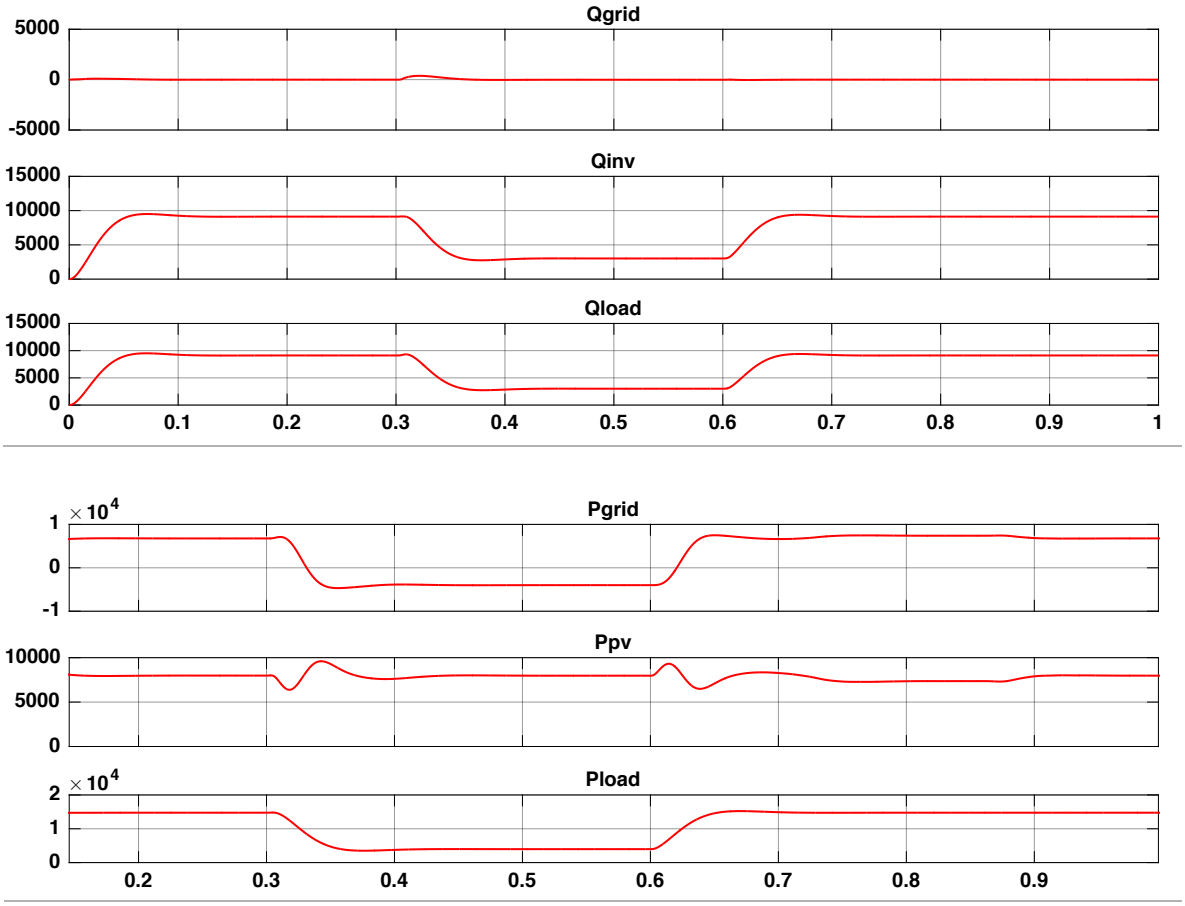

Fig.5.12 Power flow at different points in the system for linear load with varying load and changing temperature(SRFT).

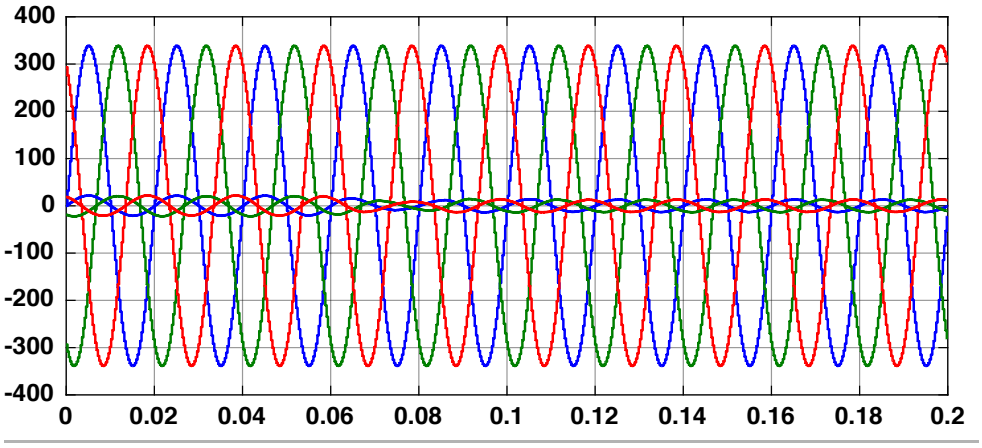

Fig.5.13 In phase grid side voltage and current under linear load(SRFT).

***B. Performance of grid connected Solar PV system with balanced non-linear load**:*

The simulation results of grid interfaced Solar PV system with balanced non-linear load are shown in Fig. 5.14 and Fig. 5.15. From 0.3sec to 0.6sec,the load is instantaneously decreased. Thus the respective variation in various parameters can be observed due to the load change. The simulation results show that V_{dc} remains constant and grid current decreases to meet the load demand, maintaining balanced, sinusoidal waveform with unity power factor. Keeping temperature constant the irradiation of the solar PV system is decreased from 1000 W/m^2 to 500 W/m^2 from 0.7 sec. to 0.85 sec, as shown in Fig. 5.14. Keeping irradiation constant the temperature is increased from 25^0C to 50^0C as shown in Fig. 5.15 respectively. With the variation in these input parameters i.e reduction in solar irradiation or increased temperature, solar PV power generation gets reduced. So, the grid supplies the remaining load demand. Under all the parameter variations mentioned above, DC bus and PCC voltages are maintained and grid current remains balanced. The THD level of grid current is 1.05% and THD level of load current is 17.19% as shown in Fig.5.16, which is maintained within the IEEE limits. The grid side supply is maintained at unity power factor as shown in Fig. 5.17.

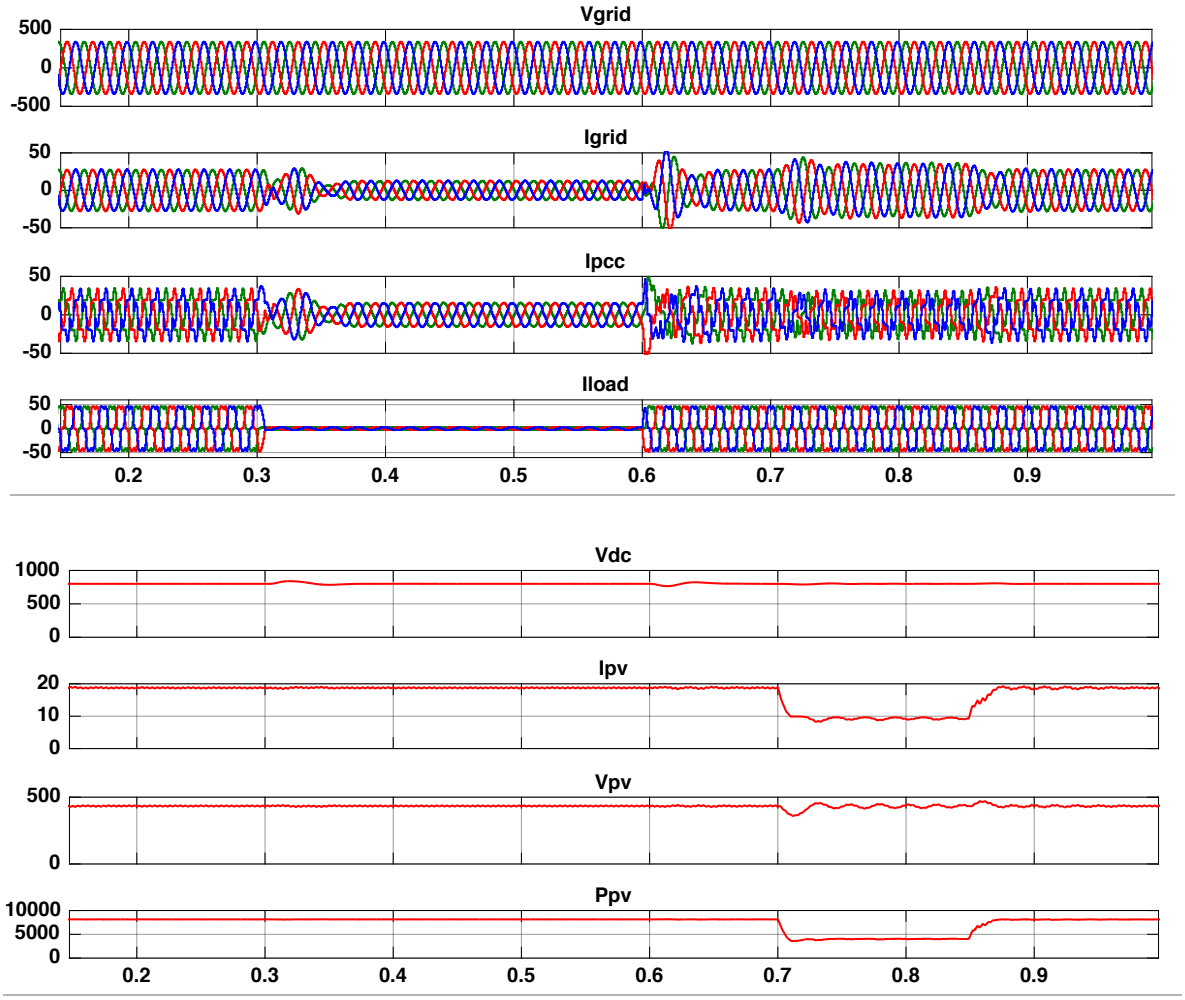

Fig. 5.14. Performance of grid interfaced PV system for non-linear load under varying load and changing radiation(SRFT).

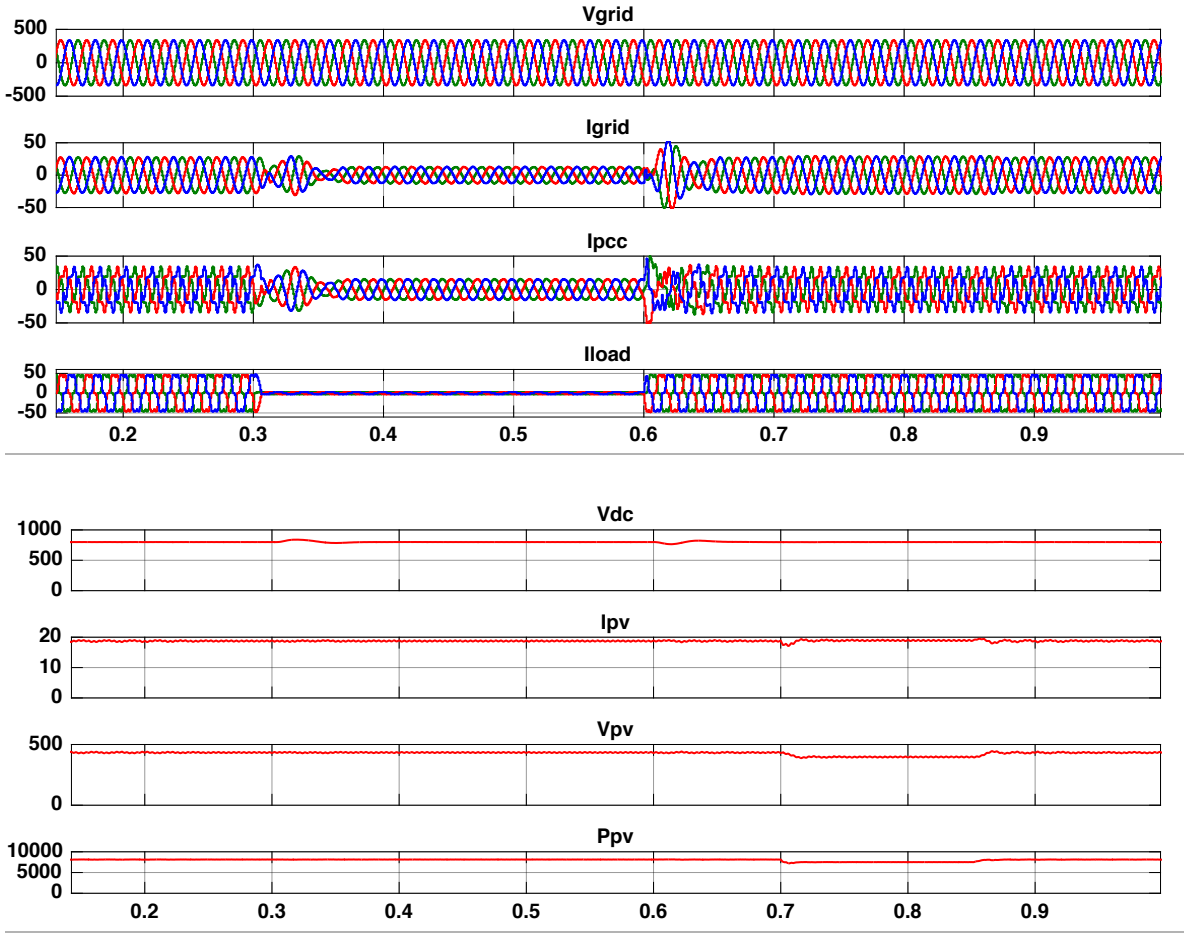

Fig 5.15.Performance of grid interfaced PV system for non-linear load under varying load and changing temperature(SRFT).

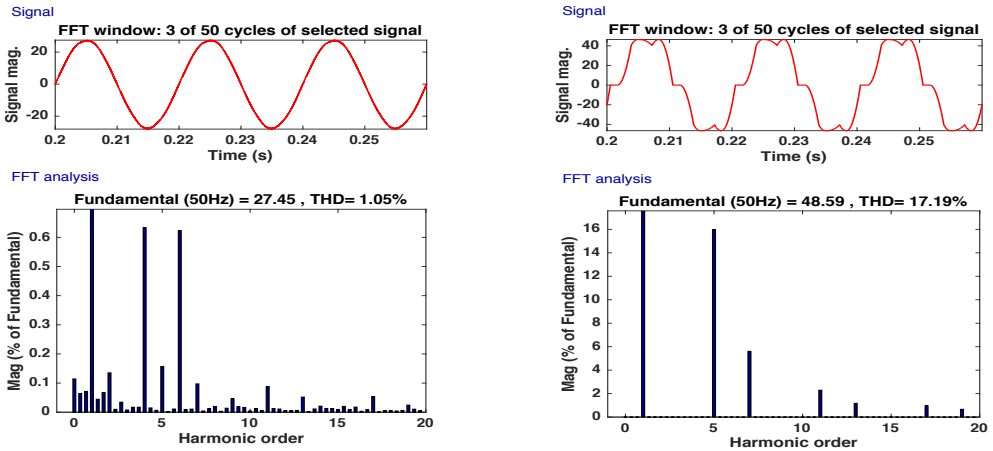

Fig.5.16 .Waveform and harmonic analysis for Grid Current (I_{grid}) and Load current (I_{Load}) for non-linear load(SRFT).

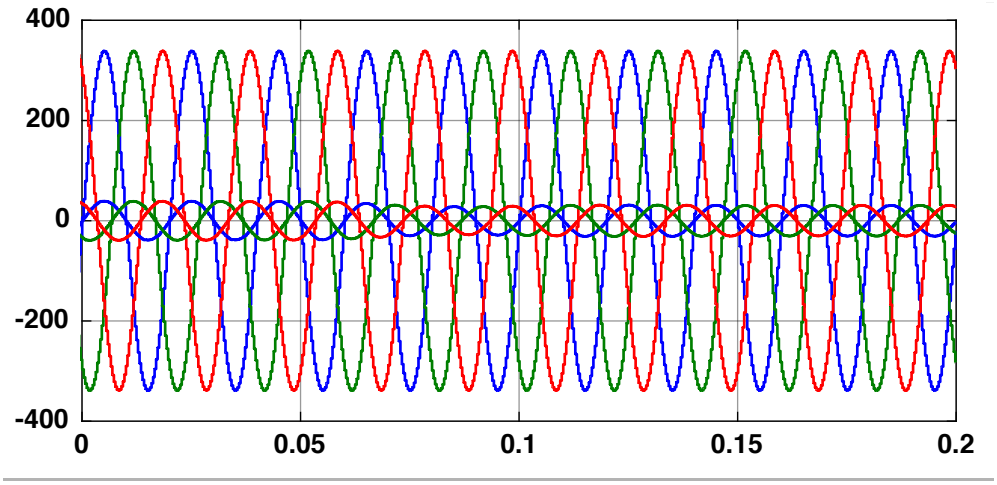

Fig. 5.17. In phase grid side voltage and current for non-linear load conditions(SRFT).

C. Performance of grid connected Solar PV system with unbalanced non-linear load

The simulation results for non-linear unbalanced load is shown in Fig.5.18.The 'B' phase of the load is disconnected from 0.3 sec to 0.6 sec and at t=0.5 sec this 'B' phase of the load is again applied and the system regains its balanced state. Thus the respective variation in various parameters can be observed due to the load unbalancing. The simulation results show that V_{dc} remains constant and source current decreases to meet the load demand, maintaining balanced, sinusoidal waveform with unity power factor. Irradiation of the Solar PV system is decreased from 1000 W/mm^2 to 500 W/mm^2 from 0.7 sec. to 0.85 sec, as shown by fig 5.18. In this situation, solar PV power generation gets reduced. So, the grid supplies the remaining load demand. Under all the parameter variations mentioned above, DC bus and PCC voltages are maintained and grid current remains balanced. The THD level of grid current is 3.85% which is well within the IEEE limits as shown in Fig.5.19.

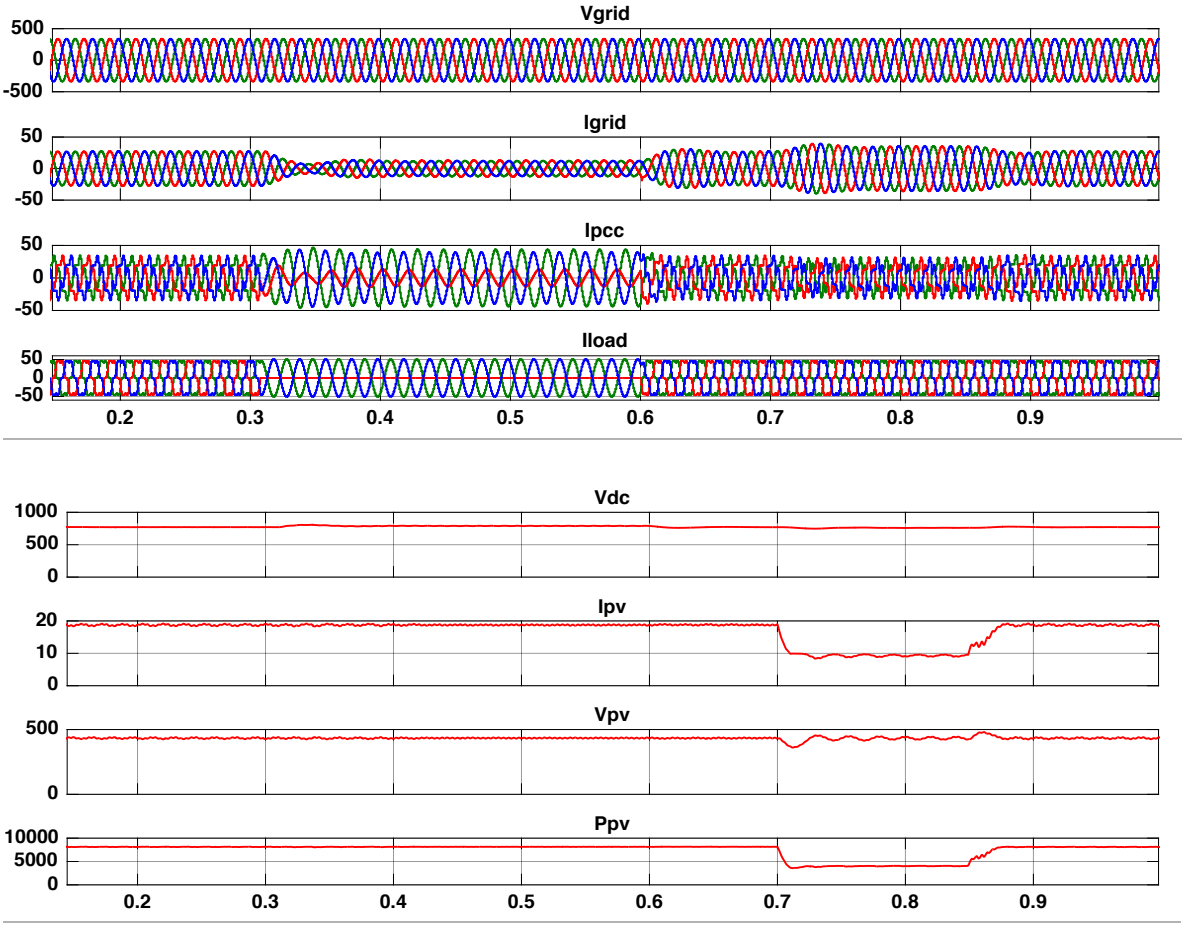

Fig. 5.18. Performance of grid interfaced PV system for non-linear load under unbalancing with changing radiation(SRFT).

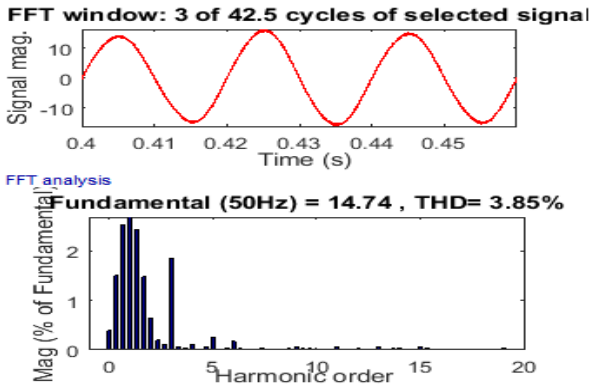

Fig.5.19 .Waveform and harmonic analysis for Grid Current (I_{grid}) for non- linear load during unbalancing time(SRFT).

D. Performance of grid connected Solar PV system with dynamic load.

The simulation results for dynamic load are shown in Fig. 5.20. The motor torque is increased to full load torque value i.e 20 N-m at 0.3 sec, and is decreased to half of the load torque i.e 10N-m after 6sec, and hence its effect on the various parameters can be observed. The simulation results show that V_{dc} remains constant and source current decreases to meet the load demand, maintaining balanced, sinusoidal waveform with unity power factor. The THD level of grid current is 1.92% and PCC current is 1.86%, which is well within IEEE limits as given by Fig. 5.21.

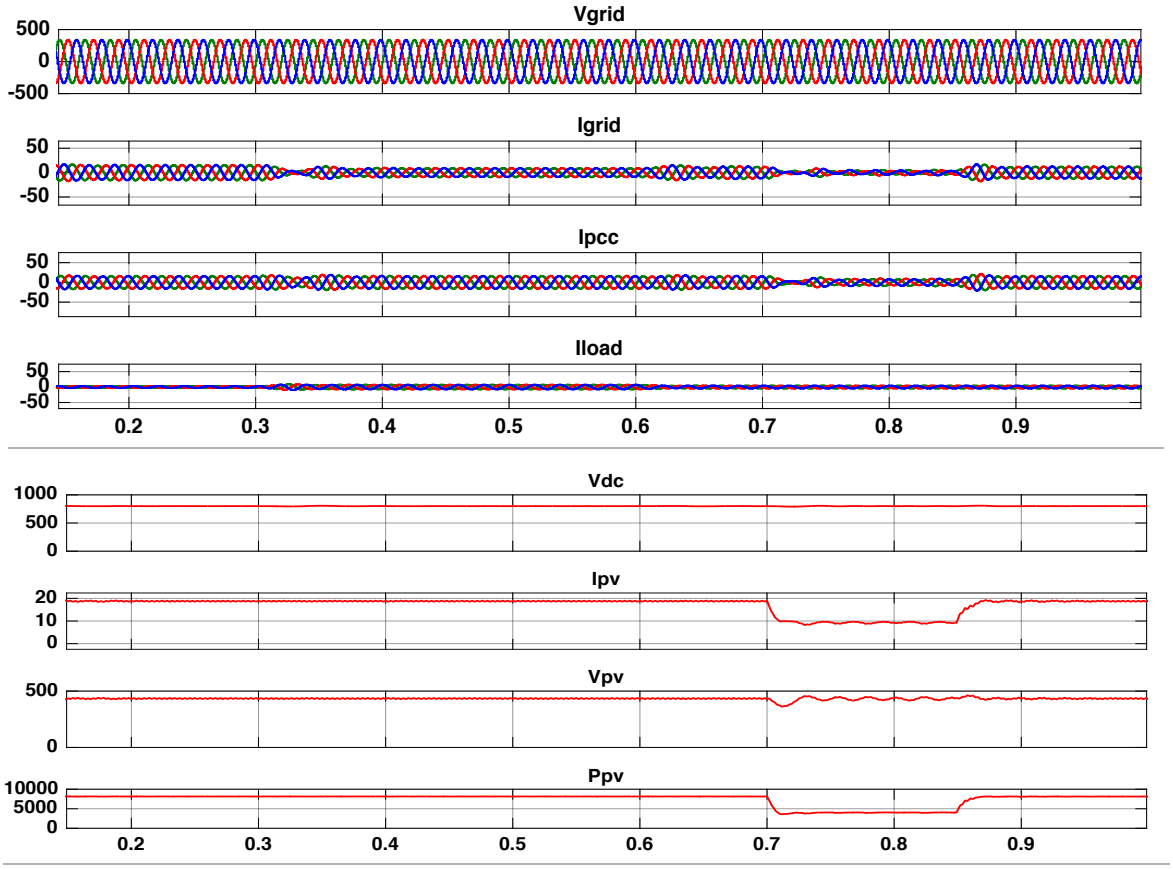

Fig. 5.20.Performance of grid interfaced PV system for dynamic load under torque variation with changing radiation(SRFT).

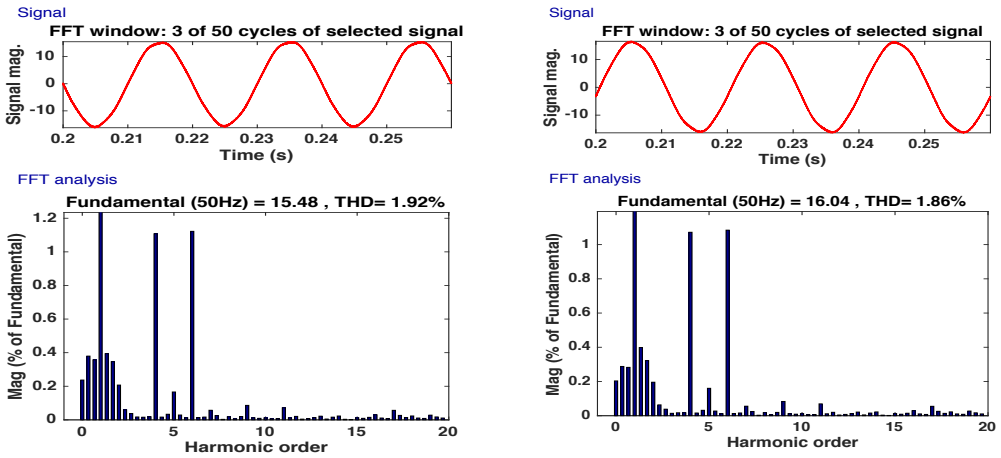

Fig.5.21 .Waveform and harmonic analysis for Grid Current (I_{grid}) and PCCcurrent (I_{PCC}) for dynamic load(SRFT).

5.3.2.2 Instantaneous Symmetrical Component Theory based control algorithm

An elaborate description of the theory and its control technique has already been covered in section 4.2.2. The Simulink model for the ISCT control technique is shown in Fig. 5.22.

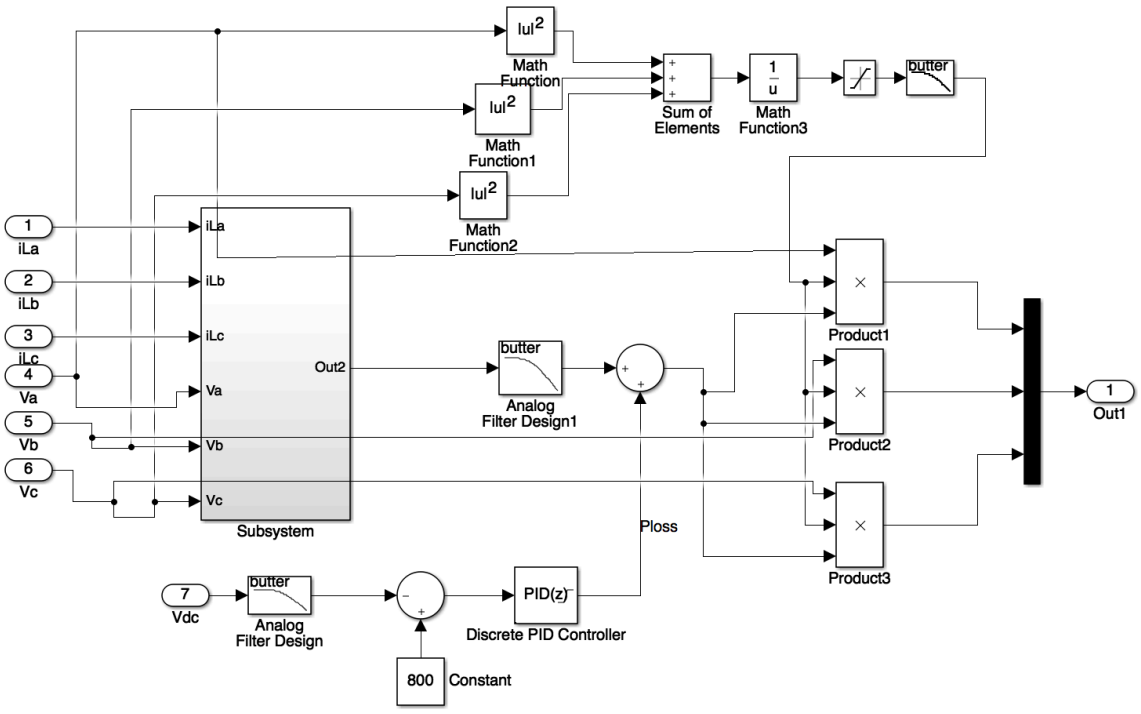

Fig.5.22. ISCT controller for reference current extraction

A) Performance of grid connected Solar PV system with balanced linear load

The simulation results of grid interfaced Solar PV system with balanced linear load are shown in Fig. 5.23 and Fig. 5.24. The load is instantaneously decreased from 0.3sec to 0.6sec. Thus the respective variation in various parameters can be observed due to the load change. The simulation results show that V_{dc} remains constant and grid current decreases to meet the load demand, maintaining balanced, sinusoidal waveform with unity power factor. Keeping temperature constant the irradiation of the solar PV system is decreased from 1000 W/m^2 to 500 W/m^2 from 0.7 sec. to 0.85 sec, as shown in Fig. 5.23. Keeping irradiation constant the temperature is increased from 25^0C to 50^0C as shown in Fig. 5.24 respectively. With the variation in these input parameters i.e reduction in solar irradiation or increased temperature, the solar PV power generation gets reduced and vice versa. So, the grid supplies the remaining load demand. Under all the parameter variations mentioned above, DC bus and PCC voltages are maintained and grid current remains balanced. The THD level of grid current is 3.02% and PCC current is 1.71% as shown in Fig. 5.25, which is well within the IEEE limits. The grid side supply is maintained at unity power factor as shown in Fig. 5.26.

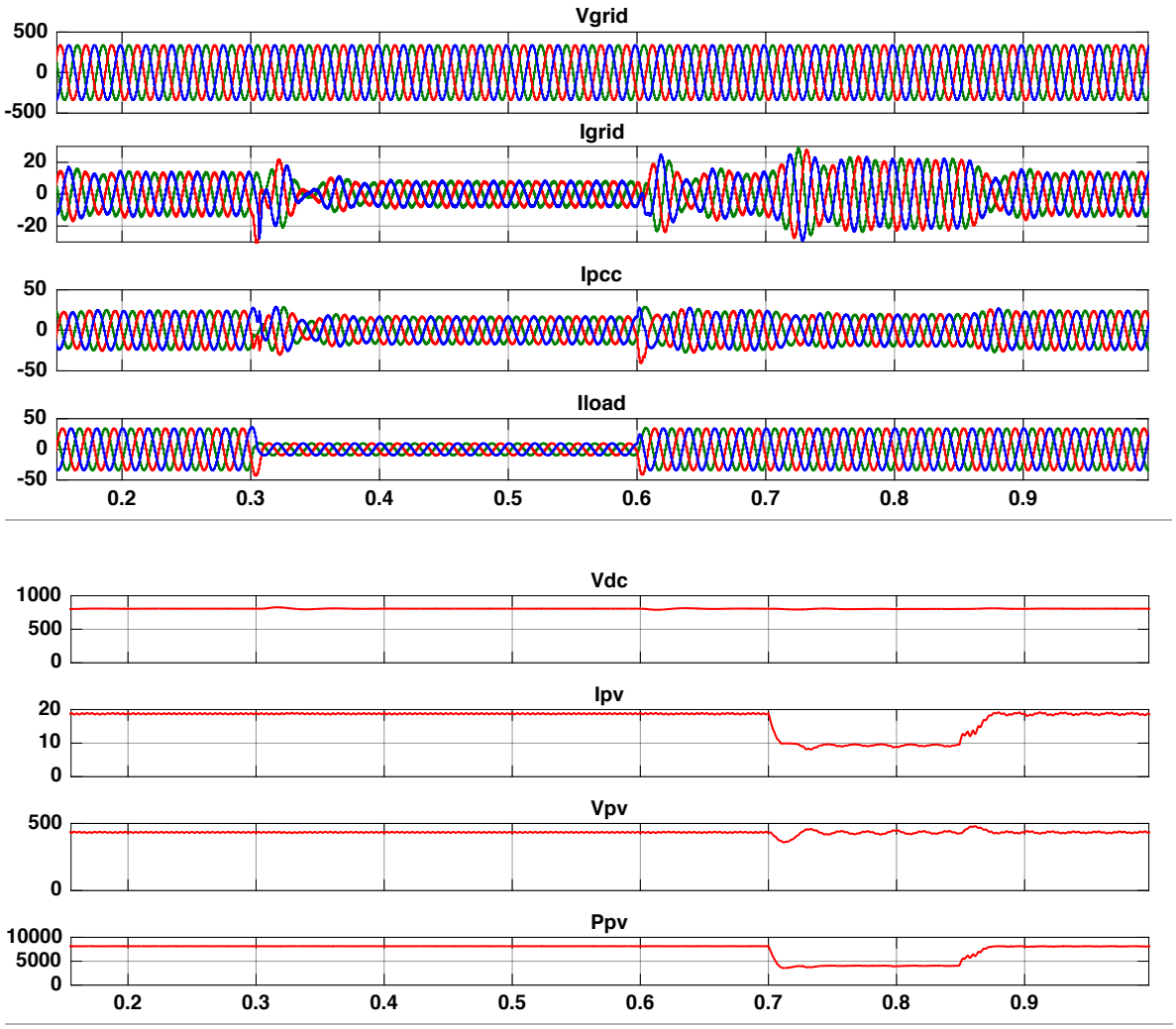

Fig. 5.23. Performance of grid interfaced PV system for linear load under varying load and changing radiation(ISCT).

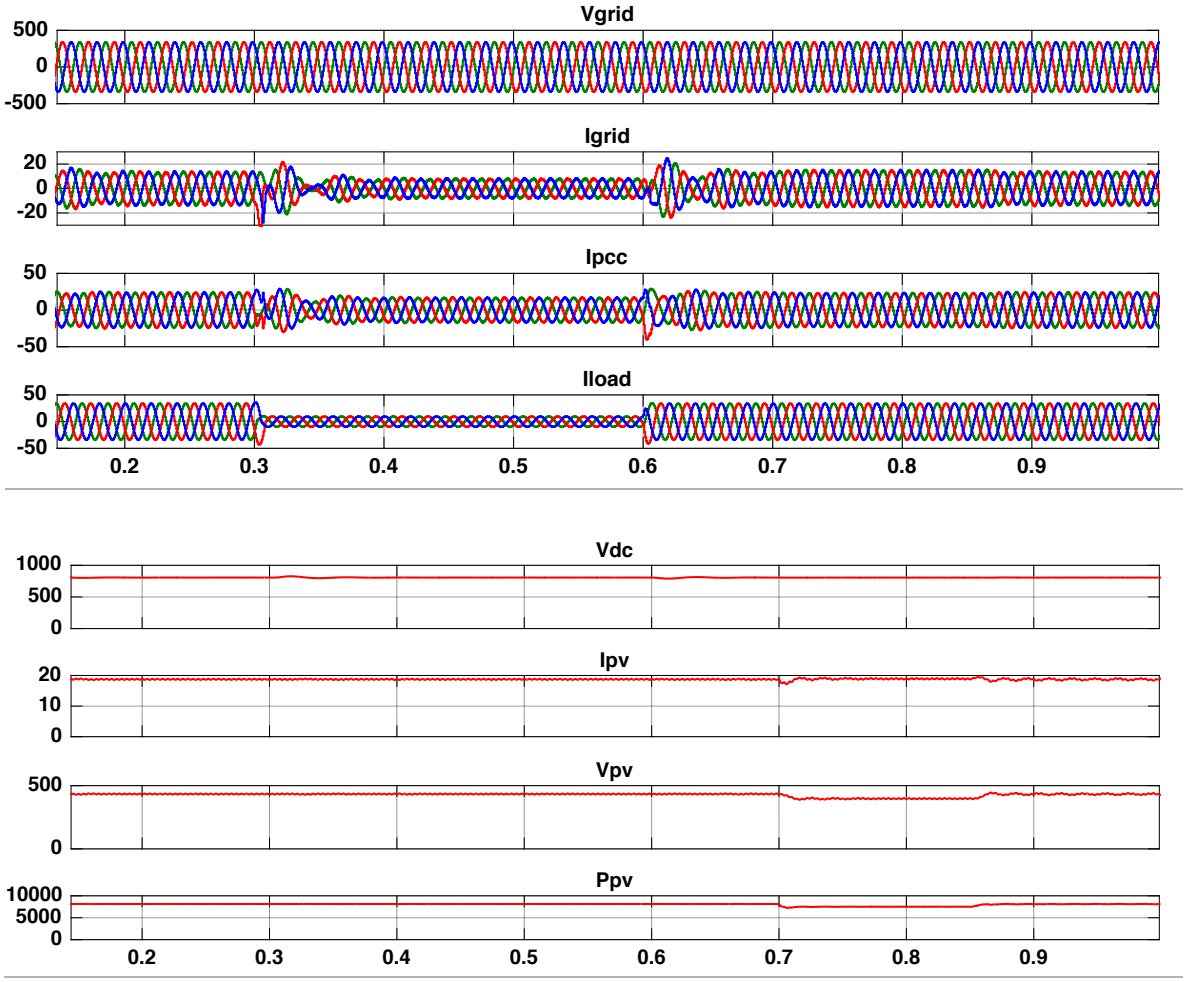

Fig 5.24.Performance of grid interfaced PV system for linear load under varying load and changing temperature (ISCT).

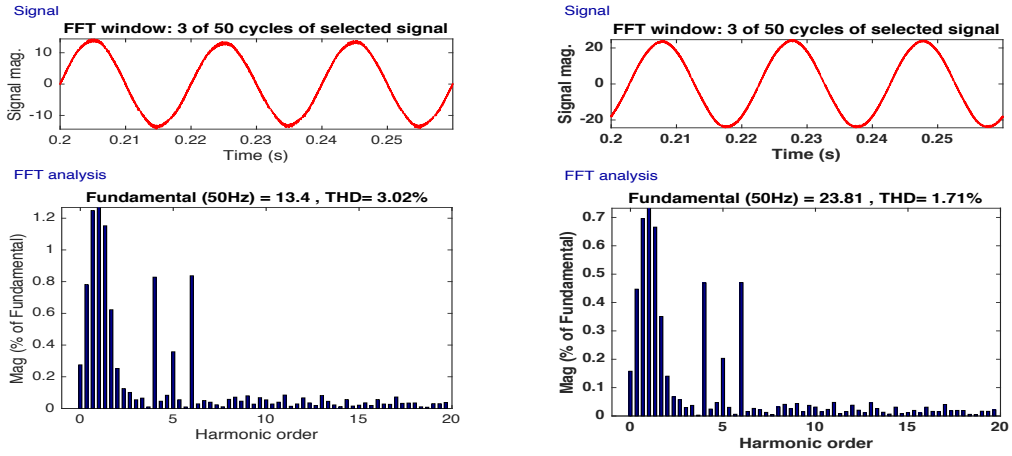

Fig.5.25.Waveform and harmonic analysis for Grid Current (I_{grid}) and PCC current (I_{PCC}) for linear load (ISCT).

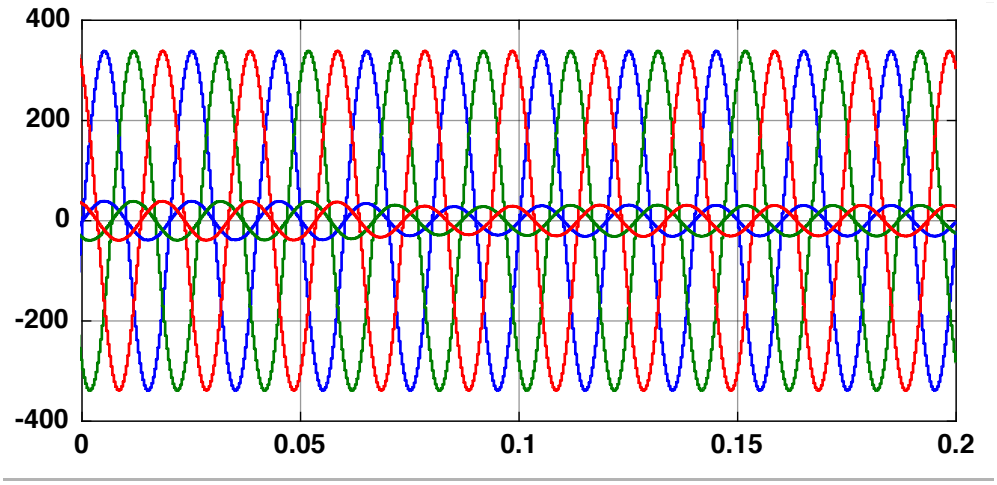

Fig.5.26. In phase grid side voltage and current for linear load conditions (ISCT).

B. Performance of grid connected Solar PV system with balanced non-linear load

The simulation results of grid interfaced Solar PV system with balanced non-linear load are shown in Fig. 5.27 and Fig. 5.28. From 0.3sec to 0.6sec,the load is instantaneously decreased. Thus the respective variation in various parameters can be observed due to the load change. The simulation results show that V_{dc} remains constant and source current decreases to meet the load demand, maintaining balanced, sinusoidal waveform with unity power factor. Keeping temperature constant the irradiation of the solar PV system is decreased from 1000 W/m^2 to 500 W/m^2 from 0.7 sec. to 0.85 sec, as shown in Fig. 5.27. Keeping irradiation constant the temperature is increased from 25^{0}C to 50^{0}C as shown in Fig. 5.28 respectively.With the variation in these input parameters i.e reduction in solar irradiation or increased temperature, solar PV power generation gets reduced. So, the grid supplies the remaining load demand. Under all the parameter variations mentioned above, DC bus and PCC voltages are maintained and grid current remains balanced. The THD level of grid current is 1.42% and THD level of load current is 17.19% as shown in Fig. 5.29, which is well within the IEEE limits. The grid side supply is maintained at unity power factor as shown in Fig. 5.30.

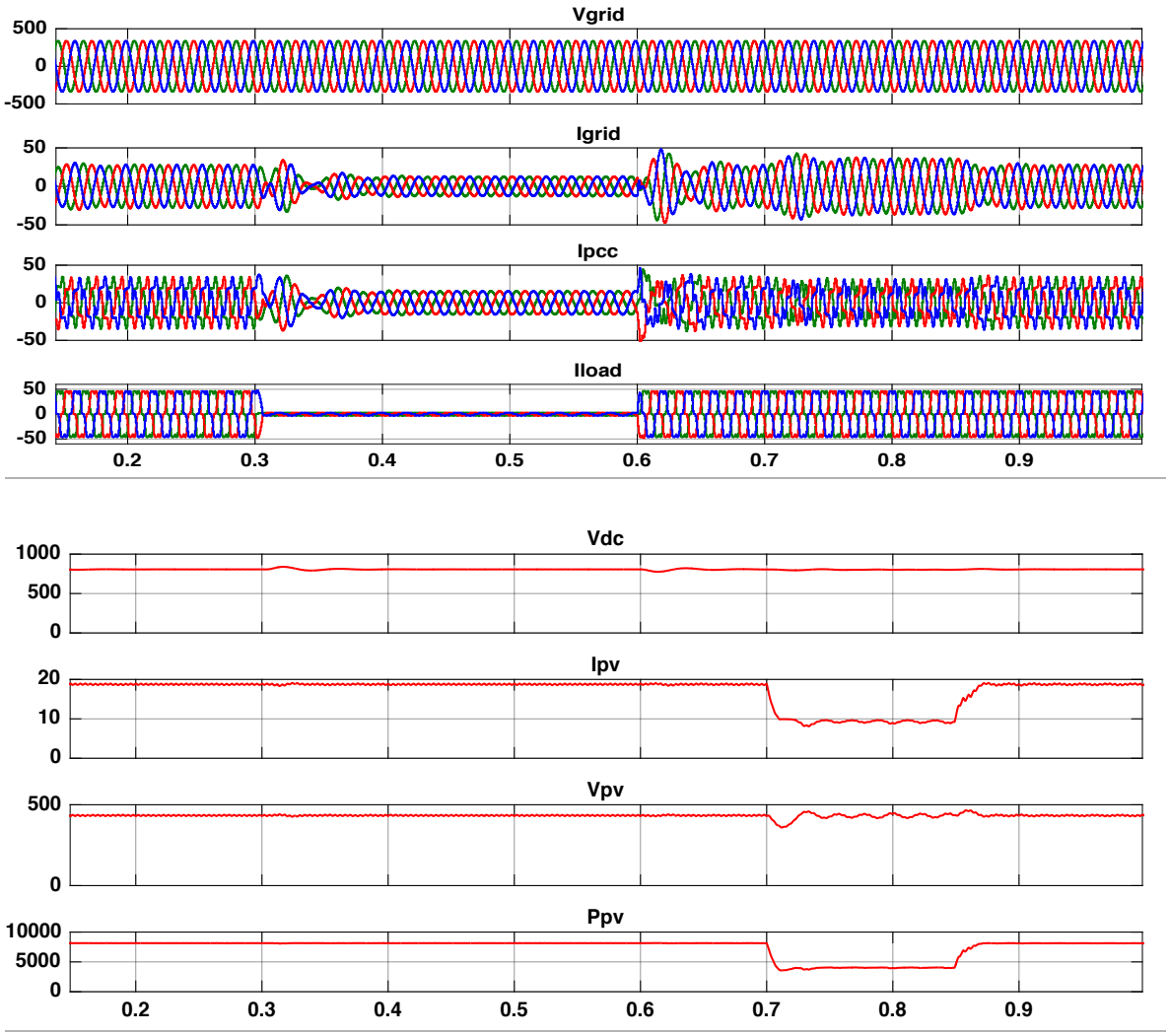

Fig. 5.27. Performance of grid interfaced PV system for non-linear load under varying load and changing radiation (ISCT).

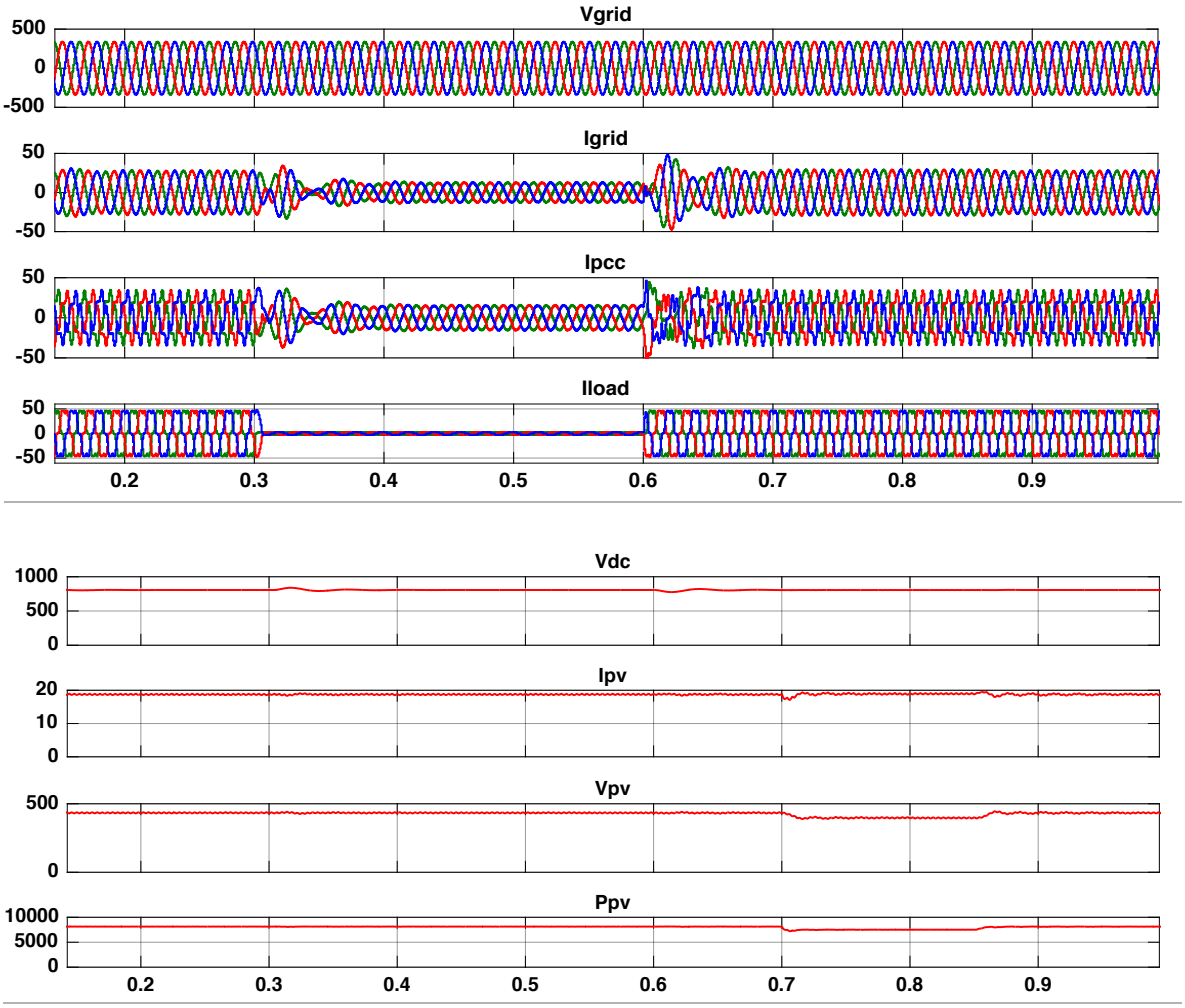

Fig 5.28. Performance of grid interfaced PV system for non-linear load under varying load and changing temperature (ISCT).

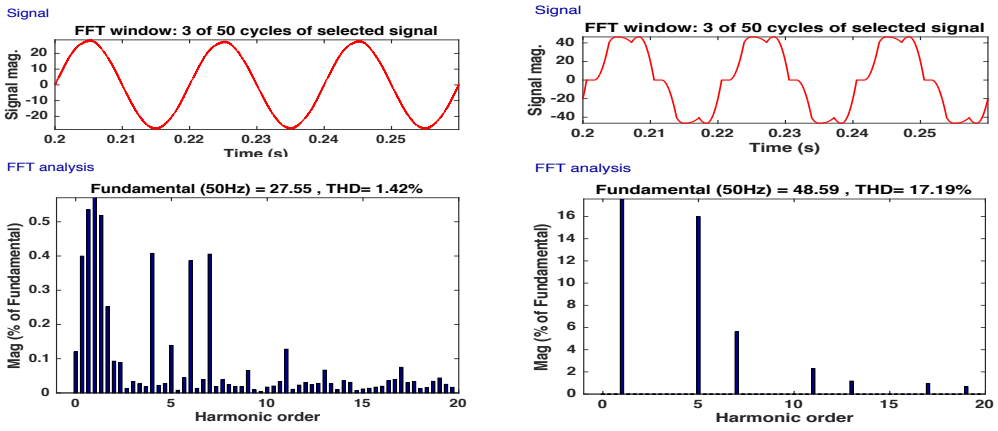

Fig.5.29 . Waveform and harmonic analysis for Grid Current (I_{grid}) and Load current (I_{Load}) for non- linear load (ISCT).

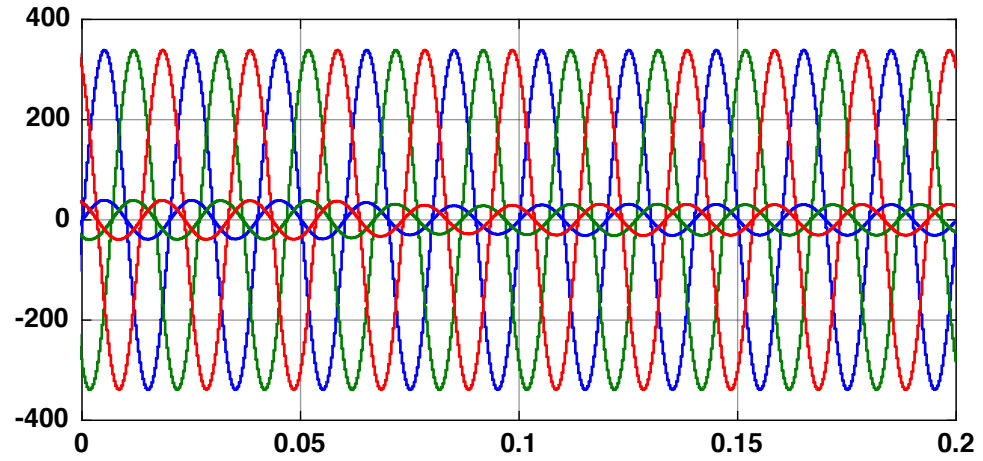

Fig.5.30. In phase grid side voltage and current for non-linear load conditions (ISCT).

C. Performance of grid connected Solar PV system with unbalanced non-linear load

The simulation results for non-linear unbalanced load is shown in Fig.5.31.The 'B' phase of the load is disconnected from 0.3 sec to 0.6 sec and at t=0.6 sec this 'B' phase of the load is again applied and the system regains its balanced state. Thus the respective variation in various parameters can be observed due to the load unbalancing. The simulation results show that V_{dc} remains constant and source current decreases to meet the load demand, maintaining balanced, sinusoidal waveform with unity power factor. Irradiation of the Solar PV system is decreased from 1000 W/mm^2 to 500 W/mm^2 from 0.7 sec. to 0.85 sec, as shown by Fig 5.31. In this situation, solar PV power generation gets reduced. So, the grid supplies the remaining load demand. Under all the parameter variations mentioned above, DC bus and PCC voltages are maintained and grid current remains balanced. The THD level of grid current is 4.61%, which is well within the IEEE, limits as shown in Fig.5.32

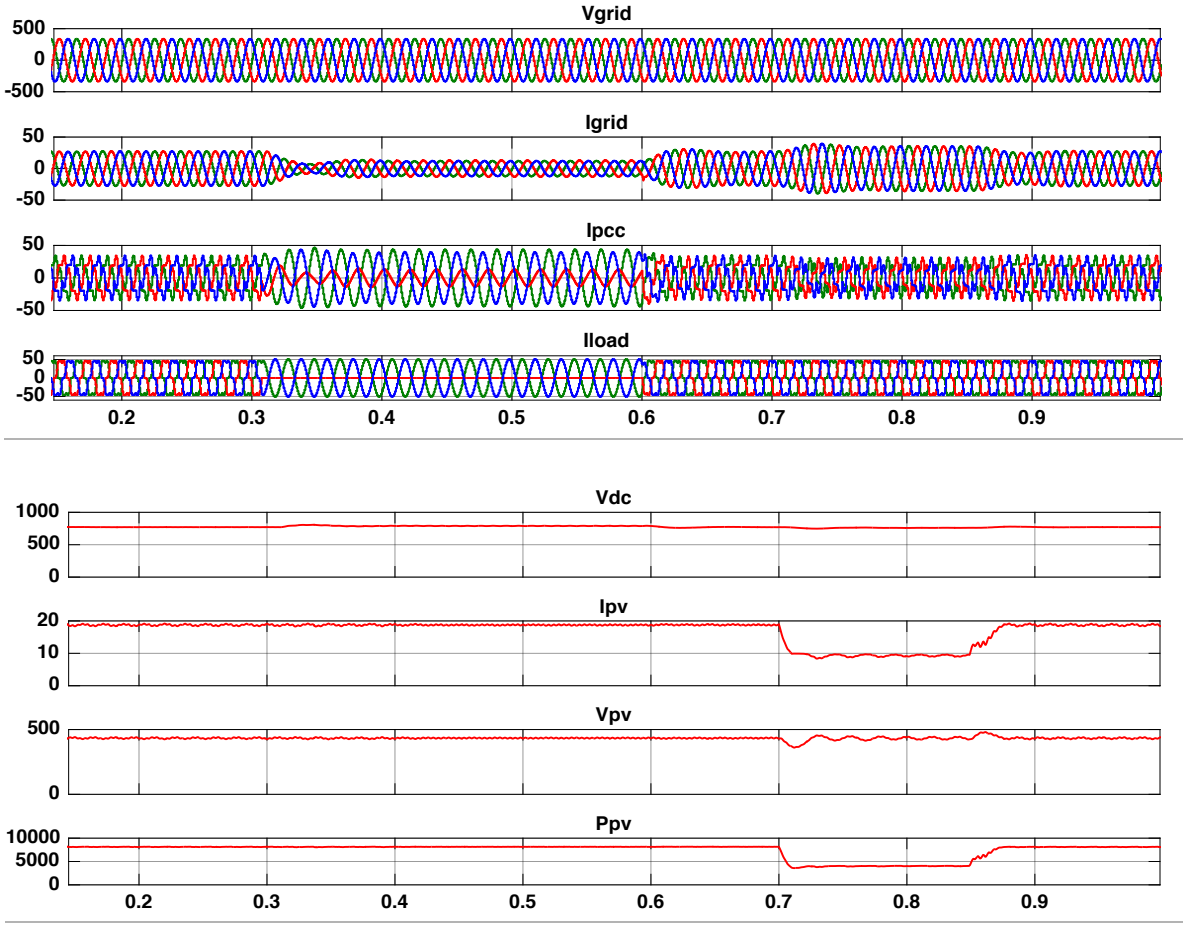

Fig. 5.31. Performance of grid interfaced PV system for non-linear load under unbalancing with changing radiation (ISCT).

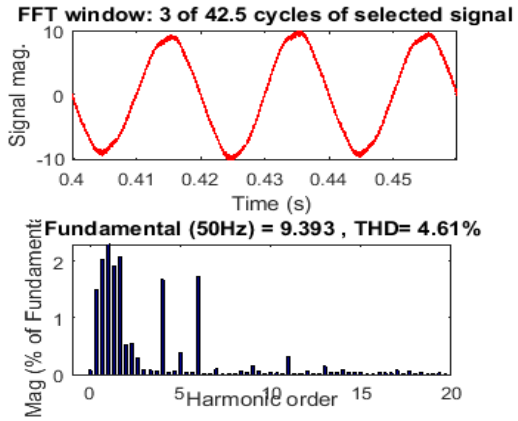

Fig.5.32. Waveform and harmonic analysis for Grid Current (I_{grid}) for non- linear load during unbalancing time(ISCT).

D. Performance of grid connected Solar PV system with dynamic load.

The simulation results for dynamic load are shown in Fig. 5.33. The motor torque is increased to full load torque value i.e 20 N-m at 0.3 sec, and is decreased to half of the load torque i.e 10N-m after 6sec, and hence its effect on the various parameters can be observed. The simulation results show that V_{dc} remains constant and source current decreases to meet the load demand, maintaining balanced, sinusoidal waveform with unity power factor. The THD level of grid current is 2.44% and PCC current is 2.33%, which is well within IEEE limits as given by Fig. 5.34.

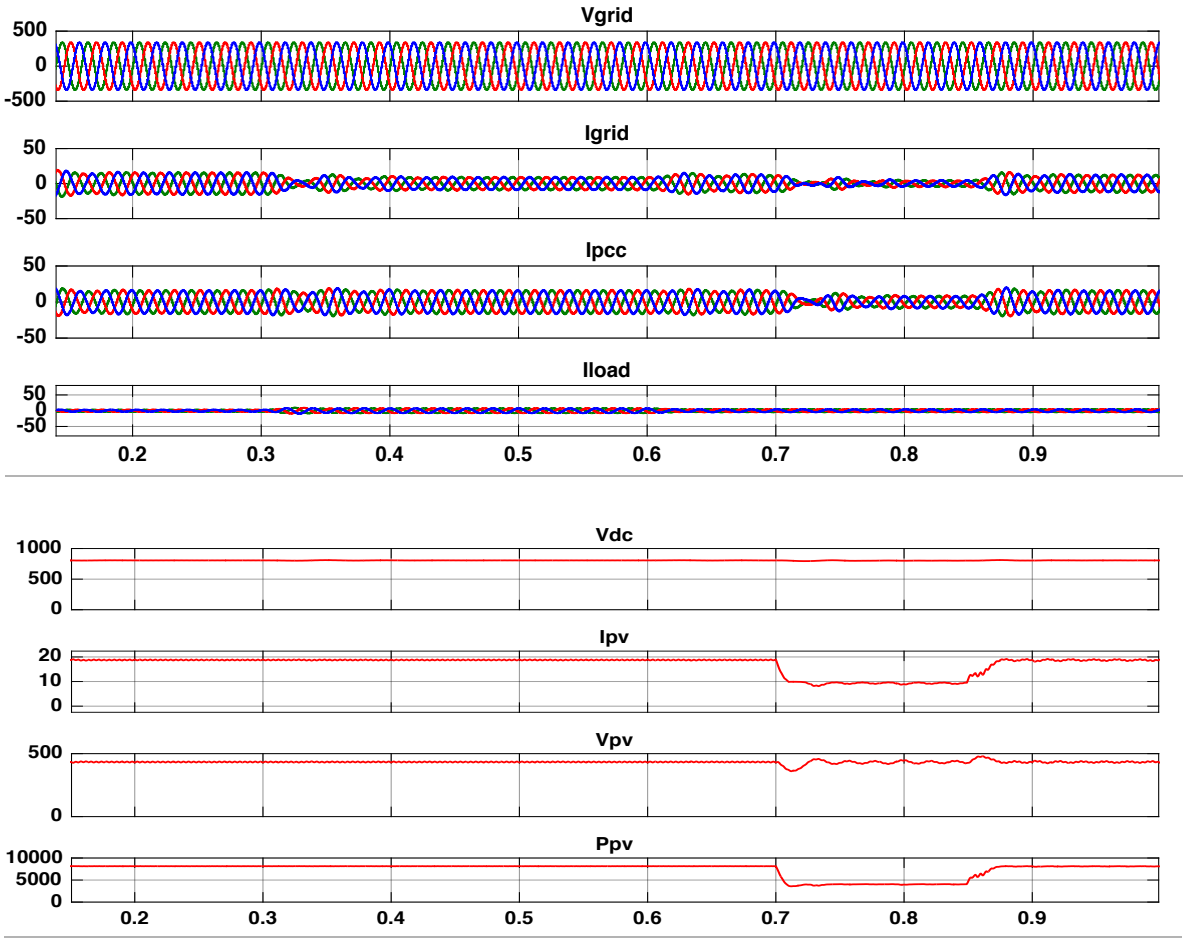

Fig. 5.33. Performance of grid interfaced PV system for dynamic load under torque variation and changing radiation (ISCT).

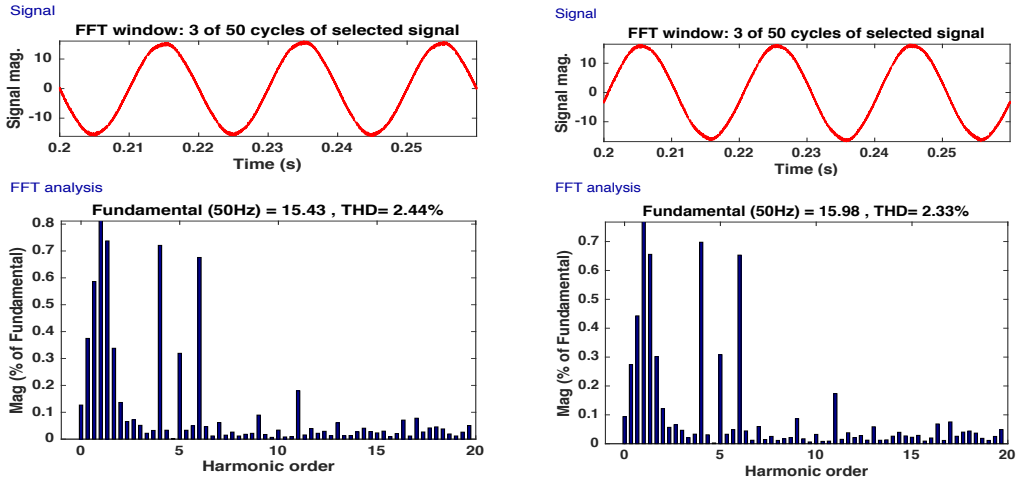

Fig.5.34. Waveform and harmonic analysis for Grid Current (I_{grid}) and PCC current (I_{PCC}) for dynamic load (ISCT).

5.3.2.3 IcosØ Theory based control algorithm

The theory and its control technique is already explained in section 4.2.3. The Simulink model for the control technique is shown in Fig 5.35.

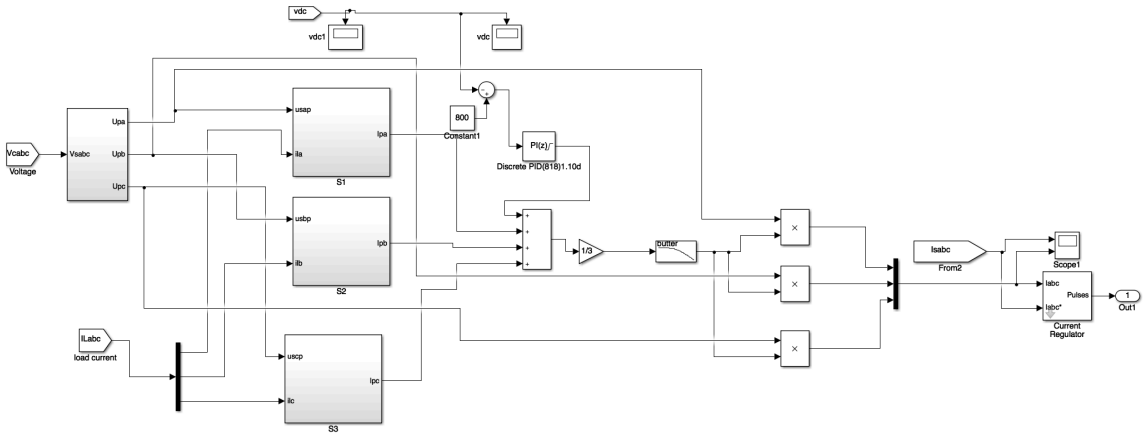

Fig.5.35. IcosØ controller for reference current extraction

A. Performance of grid connected Solar PV system with balanced linear load

The simulation results of grid interfaced Solar PV system with balanced linear load are shown in Fig. 5.36 and Fig. 5.37. The load is instantaneously decreased from 0.3sec to 0.6sec. Thus the respective variation in various parameters can be observed due to the load change. The simulation results show that V_{dc} remains constant and grid current decreases to meet the load demand, maintaining balanced, sinusoidal waveform with unity power factor.

Keeping temperature constant the irradiation of the solar PV system is decreased from 1000 W/m^2 to 500 W/m^2 from 0.7 sec. to 0.85 sec, as shown in Fig. 5.36. Keeping irradiation constant the temperature is increased from 25^0C to 50^0C as shown in Fig. 5.37 respectively. With the variation in these input parameters i.e reduction in solar irradiation or increased temperature, the solar PV power generation gets reduced and vice versa. So, the grid supplies the remaining load demand. Under all the parameter variations mentioned above, DC bus and PCC voltages are maintained and grid current remains balanced. The THD level of grid current is 1.32% and PCC current is .74% as shown in Fig. 5.38, which is well within the IEEE limits. The grid side supply is maintained at unity power factor as shown in Fig. 5.39.

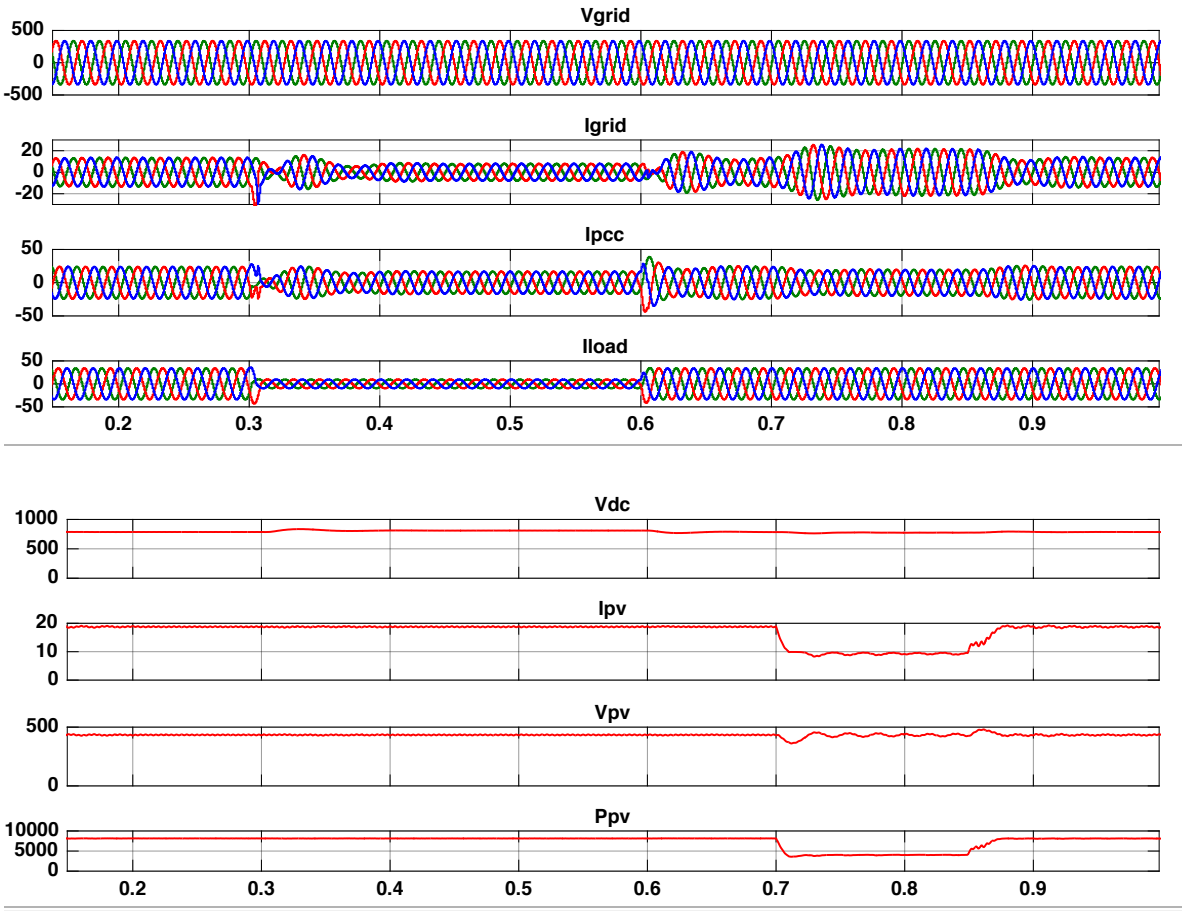

Fig. 5.36. Performance of grid interfaced PV system for linear load under varying load with changing radiation (Icosø).

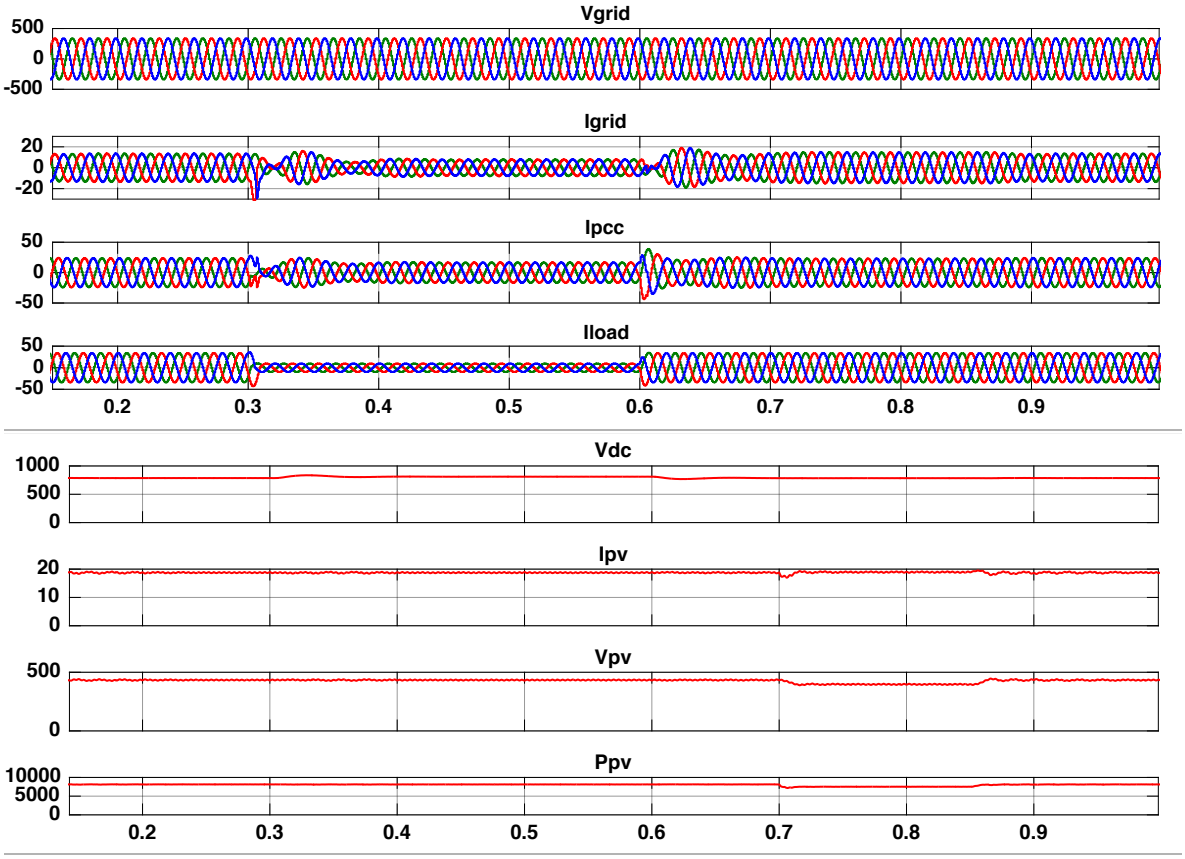

Fig 5.37. Performance of grid interfaced PV system for linear load under varying load and changing temperature (IcosØ).

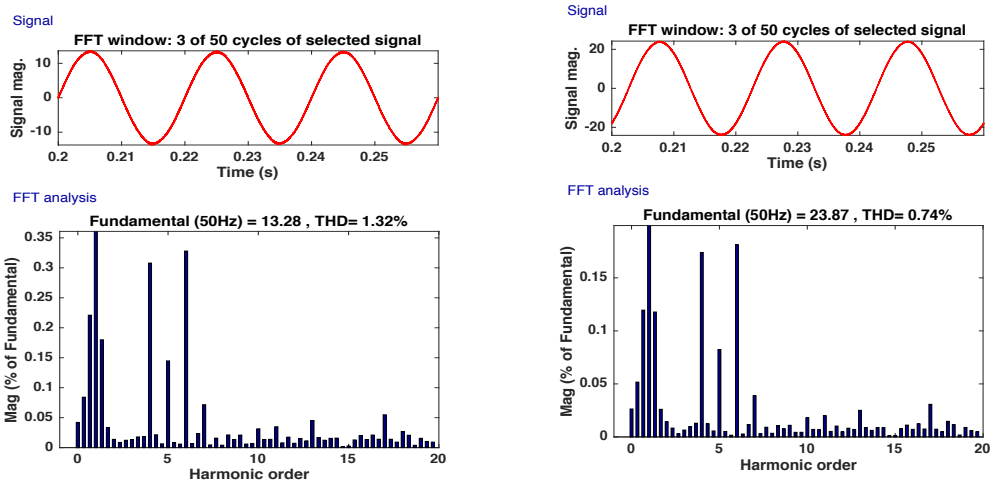

Fig.5.38. Waveform and harmonic analysis for Grid Current (I_{grid}) and PCC current (I_{PCC}) for linear load (IcosØ).

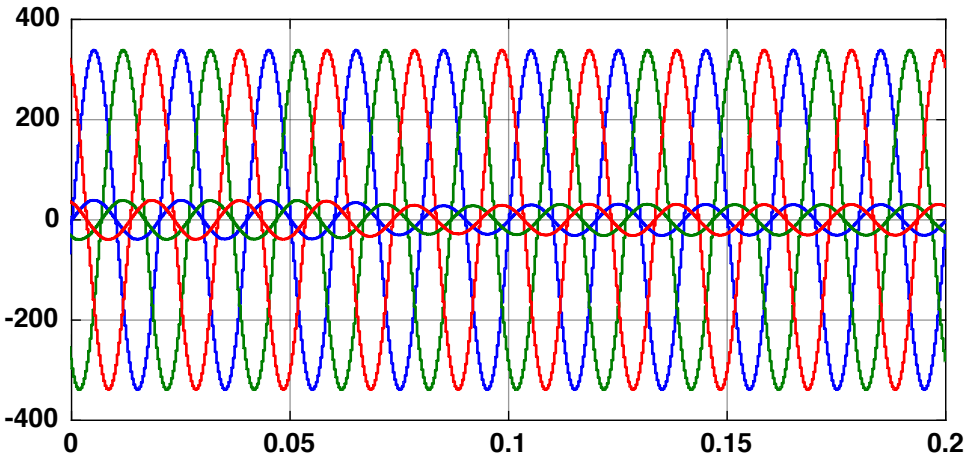

Fig. 5.39. In phase grid side voltage and current for linear load conditions (IcosØ).

B. Performance of grid connected Solar PV system with balanced non- linear load

The simulation results of grid interfaced Solar PV system with balanced non-linear load are shown in Fig. 5.40 and Fig. 5.41. From 0.3sec to 0.6sec,the load is instantaneously decreased. Thus the respective variation in various parameters can be observed due to the load change. The simulation results show that V_{dc} remains constant and source current decreases to meet the load demand, maintaining balanced, sinusoidal waveform with unity power factor. Keeping temperature constant the irradiation of the solar PV system is decreased from 1000 W/m^2 to 500 W/m^2 from 0.7 sec. to 0.85 sec, as shown in Fig. 5.40. Keeping irradiation constant the temperature is increased from 25^{0}C to 50^{0}C as shown in Fig. 5.41 respectively.With the variation in these input parameters i.e reduction in solar irradiation or increased temperature, solar PV power generation gets reduced. So, the grid supplies the remaining load demand. Under all the parameter variations mentioned above, DC bus and PCC voltages are maintained and grid current remains balanced. The THD level of grid current is .70% and THD level of load current is 17.20% as shown in Fig. 5.42, which is well within the IEEE limits. The grid side supply is maintained at unity power factor as shown in Fig. 5.43

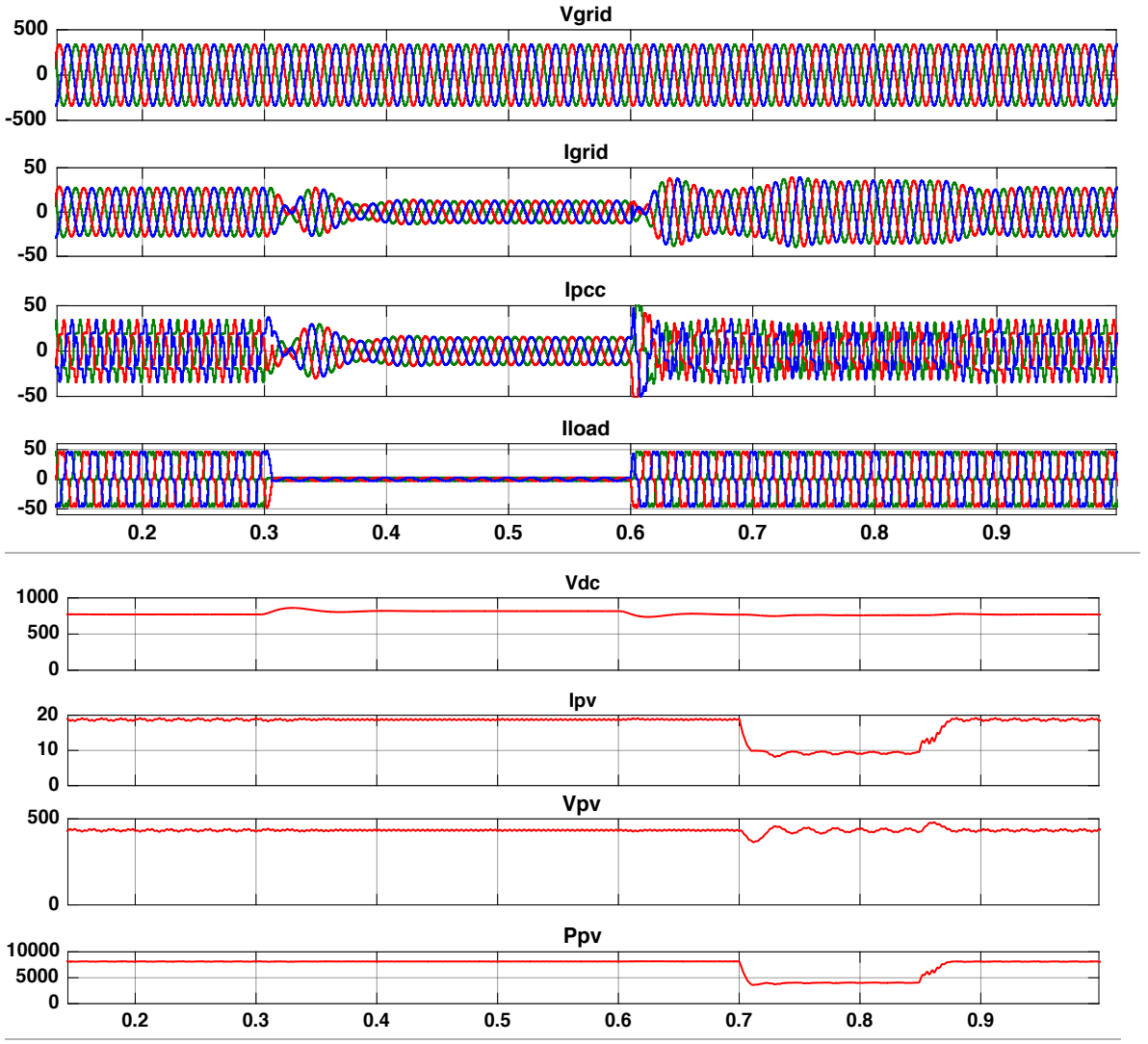

Fig. 5.40. Performance of grid interfaced PV system for non-linear load under varying load and changing radiation (IcosØ).

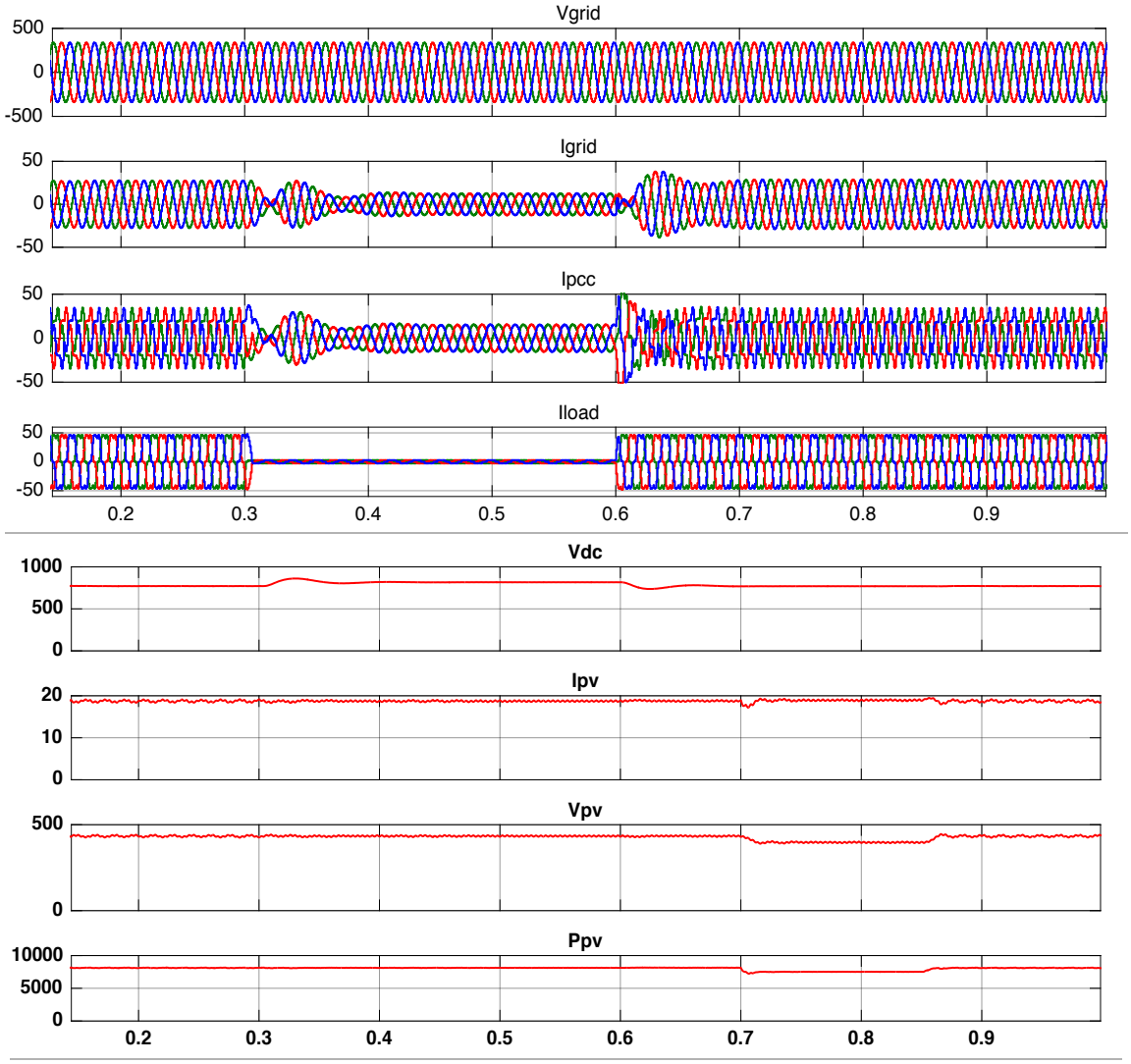

Fig.3.41. Performance of grid interfaced PV system for non-linear load under varying load and changing temperature (IcosØ).

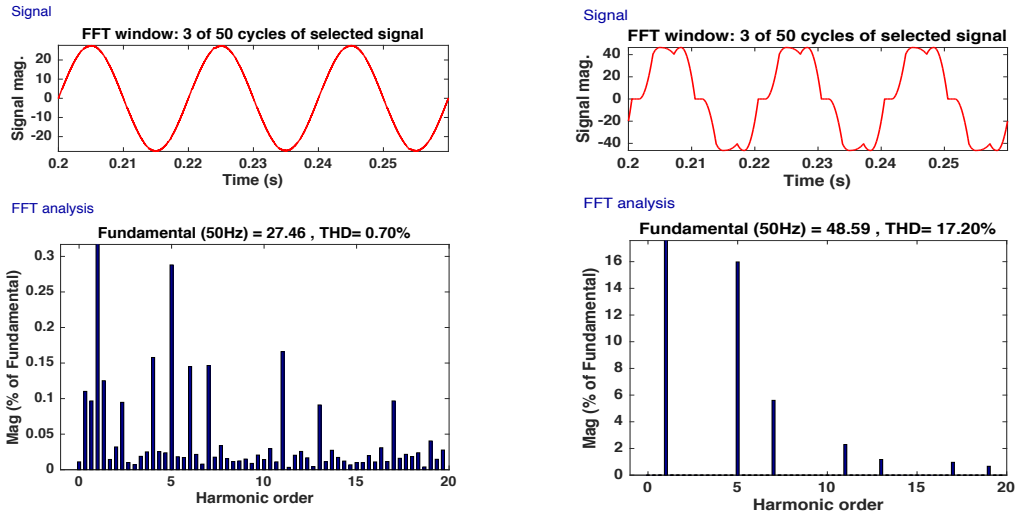

Fig.3.42. Waveform and harmonic analysis for Grid Current (I_{grid}) and Load current (I_{Load}) for non-linear load (IcosØ).

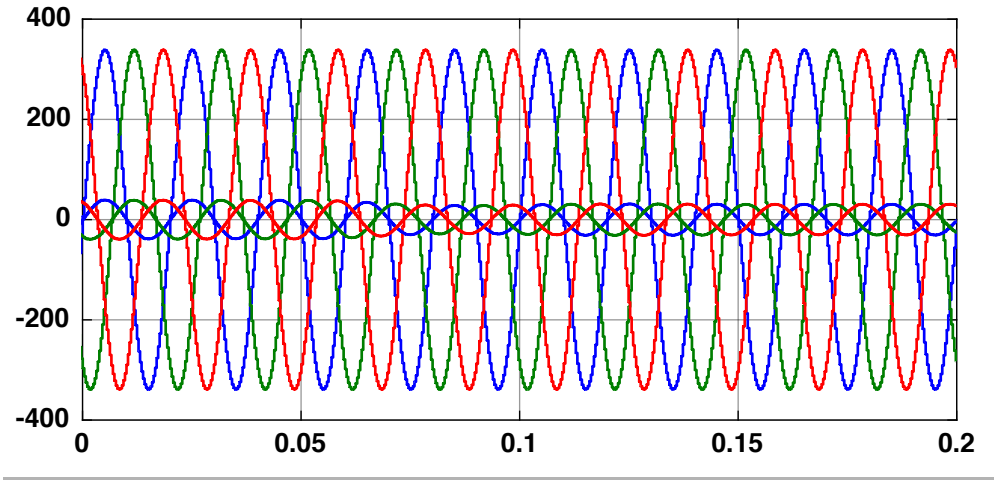

Fig. 5.43. In phase grid side voltage and current for non-linear load conditions (IcosØ).

C. *Performance of grid connected Solar PV system with unbalanced non-linear load*

The simulation results for non-linear unbalanced load is shown in Fig.5.44.The 'B' phase of the load is disconnected from 0.3 sec to 0.6 sec and at t=0.6 sec this 'B' phase of the load is again applied and the system regains its balanced state. Thus the respective variation in various parameters can be observed due to the load unbalancing. The simulation results show that V_{dc} remains constant and source current decreases to meet the load demand, maintaining balanced, sinusoidal waveform with unity power factor. Irradiation of the Solar

PV system is decreased from 1000 W/mm^2 to 500 W/mm^2 from 0.7 sec. to 0.85 sec, as shown by fig 5.44. In this situation, solar PV power generation gets reduced. So, the grid supplies the remaining load demand. Under all the parameter variations mentioned above, DC bus and PCC voltages are maintained and grid current remains balanced. The THD level of grid current is 3.38%, which is well within the IEEE, limits as shown in Fig.5.45.

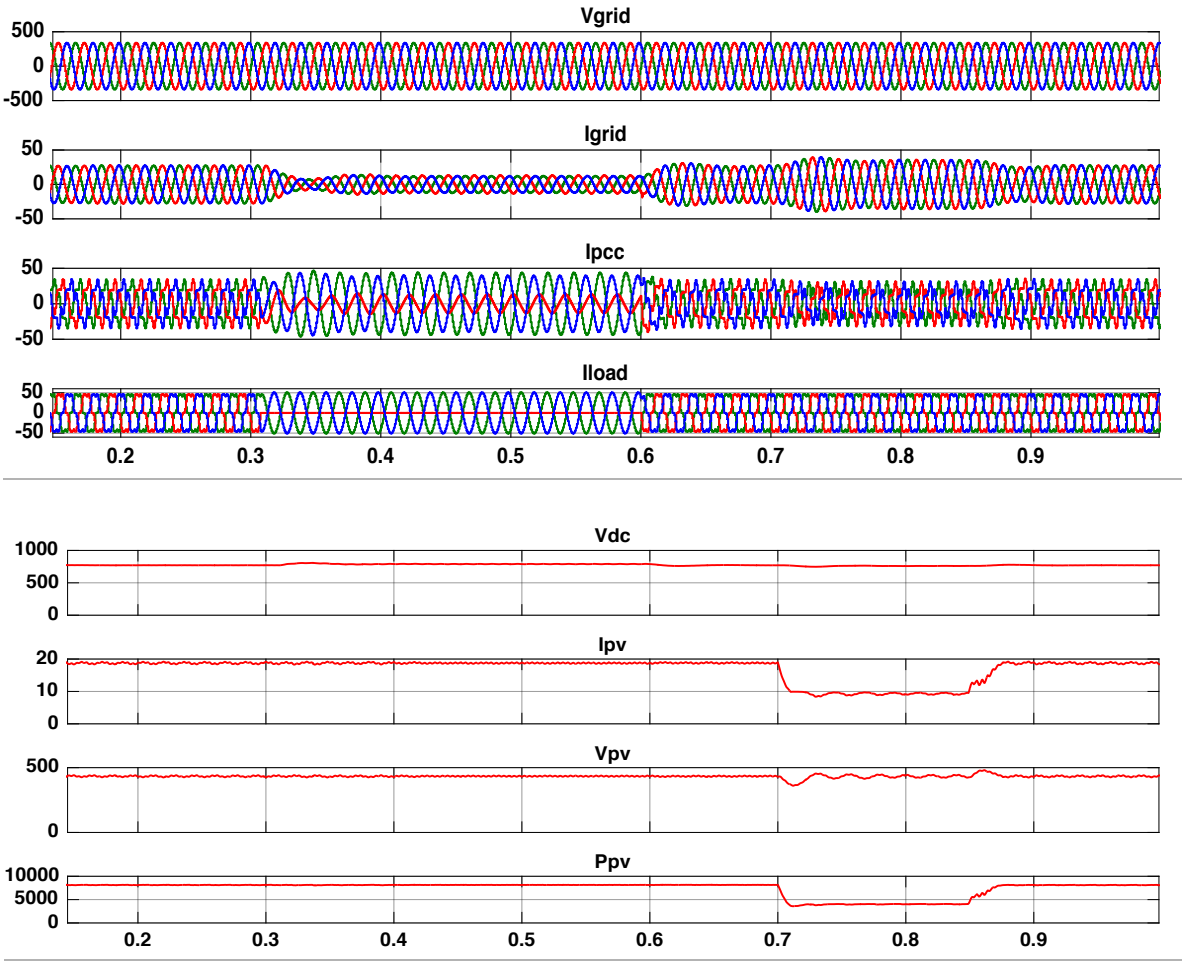

Fig.5.44. Performance of grid interfaced PV system for non-linear load under unbalancing with changing radiation (IcosØ).

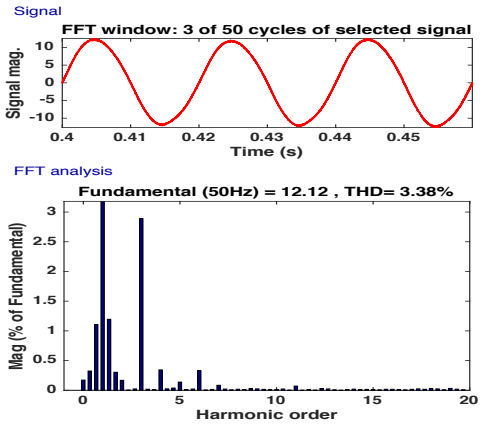

Fig.5.45. Waveform and harmonic analysis for Grid Current (I_{grid}) for non- linear load during unbalancing time (IcosØ).

D. Performance of grid connected Solar PV system with dynamic load.

The simulation results for dynamic load are shown in Fig. 5.46. The motor torque is increased to full load torque value i.e 20 N-m at 0.3 sec, and is decreased to half of the load torque i.e 10N-m after 6sec, and hence its effect on the various parameters can be observed. The simulation results show that V_{dc} remains constant and source current decreases to meet the load demand, maintaining balanced, sinusoidal waveform with unity power factor. The THD level of grid current is 1.03% and PCC current is .98%, which is well within IEEE limits as given by Fig. 5.47.

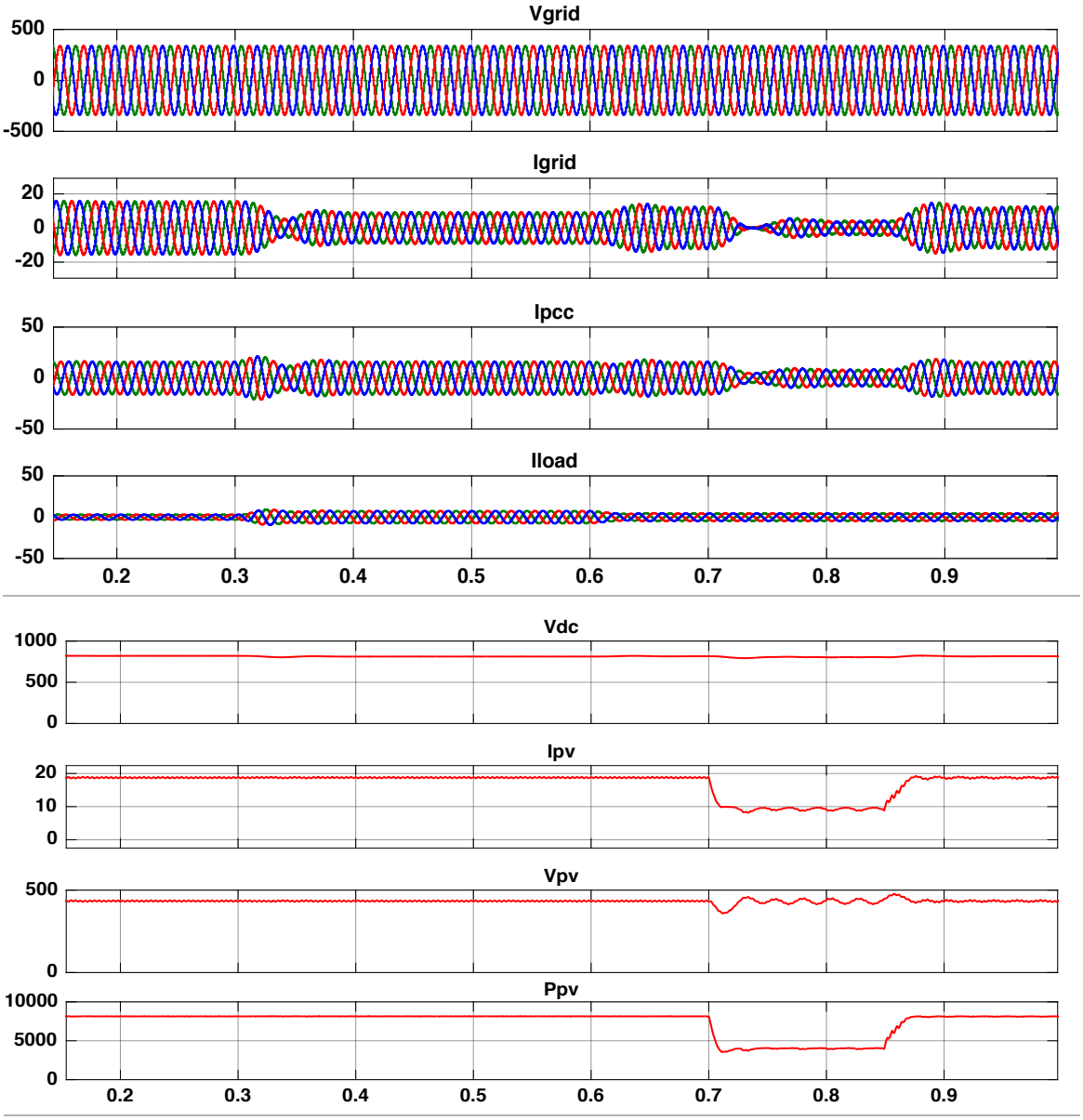

Fig. 5.46. Performance of grid interfaced PV system for dynamic load under torque variation with changing radiation (Icos∅).

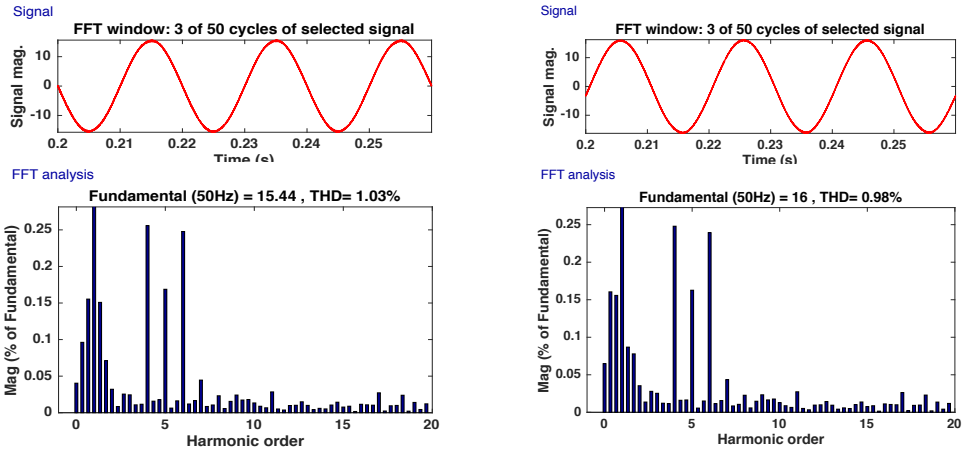

Fig.5.47. Waveform and harmonic analysis for Grid Current (I_{grid}) and PCC current (I_{PCC}) for dynamic load (Icosø).

5.4 Comparison of THD using SRF, ISC and ICOSØ Theory

Performance of all three algorithms in terms of harmonic filtering when 5% THD is introduced in source current.

Table II. Comparision of THD of grid current, PCC current and load current under different loads and inverter controllers.

Inverter Control Algorithms	DC-link voltage (V_{dc})	Linear load		Non-linear load		Dynamic load		Unbalanced Non-linear load
		Grid current THD (in %)	Point of common coupling current THD (in %)	Grid current THD (in %)	Load current THD (in %)	Grid current THD (in %)	Point of common coupling current THD (in %)	Grid current THD during unbalancing time (in %)
SRFT	800	2.23	1.25	1.05	17.19	1.92	1.86	3.85
ISCT	802	3.02	1.71	1.42	17.19	2.44	2.33	4.61
ICOSØ	818	1.32	.74	0.70	17.20	1.03	.98	3.38

5.5 Replacement of L filter by LCL filter with Icosϕ algorithm

On comparison of THD levels in different inverter control implemented so far, it is observed that minimum THD is obtained with Icosϕ algorithm. In order to improve the THD level further, LCL filter is implemented between the distribution grid and the inverter.

The simulation results obtained by both L filter and LCL filter are then compared. The bode plot of LCL filter under damped (blue) and undamped (red) conditions is shown in Fig.5.48

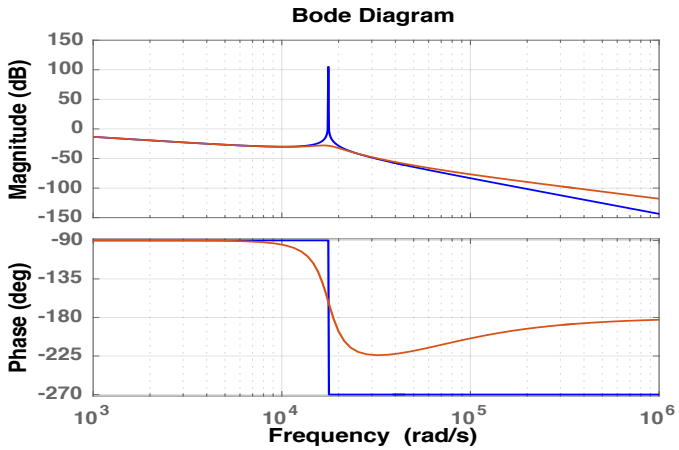

Fig.5.48. Bode plot for LCL filter under damped and undamped condition.

A. Performance of grid connected Solar PV system with balanced linear load

The simulation results of grid interfaced solar PV system with LCL filter under balanced linear load are shown in fig. 5.49. The simulation is carried out on constant load, irradiance and temperature i.e. 15000W active power and 9000Var reactive power, 1000W/m^2 and 25^0 C respectively. The THD level of grid current reduced from 1.16% to 0.73%and PCC current reduced from 0.65% to 0.45%, which is well within IEEE limits as given by fig. 5.50 and 5.51 respectively.

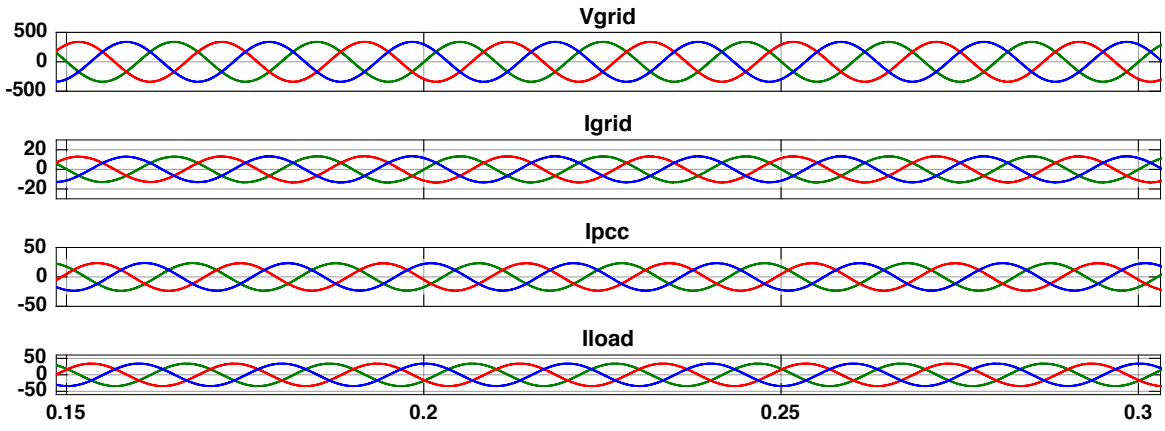

Fig.5.49. Performance of grid interfaced PV system for linear load with LCL filter (ICOSϕ).

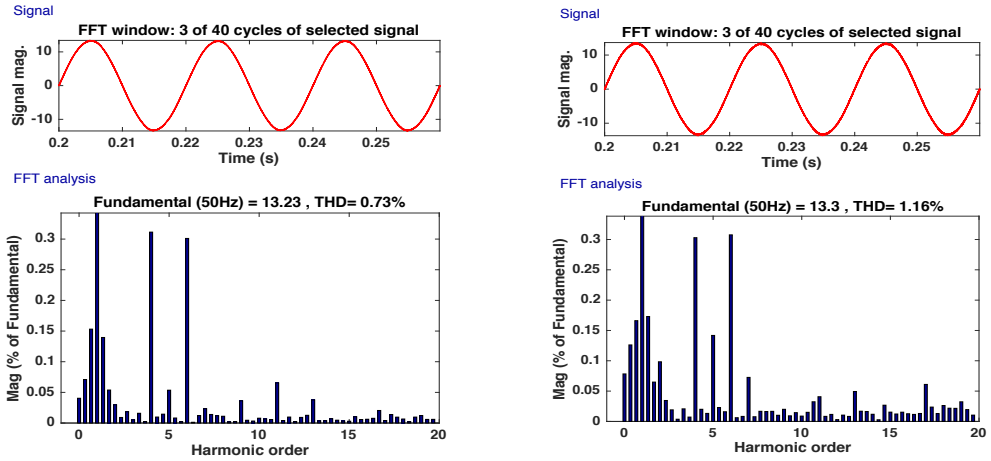

Fig.5.50. Waveform and harmonic analysis for Grid Current (I_{grid}) with LCL filter and L filter for linear load.

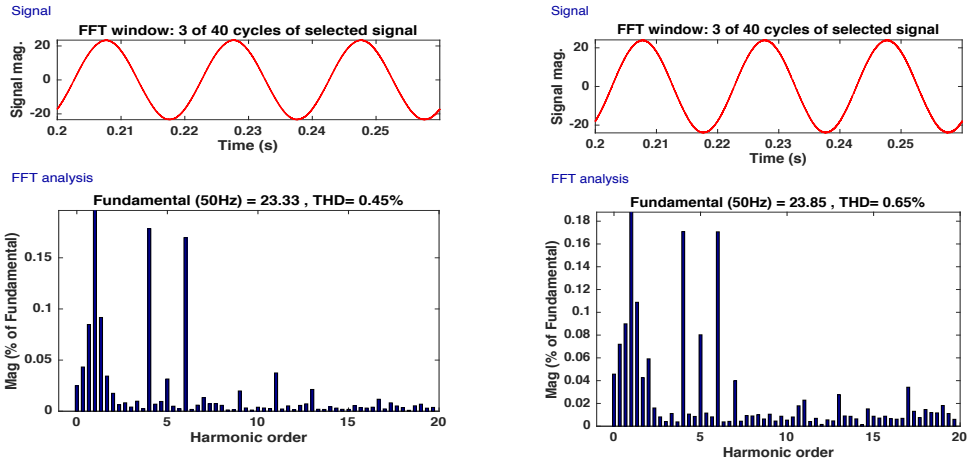

Fig.5.51. Waveform and harmonic analysis for PCC Current (I_{PCC}) with LCL filter and L filter for linear load.

B. Performance of grid connected Solar PV system with balanced non- linear load

The simulation results of grid interfaced solar PV system with LCL filter under non-linear load are shown in fig. 5.52.The simulation is carried out on constant load, irradiance and temperature i.e. nonlinear load-universal bridge with 200 ohms, 400mH RL load, 1000W/m^2 and 25^0 C respectively. It is observed that the THD on grid side got reduced from 1.36 % to 0.81 % and load THD remained constant i.e. 27.21% which is well within the IEEE standards as shown in fig 5.53 and 5.54 respectively.

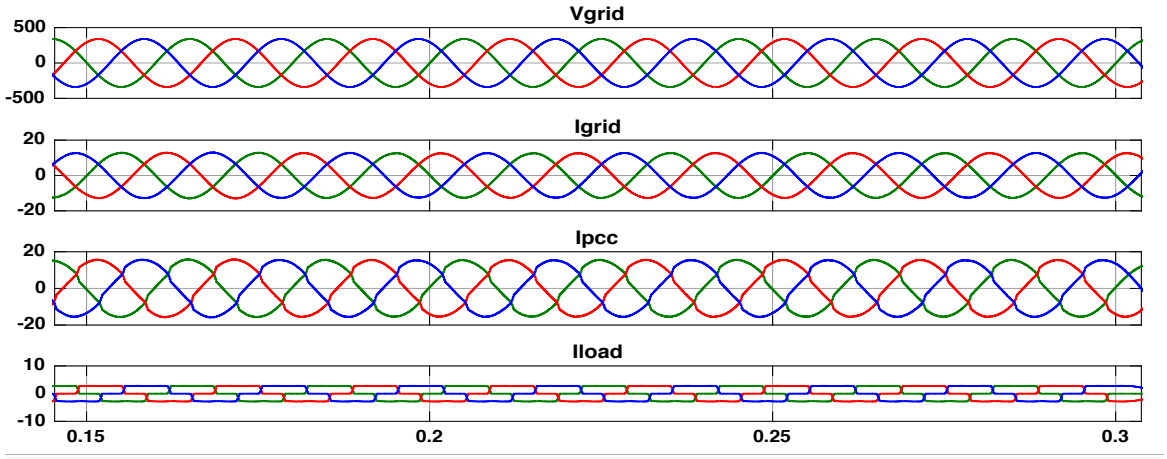

Fig.5.52. Performance of grid interfaced PV system for non-linear load with LCL filter (Icosϕ).

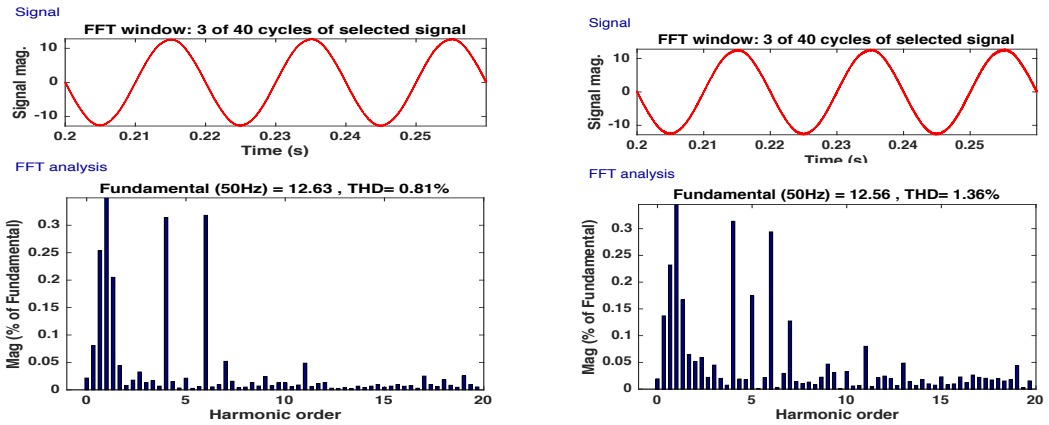

Fig.5.53. Waveform and harmonic analysis for Grid Current (I_{grid}) with LCL filter and L filter for non-linear load.

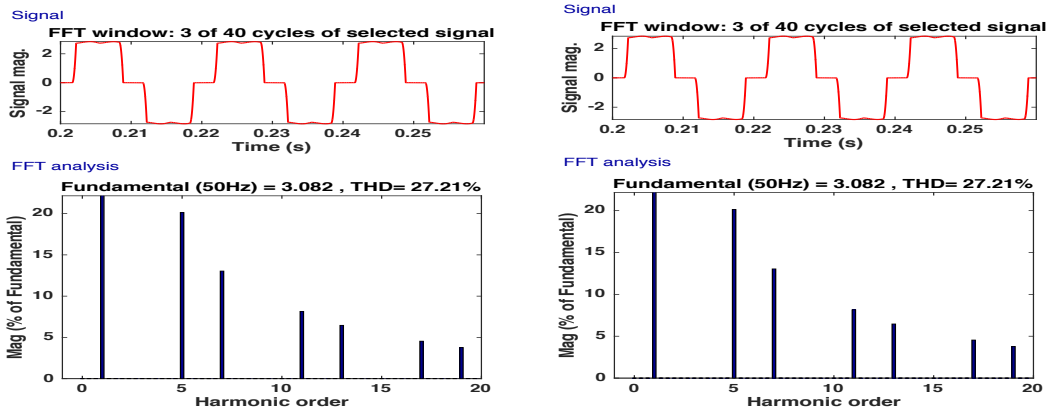

Fig.5.54. Waveform and harmonic analysis for Load Current (I_{load}) with LCL filter and L filter for non-linear load

C. Performance of grid connected Solar PV system with dynamic load.

The simulation results of grid interfaced solar PV system with LCL filter under dynamic load are shown in fig. 5.55.The simulation is carried out on constant load, irradiance and temperature i.e. Induction motor of 5HP, 1750 rpm; 1000W/m^2 and 25^0 C respectively. It is observed that the THD on grid side got reduced from 1.03 % to 0.66 % and PCC current THD reduced from 0.98% to 0.72% which is well within the IEEE standards as shown in Fig 5.56 and 5.57 respectively.

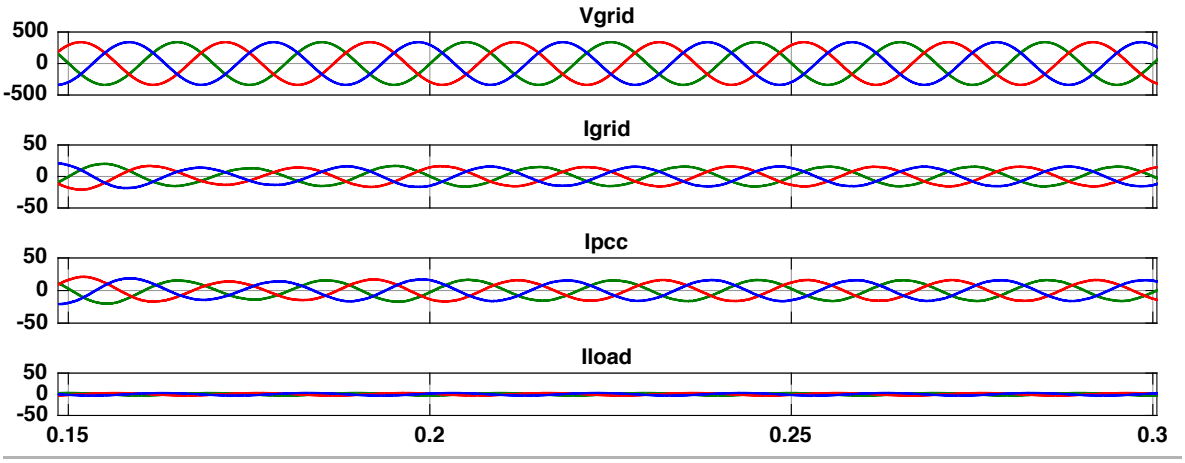

Fig.5.55. Performance of grid interfaced PV system for dynamic load with LCL

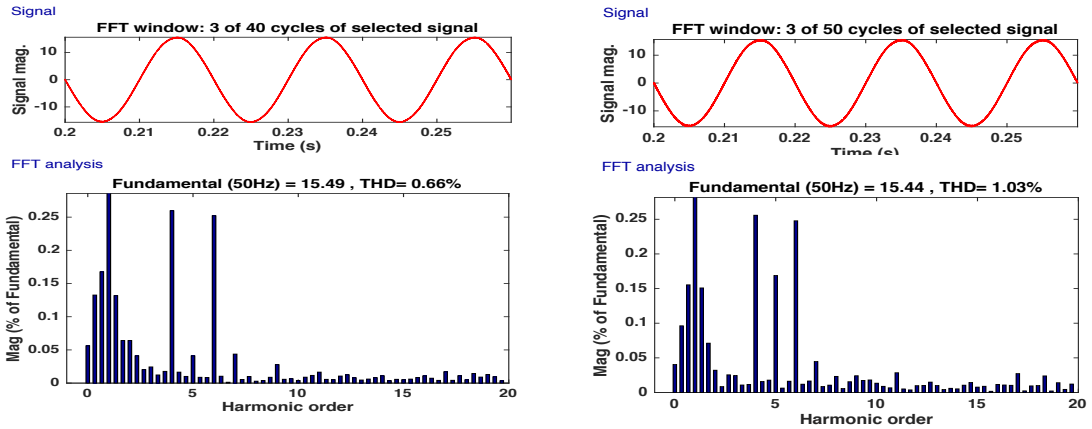

Fig.5.56. Waveform and harmonic analysis for Grid Current (I_{grid}) with LCL filter and L filter for dynamic load.

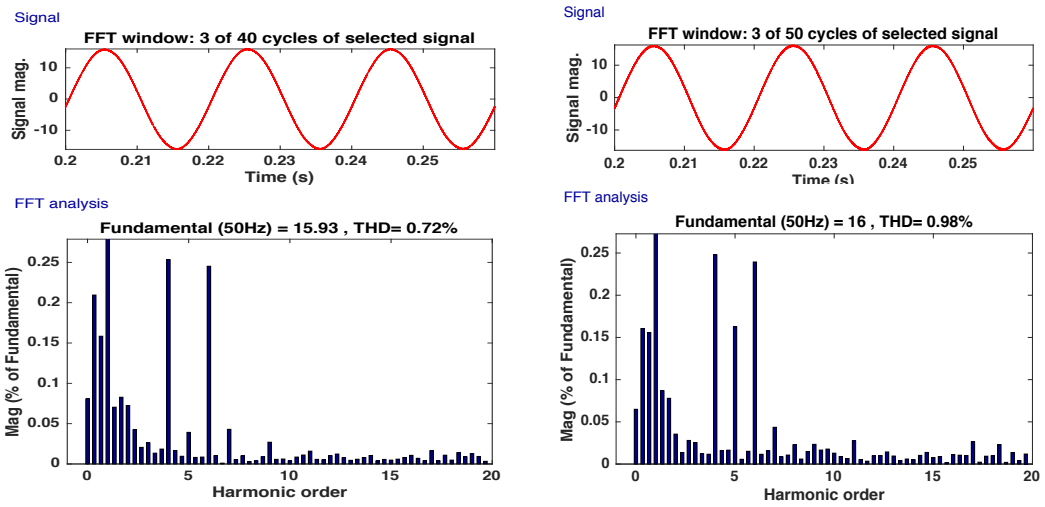

Fig.5.57. Waveform and harmonic analysis for PCC Current (I_{PCC}) with LCL filter and L filter for dynamic load

TABLE III Comparision of THD of grid current, PCC current and load current using L and LCL Filter under different loads and ICOSϕ inverter control .

FILTER	Linear Load		Non-Linear Load		Dynamic Load	
	Grid current THD (in %)	Point of common coupling current THD (in %)	Grid current THD (in %)	Load current THD (in %)	Grid current THD (in %)	Point of common coupling current THD (in %)
L- Filter	1.16	.65	1.36	27.21	1.03	.98
LCL- Filter	.73	.45	.81	27.21	.66	.72

5.6. Conclusion

The two MPPT algorithms P&O and INC and three inverter control techniques SRFT, ISCT and ICOSØ and two filter L and LCL are simulated in MATLAB/ SIMULINK and the simulation result for harmonic reduction in grid current and power balancing with different loads and varying atmospheric conditions are shown. The three control techniques are compared and it is noticed that the THD in each control algorithm for different loads is

well within IEEE Standard 519, 1992 and unity power factor on grid side is maintained. The THD level is further improved by implementing LCL filter between distribution grid and inverter end.

CHAPTER 6
CONCLUSIONS AND FURTHER SCOPE OF WORK

6.1 Conclusion

This thesis work includes the modeling and simulation of grid interfaced solar PV system. The Power versus Voltage characteristic curve and Current versus Voltage characteristic curve of given solar PV array is plotted and it is observed that the PV power output varies with the variation in the solar irradiation and temperature. The PV current decreases with the reduction in irradiance. As PV current is proportional to irradiance; this results in reduced output power. Similarly temperature holds inverse relation to voltage. Thus when the temperature increases, the open circuit voltage decreases. Therefore, the power of the solar PV array is reduced. The PV array exhibits non-linear characteristics. Therefore MPPT algorithm is used to track the maximum power point from the PV array according to the variation in the temperature and irradiation. MPPT technique is realized through a boost converter. Two different MPPT algorithms namely P&O and INC are implemented in the simulation studies and the one with better tracking of MPP (P&O) is implemented in the grid interfaced SPV system.

The SPV inverter is designed and simulated using three different control algorithms namely SRFT, ISCT, and ICOSØ. Simulation studies are carried out on the SPV system integrated with distribution grid. These studies are analyzed with various inverter control techniques under different load and environmental conditions. The DC bus voltage and power balance is maintained under all the conditions. The source side current is maintained at unity power factor with THD within IEEE standard limits. The inverter control technique(i.e. ICOSØ) giving minimum harmonic distortion is further improved by using LCL filter.

6.2 Future scope

Further research works that can be followed using the designed model of grid interfaced solar PV system can be the implementation of intelligent and adaptive control algorithms for maximum power point tracking and inverter control. Effect of partial shading condition on the performance of MPPT is to be studied both in stand-alone system and grid-

connected system. The hardware implementation of the grid interfaced SPV system can be done to confirm the simulation results.

The inverter may be examined to have immunity to grid operating in critical conditions, e.g. voltage swelling and sagging, and phase jumps etc.

REFERENCES

[1] "International Energy Outlook, 2016", U.S. Energy Information Administration.

[2] Ministry of New and Renewable Energy (MNRE) 2016.

[3] Gireesh Shrimali, Sunali Rohra,(2012, October), "India's solar mission: A review" Renewable and Sustainable Energy Reviews, Vol.16, Issue 8, Pg 6317-6332.

[4] Gupta, Sandeep Kumar, and Raghubir Singh Anand (2013) "Development of Solar Electricity Supply System in India: An Overview." Journal of Solar Energy 2013.

[5] Rachid Belaidi , A. Haddouche, "Shunt active power filter connected to a photovoltaic array for compensating harmonics and reactive power simultaneously" IEEE 4th International Conference on Power Engineering, Energy and Electrical Drives.

[6] Pritam Chowdhury, Indrajit Koley, Sougata Sen, Dr.Pradip Kumar Saha , Dr.Gautam Kumar Panda, "Modelling, Simulation And Control of A Grid Connected Non Conventional Solar Power Generation System Using Matlab" International Journal of Advanced Research in Electrical, Electronics and Instrumentation Engineering Vol. 2, Issue 4, April 2013.

[7] Jincy Philip, Chinmay Jain, Krishan Kant, Bhim Singh, Sukumar Mishra,Ambrish Chandra, Kamal Al-Haddad, "Control and implementation of a standalone solar photovoltaic hybrid system" IEEE Transaction on Industry applications, vol.52,no. 4, july/august 2016.

[8] S. Sumathi, L. Ashok Kumar, P. Surekha, "Solar PV and Wind Energy Conversion Systems" an Introduction to Theory, Modeling with MATLAB/SIMULINK, and the Role of Soft Computing Techniques ISSN 1865-3529 ISSN 1865-3537 (electronic) Green Energy and Technology ISBN 978-3-319-14941-7 (eBook)

[9] S. Dasgupta, S. K. Sahoo, and S. K. Panda, "Single-phase inverter control techniques for interfacing renewable energy sources with microgrid—Part I: Parallel-connected

inverter topology with active and reactive power flow control along with grid current shaping," Power Electronics, IEEE Transactions on, vol. 26, pp. 717-731, 2011.

[10] Augustin McEvoy, Tom Markvart and Luis Castaner, “Practical Handbook of Photovoltaics-Fundamentals and Applications”, Second Edition, Elsevier, Wyman Street, USA, 2012

[11] Himanshu Sekhar Sahu, Sisir Kumar Nayak and Sukumar Mishra, “Maximizing the Power Generation of a Partially Shaded PV Array”,IEEE Journal of emerging and selected topics in power electronics, vol. 4,no. 2, june 2016.

[12] M. G. Villalva, J. R. Gazoli, and E. R. Filho, "Comprehensive Approach to Modeling and Simulation of Photovoltaic Arrays," Power Electronics IEEE Transactions on, vol. 24, pp. 1198-1208, 2009.

[13] J. A. Gow and C. D. Manning, “Development of a photovoltaic array model for use in power-electronics simulation studies,” IEEE Proc. Elect.Power Appl., vol. 146, no. 2, pp. 193–200, 1999.

[14] Wei Jiang, Yu-fei Zhou and Jun-ning Chen, “Modeling andSimulation of Boost Converter in CCM and DCM,” IEEE Conference on Power Electronics and Intelligent Transportation System (PEITS), pp. 288-291, 2009.

[15] Nikita Gupta, Rachana Garg and Parmod Kumar, “characterization study of PV module connected to Microgrid”, In IEEE India International Conference JMI, DOI: 10.1109/INDICON.2015.7443356, India, 2015.

[16] Mukhtiar Singh, Vinod Khadkikar, Ambrish Chandra and Rajiv K. Varma, “Grid Interconnection of Renewable Energy Sources at the Distribution Level with Power Quality Improvement Features”, IEEE Transactions on Power Delivery, vol. 26, no. 1, pp. 307-315, 2011.

[17] S. Rustemli, F. Dincer, “Modeling of Photovoltaic Panel and Examining Effects of Temperature in Matlab/Simulink”, Electronics and Electrical Engineering, ISSN 1392-1215, no. 3(109), pp. 35-40,2012.

[18] Kinal Kachhiya, Makarand Lokhande, Mukesh Patel, "MATLAB/Simulink Model of Solar PV Module and MPPT Algorithm", Proceedings of the National Conference on Recent Trends in Engineering and Technology, 2011.

[19] I.H. Atlas, A.M. Sharaf, "A Photovoltaic Array Simulation Model for Matlab-Simulink GUI Environment", International Conference on Clean Power, pp. 341-345, 2007.

[20] M. Latha Devi and M.Chilambarasan, "Design and simulation of Incremental Conductance MPPT Using self lift cuk converter," International conference on Renewable Energy and Sustainable Energy, IEEE 2013.

[21] M.Abdulkardir, A.S.Samosir and A. H. M Yatim, "Modelling and Simulation of Maximum Power Point Tracking of Photovoltaic System in Simulink model", International Conference on Power and Energy, IEEE 2012.

[22] Muhammad Afroz Akhtar and Hanumath Prasad Ikkurti, "A new controller for Maximum power extraction from Photovoltaic system using Phase modulated converter", IEEE 2012.

[23] Himanshu Kumar and Dr. R.K Tripathi, "Simulation of Variable Incremental Conductance Method using boost converter", IEEE 2012.

[24] Trishan Esram, "Comparison of Photovoltaic Array Maximum Power Point Tracking Techniques" IEEE Transactions On Energy Conversion, Vol. 22, No. 2, June 2007

[25] Tarek Selmi, Mohamed Abdul-Niby, Laura Devis and Andrew Davis, "P&O MPPT Implementation Using MATLAB/Simulink" Ninth International Conference on Ecological Vehicles and Renewable Energies (EVER), IEEE 2014.

[26] M. A. Elgendy and B. Zahawi, "Assessment of perturb and observe MPPT algorithm implementation techniques for PV pumping applications," IEEE Transactions on Sustainable Energy, vol. 3, no. 1, pp. 21-33, 2012.

[27] Marco Liserre, Frede Blaabjerg and Steffan Hansen “Design and control of an LCL-filter based three phase active rectifier”, IEEE Transaction on industry applications, Vol. 41, no. 5, September/October 2005.

[28] Leonardo Augusto Serpa, Srinivas Ponnaluri, Peter Mantovanelli Barbosa and Johann Walter Kolar, “A modified direct power control strategy allowing the connection of three-phase inverters to the grid through LCL filters”, IEEE Transaction on industry applications, Vol. 43, no. 5, September/October 2007.

[29] A. Reznik, M. Godoy Simoes, Ahmed Al-Durra and S. M. Muyeen, “LCL filter design and performance analysis for grid interconnected systems”.

[30] Prakash Chittora, Alka Singh and Madhusudan Singh, “Harmonic Current Extraction and Compensation in three phase three wire system using Notch filter,” 2015 IEEE Recent Advanced in Intelligent Computational Systems.

[31] Bhim Singh, Sabha Raj Arya, “Design and control of a DSTATCOM for power quality improvement using cross correlation function approach” International Journal of Engineering, Science and TechnologyVol. 4, No. 1, 2012, pp. 74-86.

[32] B. N. Singh, P. Rastgoufard, B. Singh, A. Chandra, and K. A. Haddad, “Design, simulation and implementation of three pole/four pole topologies for active filters,” Inst. Electr. Eng. Proc. Electr. PowerAppl.,vol. 151, no. 4, pp. 467–476, Jul. 2004

[33] El-Samahy and E. El-Saadany, "The effect of DG on power quality in a deregulated environment," IEEE Power Engineering Society General Meeting, vol. 3, Jun 2005, pp. 2969- 2976.

[34] Bhattacharya, S. Divan, and B. Benejee, “Synchronous Reference Frame HarmonicIsolator Using Series Active Filter”, 4th European Power Electronic Conf., Florence,vol. 3, 1991, pp. 30-35.

[35] A. K. Verma, B. Singh and D.T. Shahani, “Grid interfaced solar photovoltaic power generating system with power quality improvement at AC mains,” in IEEE ICSET-2012, 24-27 Sept. 2012, pp. pp.177-182.

[36] Rejil C, AnzariM and Arun Kumar R, "Design and Simulation of Three Phase Shunt Active Power Filter Using SRF Theory". Advance in Electronic and Electric Engineering.ISSN 2231-1297, Volume 3, Number 6 (2013), pp. 651-660

[37] Nikita Gupta, Rachana Garg and Parmod Kumar, "Asymmetrical fuzzy logic control to PV module connected micro-grid", In IEEE India International Conference JMI, DOI: 10.1109/INDICON.2015.7443356, India, 2015.

[38] Ravi Nath Tripathi, Alka Singh , "SRF Theory Based Grid Interconnected Solar Photovoltaic (SPV) System with Improved Power Quality" Emerging Trends in Communication, Control, Signal Processing & Computing Applications (C2SPCA), 2013 International Conference

[39] Da silva, CH., Pereira, R.R., da silva, "A digital PLL scheme for three-phase system using modified synchronous reference frame", IEEE Transactions Industrial Electronics, 2010, 57; 3814-21.

[40] http://in.mathworks.com/help/physmod/sps/powersys/ref/pll3ph.html

[41] U. Koteswara Rao, Mahesh K. Mishra, and Arindam Ghosh, "Control Strategies for Load Compensation Using Instantaneous Symmetrical Component Theory Under Different Supply Voltages," IEEE Trans on Power Delivery, vol.23, no.4, pp.2310-2317, 2008.

[42] Sunil Kumar and Bhim Singh, "Control of 4-Leg VSC Based DSTATCOM Using Modified Instantaneous Symmetrical Component Theory," International Conf. on Power System(ICPS), pp.1-6, 2009.

[43] Arindam Ghosh, and Avinash Joshi, "A New Approach to Load Balancing and Power Factor Correction in Power Distribution System," IEEE Trans on Power Delivery, vol.15, no.1, pp. 417-422, 2000.

[44] Mahesh K. Mishra, Arindam Ghosh, Avinash Joshi and Hiralal M. Suryawanshi, "A Novel Method of Load Compensation Under Unbalanced and Distorted Voltages," IEEE Trans on Power Delivery, vol.22, no.1, pp. 288-295, 2007.

[45] Naresh K. Kummari, Asheesh K. Singh and Pradeep Kumar, "Comparative Evaluation of DSTATCOM Control Algorithms for Load Compensation" conf. IEEE ICHQP, 2012.

[46] Dinesh Kumar, Rajesh, "Modelling, Analysis and Performance of a DSTATCOM for Unbalanced and Non-Linear Load" 2005 IEEE/PES Transmission and Distribution Conference & Exhibition: Asia and Pacific Dalian, China.

[47] Arun Kumar Verma, Bhim Singh, D.T Shahani, Ambrish Chandra and Kamal Al-Haddad, "Combined Operation of a VSC Based Grid Interfaced Solar Photovoltaic Power Generation System with Night Time Application". IEEE /PES General meeting, Conference & Exhibition 2014.

[48] Manoj Kumar, Mahesh K. Mishra, "A Grid-Connected Dual Voltage Source Inverter With Power Quality Improvement Features" IEEE Trans. on Sustainable Energy, Vol. 6, No. 2, April 2015.

[49] G. Bhuvaneswari and M.G. Nair , "Design, Simulation and Analog Circuit Implementation of a Three-phase Shunt Active Filter using the Icosφ Algorithm", Conf. IEEE PEDS '05, vol. 1, Jan. 2006, pp. 553 –55.

[50] Singh, B. and Kumar S., "Control of DSTATCOM using IcosΦ Algorithm," IEEE Conference in Industrial Electronics IECON'09, pp. 322_327 (2009).

[51] Kamatchi Kannan, V. and Rengarajan, N.,"PhotovoltaicBased Distribution Static Compensator for PowerQuality Improvement," International Journal of Electrical Power & Energy Systems, Vol. 42, No. 1, pp.685_692 (2012).

[52] G. Bhuvaneswari, M.G. Nair and S. Kumar Reddy, "Comparison of Synchronous Detection and IcosΦ Shunt Active Filtering Algorithms", Conf. IEEE PEDES, Dec. 2006, pp. 1 – 5.

[53] IEEE Recommended Practices and Requirements for Harmonics Control in Electric Power Systems, IEEE Standard 519, 1992.

Appendix 1

Data for SPV system:

TABLE IV PV MODULE DATA

Parameters	Values (unit)
Peak power (P_{max})	315.07W
Open circuit voltage (V_{oc})	64.6V
Short circuit current (I_{sc})	6.14A
Voltage at max power (V_{mp})	54.7V
Current at max power (I_{mp})	5.76A
No. of cells (n_s)	96
Shunt Resistance (R_{sh})	430 Ω
Series Resistance (R_s)	0.43 Ω

TABLE V SPECIFICATIONS FOR THE GRID-CONNECTED PV SYSTEM.

Parameters	Values (unit)
PV array	8kW
Grid Voltage	3Φ, 415V
Grid frequency	50Hz
Switching frequency	10kHz
DC link voltage (V_{dc})	800V
DC link capacitor (C_d)	3000μF
L_f	7 mF
Output filter (LCL)	$L_i = 12$mH $L_g = .012$mH $C_f = 7.39\mu F$ R_f = 8.73

TABLE VI DATA FOR DIFFERENT LOADS

Load Specification	**Time(upto .3 sec)**	**(.3 to .6 sec)**
Balanced Linear Load (RL)	P = 15kW	P = 4kW
	Q = 9kVar	Q = 3kVar
	p.f = .85	p.f = .8
Nonlinear load-universal bridge with RL load	11Ω	200Ω
	0.9mH	400mH
Dynamic load(induction motor) 5 HP, 1750 rpm.		